



---

**Forschungszentrum Karlsruhe**  
in der Helmholtz-Gemeinschaft

---

**Wissenschaftliche Berichte**  
FZKA 7421

# **Effects of N-terminal Mutations of Human Androgen Receptor on Polyglutamine Toxicity**

**S.F. Funderburk**

**Institut für Toxikologie und Genetik**

**Juli 2008**



**Forschungszentrum Karlsruhe**

in der Helmholtz-Gemeinschaft

Wissenschaftliche Berichte

FZKA 7421

**Effects of N-terminal mutations of human  
androgen receptor on polyglutamine toxicity**

Sarah F. Funderburk

Institut für Toxikologie und Genetik

Von der Fakultät Naturwissenschaften

der Universität Hohenheim

Institut für Zoologie

genehmigte Dissertation

**Forschungszentrum Karlsruhe GmbH, Karlsruhe**

**2008**

Für diesen Bericht behalten wir uns alle Rechte vor

Forschungszentrum Karlsruhe GmbH  
Postfach 3640, 76021 Karlsruhe

Mitglied der Hermann von Helmholtz-Gemeinschaft  
Deutscher Forschungszentren (HGF)

ISSN 0947-8620

urn:nbn:de:0005-074214

**Effects of N-terminal mutations of human androgen  
receptor on polyglutamine toxicity**

**Dissertation zur Erlangung des Doktorgrades  
der Naturwissenschaften (Dr. rer. nat.)**

**Fakultät Naturwissenschaften  
Universität Hohenheim  
Institut für Zoologie**

Institut für Toxikologie und Genetik  
Forschungszentrum Karlsruhe

vorgelegt von

Sarah F. Funderburk

aus Greenville, South Carolina, USA

2008

Dekan: Prof. Dr. Heinz Breer  
1. berichtende Person: Prof. Dr. Andrew C.B. Cato  
2. berichtende Person: Prof. Dr. Martin Blum  
Eingereicht am: 20.11.2007  
Mündliche Prüfung: 18.01.2008

Die vorliegende Arbeit wurde am 14. Januar 2008 von der Fakultät Naturwissenschaften der Universität Hohenheim als „Dissertation zur Erlangung des Doktorgrades der Naturwissenschaften“ angenommen.

Ich erkläre, dass ich diese Dissertation selbständig angefertigt habe. Ich habe nur die angegebenen Quellen und Hilfsmittel benutzt und wörtlich oder inhaltlich übernommene Stellen als solche gekennzeichnet.

I hereby declare that this dissertation is my own independent work. I have only used the given sources and materials, and I have cited others' works appropriately.

Sarah F. Funderburk

Karlsruhe, 20.11.2007



## *Acknowledgements*

I would first like to gratefully acknowledge all of those who have made the complicated progression from Bachelor's to PhD possible: Prof. Dr. Martin Blum, Renate Sauter, Dr. Marita Baumgarten, Prof. Dr. Heinz Breer, and Prof. Dr. Andrew Cato.

I would especially like to thank my supervisor, Prof. Dr. Andrew Cato, for initially offering me the opportunity to come to Germany and work in his lab for a “year-long” research internship. Through his encouragement, support, and constant pushing, that internship turned into an invaluable learning experience. I could not have asked for a better group leader, mentor, or confidante.

During the course of my PhD, I have also benefited greatly from those working in the lab with me. I'd like to thank Ljuba for all of her help with many critical experiments; Danilo for always listening to my many difficulties and complaints; Tobias for his patience and willingness to learn; Sandra for her good advice; and Jana for always taking care of everything.

Of course, I would not have been able to survive in Germany during these PhD years without the friends that have become my international family and have been my lifeline. Thank you Vivienne for being there for me through what have been the best and worst of times for me. Thank you Anne for sharing so much of yourself and your world. Thank you Sylwia for continuously looking out for me. And Sean, thank you for keeping me sane, always making me laugh, and keeping my focus on the future.

I also could not have made it through my PhD without my family being behind me every step of the way. I would like to thank my mom and dad for always being only a phone call away. I never had any difficulty in feeling their love and support from across the Atlantic. My brother David also deserves a special “thank you” for inspiring me to be creative. Finally, I would like to dedicate my doctoral thesis to the memory of my brother, John. His crazy antics growing up inspired me to study genetics in the first place. I just could not imagine how we could be related. I miss him every day, and I know he would be proud of his little sister.



# Effekte N-terminaler Mutationen des humanen Androgenrezeptors auf die Polyglutamintoxizität

## ZUSAMMENFASSUNG

Neun neurodegenerative Krankheiten sind auf die Verlängerung einer Polyglutamin (PolyQ) Sequenz in unterschiedlichen Proteinen zurückzuführen. Die Zytotoxizität von jedem dieser Proteine ist mit einer Fehlfaltung des mutierten Proteins assoziiert. Dadurch kommt es zu Veränderungen in zellulären Prozessen und Interaktionen, sowie der damit verbundenen Bildung von unlöslichen Aggregaten und anderen toxisch wirkenden Spezies. Die Polyglutaminerkrankungen unterscheiden sich jedoch in ihrer Pathogenese und gewebespezifischen Wirkung, was auf den jeweiligen Proteinkontext bzw. PolyQ-angrenzenden Sequenzbereich zurückzuführen sein könnte.

Für die Studien der hier vorliegenden Arbeit wurde der polyglutaminhaltige humane Androgenrezeptor (AR), Auslöser der spinalen und bulbären Muskelatrophie (SBMA), als Modell verwendet, um die Toxizität der PolyQ-Verlängerung zu analysieren. In früheren Experimenten wurden zwei mögliche Phosphorylierungsstellen im AR identifiziert, und die Mutation dieser Stellen schien eine Konformationsänderung im Protein hervorzurufen. Ausgehend von diesen Befunden wurden nun diese N-terminalen Serin-Reste im Wildtyp AR (ARQ22) sowie in einem Rezeptor mit einer verlängerten PolyQ Sequenz (ARQ77) gegen Alanin ausgetauscht (ARQ22dm bzw. ARQ77dm). Mit Hilfe dieser Mutanten wurde dann der Effekt der durch die Serinmutation erzeugten Konformationsänderung auf die jeweiligen Aggregatformen und die damit verbundenen Toxizitätsprofile charakterisiert.

Die Untersuchungen der Aggregation und Toxizität in kultivierten Zellen und in einem SBMA *Drosophila* Modell ergaben, dass sich die Effekte der Konformationsänderungen in Abhängigkeit von der Länge der PolyQ Sequenz unterscheiden. Im ARQ22 verursachten die Mutationen eine deutliche Verstärkung der Aggregation, sowie eine verminderte Überlebensrate und ein verändertes Bewegungsverhalten in *Drosophila*. Diese Veränderungen ähnelten dem Phänotyp des ARQ77/SBMA Modells, waren jedoch etwas schwächer ausgeprägt. Im Gegensatz dazu

fürten die Mutationen im ARQ77 zu einer Herabsetzung und Abschwächung der Aggregatbildung und Toxizität. Darüber hinaus erwiesen sich Inhibitoren, die zur Milderung der PolyQ Toxizität eingesetzt werden, als nicht sehr effektiv in der Hemmung der durch den ARQ22dm und AR77dm verursachten Toxizität. Somit wurden in dieser Arbeit zwei Aminosäurestellen identifiziert, welche die PolyQ-Toxizität des AR in gravierender Weise modulieren. Diese Ergebnisse können zukünftig genutzt werden, um zu klären, welche konformationellen Veränderungen im AR zur Aggregation führen und welche Aggregatformen für dessen toxische Wirkung verantwortlich sind.

## ABSTRACT

Nine neurodegenerative diseases are caused by polyglutamine (polyQ) tract amplification in different proteins. The cytotoxicity of each of these proteins is associated with a misfolding of the mutant protein, resulting in the subsequent alteration of cellular processes and interactions as well as the interrelated formation of insoluble aggregates and other conformationally toxic species. However, the diseases differ in their pathology and tissue specificity of action, which may be due to protein context/regions neighboring the polyQ stretch.

For the purpose of the studies presented in this work, the polyQ containing human androgen receptor (AR) that causes the disorder spinal and bulbar muscular atrophy (SBMA) was used to model polyQ toxicity. In previous investigations, two putative phosphorylation sites of the AR were identified, and it was demonstrated that mutation of these sites appeared to cause conformational change in the protein. Therefore, these N-terminal serine residues were exchanged to alanine in the wild type AR (ARQ22/ARQ22dm) or a receptor with an amplified polyQ stretch (ARQ77/ARQ77dm). These mutants were then used to characterize variance in types of aggregates and the associated toxic profiles due to the different protein conformations that arose from the serine mutations.

Evaluating changes in aggregation and toxicity in cultured cells and in a *Drosophila* model of SBMA, it was found that the effects of the conformational changes differed depending on the length of the polyQ stretch. Mutations in the ARQ22 resulted in a marked increase in aggregation as well as decreased survival rates and altered locomotion behavior in *Drosophila*. These results were similar but not as severe as the ARQ77/SBMA model. In quite the opposite manner, mutations in the ARQ77 caused a decrease in aggregation and a lessened toxic effect in *Drosophila*. Moreover, it was found that inhibitor compounds used to ameliorate polyQ toxicity were not as efficient in inhibiting the varied toxicities exhibited by both the ARQ22dm and ARQ77dm. Therefore, two distinct amino acid sites that profoundly modulate polyQ toxicity in the AR have been identified. These results can be further utilized to understand the conformational changes in the AR that lead to aggregation as well as the types of aggregates that lead to toxicity.



# TABLE OF CONTENTS

<b>Zusammenfassung</b>	i
<b>Abstract</b>	iii
<b>Table of contents</b>	v
<b>List of tables and figures</b>	x
<b>Abbreviations</b>	xii
<b>1.0 INTRODUCTION</b>	1
<b>1.1 CAG repeat / polyglutamine disorders</b>	1
1.1.1 The polyglutamine disorders are a subclass of the unstable trinucleotide repeat disorders	1
1.1.2 The common mechanism of misfolding and aggregation	2
1.1.2.1 The dynamic process of aggregation	4
1.1.2.2 The cellular localization of aggregate species	5
1.1.3 Distinguishing between the polyglutamine disorders – protein context	6
1.1.3.1 Fragments versus whole protein – caspase cleavage	6
1.1.3.2 Cis-acting modulators of polyglutamine toxicity	7
1.1.3.3 Phosphorylation of the polyglutamine proteins	9
<b>1.2 Spinal and bulbar muscular atrophy as a model for         polyglutamine disorders</b>	11
1.2.1 Kennedy’s Disease – the first polyQ disorder	11
1.2.2 The Androgen Receptor – a unique polyQ protein	13
1.2.2.1 Manipulating the AR in SBMA models – ligand binding, nuclear localization, and transcriptional activity	15
1.2.2.2 Manipulating the AR in SBMA models – mutations of sites of covalent modifications	16
1.2.2.3 Manipulating the AR in SBMA models – utilizing model system to full potential	18

<b>1.3 Animal models of the polyglutamine disorders</b>	19
1.3.1 Mouse models	19
1.3.1.1 Mouse models of SBMA	20
1.3.2 Invertebrate models – <i>Drosophila</i> and <i>C. elegans</i>	21
1.3.2.1 Modeling SBMA in <i>Drosophila</i>	24
<b>1.4 The path to therapy – therapeutic compounds for inhibiting polyglutamine toxicity</b>	26
1.4.1 SBMA specific therapies	26
1.4.2 General polyQ inhibitors	27
1.4.2.1 HDAC inhibitors	28
1.4.2.2 Melatonin as a candidate polyglutamine inhibitor	29
<b>1.5 Aims</b>	30
<b>2.0 MATERIALS AND METHODS</b>	31
<b>2.1 Materials</b>	31
2.1.1 Chemicals and consumables	31
2.1.2 Enzymes	32
2.1.3 Plasmids and constructs	33
2.1.4 Bacteria and eukaryotic cells	34
2.1.5 <i>Drosophila melanogaster</i> lines	35
2.1.6 Antibodies	35
<b>2.2 Methods</b>	37
2.2.1 DNA- cloning techniques	37
2.2.1.1 DNA fragmentation with restriction enzymes	37
2.2.1.2 Separation of DNA fragments by agarose gel electrophoresis	37
2.2.1.3 DNA extraction from agarose gel	38
2.2.1.4 Ligation of DNA fragments into plasmid vectors	38
2.2.1.5 Transformation of bacteria	38
2.2.2 Preparation of recombinant plasmid DNA from transformed bacteria	39
2.2.2.1 Mini-preparation of plasmid DNA	39

2.2.2.2 Maxi-preparation of plasmid DNA	39
2.2.2.3 Phenol/chloroform extraction of plasmid DNA	40
2.2.2.4 Ethanol precipitation of plasmid DNA	41
2.2.2.5 Determination of nucleic acid concentration	41
2.2.3 Cell culture	41
2.2.3.1 Passaging of cells	41
2.2.3.2 Freezing and thawing of cells	41
2.2.3.3 Transient transfections	42
2.2.3.4 Analysis of gene expression through luciferase assay test	42
2.2.3.5 Immunofluorescence	43
2.2.4 <i>Drosophila</i> methods	45
2.2.4.1 Culturing of fly stocks	45
2.2.4.2 Preparation of fly food	45
2.2.4.3 Injections for germ-line transformation	46
2.2.4.4 Genetic crosses	49
2.2.4.5 Scanning electron microscopy	49
2.2.4.6 Immunohistochemistry	50
2.2.4.7 Locomotion analysis	50
2.2.4.8 Survival analysis	51
2.2.5 Methods for work with protein from cells and <i>Drosophila</i>	52
2.2.5.1 Preparation of protein lysates	52
2.2.5.2 Determination of protein concentration	53
2.2.5.3 Separation of protein by SDS polyacrylamide gel electrophoresis	53
2.2.5.4 Western blotting	54
2.2.5.5 Stripping of Western blot membranes	55
2.2.5.6 Filter trap analysis of aggregates	55
2.2.5.7 Immunoprecipitation	56

<b>3.0 RESULTS</b>	58
<b>3.1 Mutation of distinct serine residues at the N-terminus of the AR</b>	58
3.1.1 Two possible phosphorylation sites shown <i>in vitro</i>	58
3.1.2 Conformational changes induced by substitution of serine residues 424 and 514	61
<b>3.2 Cell culture model used to investigate <i>in vivo</i> effects of serine site mutations</b>	63
3.2.1 Mutation of serines 424 and 514 residues affects nuclear localization and transactivation by the AR	63
3.2.1.1 Accumulation of AR in nucleus altered with AR mutants	64
3.2.1.2 Transactivation by wild type AR affected by polyQ stretch and serine mutation	66
3.2.2 Mutation of serines 424 and 514 affects the formation of intracellular inclusions by the AR	69
3.2.2.1 Inclusions differ in structural type and kinetics of formation	69
3.2.2.2 Both polyQ stretch and presence of serine mutations affect solubility of inclusions	71
3.2.2.3 1C2 antibody preferentially recognizes expanded polyQ region	74
<b>3.3 <i>Drosophila</i> model of SBMA used to analyze effects of serine site mutations</b>	75
3.3.1 Conformational changes induced by mutation of serines 424 and 514 in <i>Drosophila</i>	75
3.3.2 Mutations of serines 424 and 514 affect nuclear accumulation and aggregation of the AR in a fly model of SBMA	76
3.3.2.1 Mutant AR demonstrates altered nuclear localization in fly lines	77
3.3.2.2 Aggregation and 1C2 recognition in fly lines comparable to cell model	79
3.3.3 Neurodegeneration occurs in fly lines expressing AR with mutations at serine residues 424 and 514	80

3.3.4 Mutation of serine residues 424 and 514 affects locomotion and survival of fly lines expressing ARQ22 and ARQ77	81
3.3.4.1 Locomotion assay demonstrates subtle differences between AR mutant lines	82
3.3.4.2 Transgenic lines demonstrate changes in survival dependent upon serine site mutations	84
<b>3.4 Inhibitors of polyQ toxicity used to demonstrate differential toxicity due to serine site mutations</b>	86
3.4.1 Sodium butyrate and melatonin inhibit neurodegeneration in expanded polyQ fly lines	86
3.4.2 Serine mutations affect ability of sodium butyrate and melatonin to rescue polyQ phenotype in quantitative assays	88
3.4.2.1 Sodium butyrate and melatonin have varying effects on locomotion	88
3.4.2.2 Sodium butyrate and melatonin differ in ability to rescue AR mutants in survival analyses	91
<b>4.0 DISCUSSION</b>	93
<b>4.1 Alteration of specific residues affects AR conformation and provides model system for evaluating polyQ toxicity</b>	93
<b>4.2 Altered conformations differentially affect nuclear accumulation and transcriptional activity</b>	96
<b>4.3 Altered AR conformations yield characteristically diverse aggregates</b>	100
<b>4.4 Inhibitor compounds act on specific subsets of the varied AR toxicities</b>	103
<b>4.5 Final conclusions and outlook for AR-specific and general polyglutamine toxicity studies</b>	105
<b>REFERENCES</b>	107
<b>Curriculum Vitae</b>	129

## LIST OF TABLES AND FIGURES

### TABLES

<b>Table 1.1</b> The polyglutamine disorders	2
--	---

### FIGURES

<b>Figure 1.1</b> A proposed model of polyQ toxicity	3
<b>Figure 1.2</b> Neuronal regions affected in SBMA	12
<b>Figure 1.3</b> Androgen receptor structural domains and phosphorylation sites	15
<b>Figure 1.4</b> <i>Drosophila</i> model system	23
<b>Figure 3.1</b> <i>In vitro</i> MAP Kinase ERK2 phosphorylation of the region 360-536 of the AR reveals two possible phosphorylation sites	60
<b>Figure 3.2</b> Mutation of serine residues 424 and 514 leads to conformational changes in wild type AR and an AR with an extended polyQ stretch	62
<b>Figure 3.3</b> Kinetics of cytoplasmic-nuclear transport is altered after mutation of serine residues 424 and 514	65
<b>Figure 3.4</b> Transactivation by the AR is altered in mutant variants	67
<b>Figure 3.5</b> Mutation of serines 424 and 514 alters kinetics of formation of intracellular inclusions	70
<b>Figure 3.6</b> Differences in aggregate formation due to mutations at serine residues 424 and 514	73
<b>Figure 3.7</b> Serine mutations do not alter 1C2 activity	74
<b>Figure 3.8</b> Mutation of serine residues 424 and 514 leads to conformational changes in androgen receptors expressed in <i>Drosophila</i>	76
<b>Figure 3.9</b> Nuclear localization of AR in <i>Drosophila</i>	78
<b>Figure 3.10</b> Aggregation and conformation of AR in transgenic <i>Drosophila</i>	79
<b>Figure 3.11</b> Ligand-induced neurodegeneration of photoreceptor neurons in flies containing amplified polyQ stretch and serine 424/514 mutations	81
<b>Figure 3.12</b> Locomotive and behavioral analysis of transgenic wandering third-instar larvae	83

<b>Figure 3.13</b> Survival studies of larvae with ubiquitous neuronal expression of AR with amplified polyQ stretch and AR containing mutated serine sites	85
<b>Figure 3.14</b> Sodium butyrate and melatonin inhibit polyQ toxicity, but serine mutations alter effectivity	87
<b>Figure 3.15</b> Effects of sodium butyrate and melatonin on larval locomotion	90
<b>Figure 3.16</b> Effects of sodium butyrate an melatonin on survival	92

## ABBREVIATIONS

<b>A<math>\beta</math></b>	$\beta$ -amyloid
<b>AF</b>	AR transcriptional activation function
<b>APS</b>	ammonium persulfate
<b>AR</b>	androgen receptor
<b>ARE</b>	androgen responsive element
<b>AXH</b>	ataxin / HBP1
<b>BSA</b>	bovine serum albumin
<b>°C</b>	degrees Celcius
<b>cAMP</b>	cyclic adenosine monophosphate
<b>cDNA</b>	complementary DNA
<b>CHIP</b>	C-terminus of Hsc-70 interacting protein
<b>CBP</b>	CREB-binding protein
<b>CMV</b>	cytomegalovirus
<b>CNS</b>	central nervous system
<b>CREB</b>	cAMP-responsive element binding protein
<b>C-terminal</b>	carboxy terminal
<b>Cy</b>	Cyanine
<b>DBD</b>	DNA binding domain
<b>DHFR</b>	dihydrofolate reductase
<b>DHT</b>	5 $\alpha$ -dihydrotestosterone
<b>DMEM</b>	Dulbecco's modified eagle's medium
<b>DMSO</b>	dimethylsulfoxide
<b>DNA</b>	deoxyribonucleic acid
<b>DRPLA</b>	dentatorubral-pallidoluysian atrophy
<b>DTT</b>	dithiothreitol
<b>ECL</b>	enhanced chemiluminescence
<b>EDTA</b>	ethylenediaminetetraacetic acid
<b>ELAV</b>	embryonic lethal abnormal vision
<b>ERK</b>	extracellular signal-regulated protein kinase
<b>EtOH</b>	ethanol
<b>eg.</b>	<i>exempli gratia</i> , for instance
<b>et al.</b>	<i>et alii</i> , and others
<b>fC</b>	fibrous cytoplasmic
<b>FCS</b>	fetal calf serum

<b>Fig</b>	figure
<b>fN</b>	fibrous nuclear
<b>g</b>	gram
<b>gC</b>	globular cytoplasmic
<b>GMR</b>	glass multimer reporter
<b>gN</b>	globular nuclear
<b>h</b>	hour
<b>HAT</b>	histone acetyltransferase
<b>HBP1</b>	HMG box-containing protein-1
<b>HCL</b>	hydrogen chloride
<b>HDAC</b>	histone deacetylase
<b>HMG</b>	high mobility group
<b>HRP</b>	horseradish peroxidase
<b>Hsp</b>	heat shock protein
<b>htt</b>	huntingtin
<b>IGF-1</b>	insulin growth factor 1
<b>JNK</b>	c-Jun NH2-terminal kinase
<b>kDa</b>	kilodalton
<b>kcal</b>	kilocalorie
<b>l</b>	liter
<b>LBD</b>	ligand binding domain
<b>LM</b>	light microscopy
<b>MAPK</b>	mitogen-activated protein kinase
<b>μ</b>	micro-
<b>m</b>	milli-
<b>m</b>	meter
<b>M</b>	molar
<b>MBP</b>	myelin-based protein
<b>MeOH</b>	methanol
<b>min</b>	minute
<b>MMTV</b>	mammary tumor virus
<b>mol</b>	mole
<b>NLS</b>	nuclear localization signal
<b>NTD</b>	N-terminal domain
<b>N-terminal</b>	amino terminal
<b>n</b>	nano-
<b>OD</b>	optical density

<b>PAGE</b>	polyacrylamide gel electrophoresis
<b>PBS</b>	phosphate-buffered saline
<b>PBST</b>	PBS with tween
<b>PBT</b>	PBS with TritonX-100
<b>PI3K</b>	phosphoinositide 3-kinase
<b>polyQ</b>	polyglutamine
<b>PVDF</b>	polyvinylidene difluoride
<b>RNA</b>	ribonucleic acid
<b>rpm</b>	rotations per minute
<b>RT</b>	room temperature
<b>s</b>	second
<b>SAPK</b>	stress-activated kinase
<b>SAHA</b>	suberoylanilide hydroxamic acid
<b>SBMA</b>	spinal and bulbar muscular atrophy
<b>SCA</b>	spinocerebellar ataxia
<b>SDS</b>	sodiumdodecylsulfate
<b>SEM</b>	scanning electron microscopy
<b>TAE</b>	tri/acetate/EDTA electrophoresis buffer
<b>TEMED</b>	tetramethylethylenediamine
<b>Tris</b>	tris(hydroxymethyl)aminomethane
<b>UAS</b>	upstream activating sequence
<b>UV</b>	ultraviolet
<b>V</b>	volt
<b>VEGF</b>	vascular endothelial growth factor
<b>v/v</b>	volume on volume
<b>w/v</b>	weight on volume
<b>YAC</b>	yeast artificial chromosome

# 1.0 INTRODUCTION

## 1.1 CAG repeat / polyglutamine disorders

### 1.1.1 The polyglutamine disorders are a subclass of the unstable trinucleotide repeat diseases

Trinucleotide repeat sequences that code for runs of specific amino acids occur throughout the genomes of many different species. However, the human genome appears to have a unique mutational mechanism which causes instability of specific nucleotide repeats (Gatchel and Zoghbi, 2005). This distinct aspect of the human genome has resulted in a class of inherited neurodegenerative disorders known as the unstable trinucleotide repeat diseases. This class of disorders is marked by the phenomenon known as “anticipation”, the observation that the severity of a disorder increases while the age of onset decreases as the disorder is passed down through the generations. The diseases vary in that the underlying mechanisms of the disorders can be a loss or gain-of-function mutation at either the RNA or protein level (Riley and Orr, 2006). In this respect, the trinucleotide repeat diseases can be divided into two distinct categories. Disorders of the first category, Type I, are caused by the triplet repeat CAG, which is inserted into the open reading frame of a broadly expressed gene. The CAG nucleotide sequence encodes the amino acid glutamine, giving this subclass of unstable trinucleotide repeat diseases the title “polyglutamine (polyQ) disorders”. The category of Type II disorders is distinguished by typically longer trinucleotide repeat expansions that are contained in noncoding regions (Reddy and Housman, 1997).

The Type I polyQ disorders have only emerged as a class of inherited neurodegenerative disorders over the past 15 years (Zoghbi and Orr, 2000). This group includes Huntington’s disease, spinal and bulbar muscular atrophy (SBMA), dentatorubral-pallidoluysian atrophy (DRPLA), and a number of spinocerebellar ataxias (SCA) (Table 1.1). Each disease, taken on its own, is quite rare; however, as a group they now represent the most common form of inherited neurodegenerative disease (Riley and Orr, 2006). In all of the nine known diseases, the CAG repeat expansions that appear in

the respective unrelated disease proteins result in a characteristic pathogenesis of progressive neuronal loss. With the exception of spinocerebellar ataxia 6 (SCA6), the disease threshold of the polyQ length is 35-40 amino acids. Beyond this threshold, an inverse relationship exists between the length of the CAG repeat region and the age of onset of the neuronal loss and clinical symptoms. The clinical manifestations usually commence in adulthood and progress over 10 to 30 years to an ultimately fatal state.

Disease	Protein	Normal CAG length	Pathological CAG length	Neuronal areas affected	Clinical manifestation
Huntington's disease	Huntingtin	11-34	40-120	corpus striatum, cerebral cortex	chorea, impairment of cognitive function, emotional disturbance
Dentatorubral-pallidolusian atrophy (Smith's disease)	Atrophin1	7-35	49-88	globus pallidus, dentatorubral and subthalamic nucleus	choreoathetosis, ataxia, dementia, myoclonus and epilepsy
Spinobulbar muscular atrophy (Kennedy's disease)	Androgen receptor	9-38	40-62	anterior horn cells, bulbar neurons, dorsal root ganglia	muscle weakness, atrophy and fasciculations
Spinocerebellar ataxia type 1	Ataxin-1	25-36	41-81	cerebellar cortex, dentate nucleus, brainstem	ataxia, dysarthria, dysmetria and decreased vibration sense
Spinocerebellar ataxia type 2	Ataxin-2	15-24	35-59	cerebellum, pontine nuclei, substantia nigra	ataxia, dysarthria
Spinocerebellar ataxia type 3 (Machado-Joseph disease)	Ataxin-3	13-36	62-82	substantia nigra, globus pallidus, pontine nucleus, cerebellar cortex	ataxia, dystonia and ophthalmoplegia
Spinocerebellar ataxia type 6	Ataxin-6 / CACAA1A	4-16	21-27	cerebellum, brainstem	ataxia, dysarthria, nystagmus and vibratory loss
Spinocerebellar ataxia type 7	Ataxin-7	4-19	37-306	cerebellum, inferior olive, dentate nucleus	cerebellar ataxia, dysarthria and dysphagia, cone-rod and retinal dystrophy
Spinocerebellar ataxia type 17 (TATA-binding protein disease)	TATA-BP	25-42	47-63	cerebellum, caudate nucleus, putamen	gait ataxia, dementia, bradykinesia, dysmetria

**Table 1.1 The polyglutamine disorders**, adapted from Reddy and Housman, 1997

### 1.1.2 The common mechanism of misfolding and aggregation

Despite differences that exist between the polyQ disorders, specifically in disease symptoms and patterning of neuronal degeneration, much research has argued that there must be a common underlying pathogenic mechanism resulting from the presence of the polyQ tract. Research tends to agree on a model where one aspect of this mechanism is

the adoption of an abnormal conformation by the mutant protein. A proposed basic model by Paulson et al., demonstrates how misfolding of an expanded polyQ stretch-containing protein could lead to the neurodegeneration seen in the polyQ disorders (Fig. 1.1) (Paulson et al., 2000). In this model, misfolding of the protein disrupts normal protein function, alters protein-protein interactions, and upsets the balance of protein homeostasis.

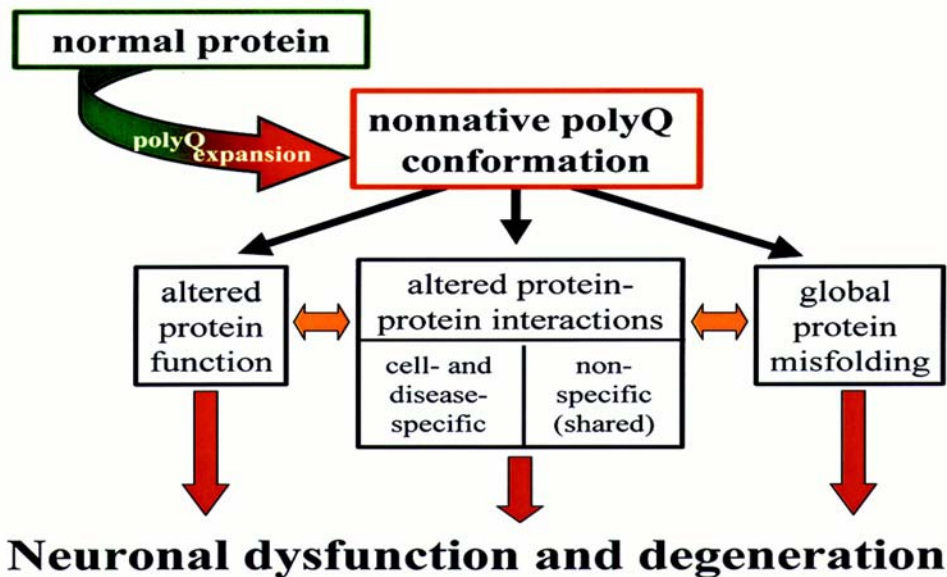


Figure 1.1 A proposed model of polyQ toxicity (Paulson et al., 2002)

Although scientists tend to study the disorders individually, there is an expectation that an advance in one of the diseases will provide relevant understanding for the group as a whole. This theory has proven true in the case of the misfolding of the polyQ proteins. An important consequence of the misfolding process is the accumulation of the mutant polyQ, resulting in protein aggregates. Deposits of the aberrant huntingtin (htt) protein, which causes Huntington’s disease, were first seen in transgenic mice (Davies et al., 1997) and human patients (DiFiglia et al., 1997) in 1997. After this breakthrough observation, aggregates and inclusions were eventually identified in all of the other polyQ disorders; and aggregation quickly became the prominent pathological hallmark of the group of disorders as well as a main focus of research (Ross, 1997; Davies et al., 1999). However, many questions soon arose around the topic of

aggregation. Were aggregated deposits of polyQ protein a cause of toxicity or just a byproduct? Or going, a step further, were aggregates actually cytoprotective? In the literature, one could find support for each of these arguments. One tempting theory is to link each of these schools of thought by looking at aggregation as a dynamic process where earlier steps in the misfolding process are more directly linked to toxicity and the final physical state is a way of sequestering the toxic protein (Ross and Poirier, 2004).

#### ***1.1.2.1 The dynamic process of aggregation***

When the story of polyQ aggregation first began to take shape, aggregates were described simply as large and poorly soluble structures. But further investigation found them to have an extensive  $\beta$ -pleated sheet structure similar to the amyloid fibril structure of protein aggregates formed in other neurodegenerative diseases such as Alzheimer's and Parkinson's (Davies et al., 1997; Scherzinger et al., 1999). Amyloid fibrils are defined as filamentous structures with a width of approximately 10 nm and a length of 0.1-10  $\mu\text{m}$  (Sunde and Blake, 1998). The particular amyloid fibril indicated in Alzheimer's disease is known as the  $\beta$ -amyloid ( $A\beta$ ) peptide, and antibodies specific for the amyloid fibril conformation of the  $A\beta$  peptide have been shown to recognize aggregate structures derived from the polyQ proteins (O'Nuallain and Wetzel, 2002).

In the search to unravel the mechanism of the misfolding process that starts from the native polyQ protein and progresses to the amyloid fibril conformation, the importance of intermediates in the aggregation process has become increasingly apparent. These amyloidal precursors can be grouped into a category of structures known as "soluble oligomeric intermediates". These structures are larger than dimers and can have a globular/micelle formation or a fibril-like morphology. Those with the latter structure type are referred to as  $A\beta$  protofibrils (Lambert et al., 1998; Ross and Poirier, 2004). Protofibrils may be able to amass to become larger fiber-like structures, which then form the final physical state of the inclusion (Ross and Poirier, 2004).

As knowledge of the aggregation process has advanced, researchers looking to the soluble oligomeric intermediates as the toxic species have honed in further on the specific subtypes. The spherical form of soluble oligomers were first represented to be the toxic species of amyloid-like  $A\beta$  peptide in Alzheimer's disease and have now also been

shown to exist in other amyloidogenic proteins and peptides, including expanded polyQ containing proteins (Kayed et al., 2003; Wacker et al., 2004). A study of a protein containing a polyQ stretch of 91 amino acids identified globular aggregates 4-50 nm in diameter as the principal cytotoxic species in protein conformational diseases (Mukai et al., 2005). In general, globules and not fibrillar conformations of the polyQ stretch amplifications have been shown to be sufficient to induce cellular pathophysiology (Quist et al., 2005).

### ***1.1.2.2 The cellular localization of aggregate species***

Yet another aspect of aggregation that is still under debate is the effect of nuclear versus cytoplasmic aggregates on the neuropathology of the polyQ disorders. The first deposits of the htt protein described in transgenic mice and patients in 1997 were of nuclear localization (Davies et al., 1997; DiFiglia et al., 1997). Since that time, much data has accumulated linking such nuclear-localized inclusions with polyQ toxicity. Most of these findings have stemmed from studies that manipulated to which cellular compartment the mutant polyQ proteins were directed. Cytoplasmic localization of the nuclear protein ataxin1 reduced toxicity and aggregate formation in a mouse model of SCA1 (Klement et al., 1998) while forced nuclear localization of an N-terminal fragment of the usually cytoplasmic htt protein resulted in an increase in toxicity (Peters et al., 1999; Schilling et al., 2004). Furthermore, nuclear localization of the androgen receptor (AR) is required for toxicity in SBMA models (Takeyama et al., 2002; Walcott and Merry, 2002).

Varying evidence exists in the literature regarding the role of cytoplasmic aggregates in polyQ toxicity. In a *Drosophila* model of Huntington's, accumulation of aggregates in the cytoplasm blocked axonal transport (Lee et al., 2004). Cytoplasmic htt aggregates were also shown to interfere with the normal mobility and trafficking of mitochondria (Chang et al., 2006). In the case of SBMA, aggregates in the cytoplasm have been suggested to act as protective "sinks", trapping the polyQ until it can be degraded through proteasomal pathways (Rusmini et al., 2007). One theory regarding cytoplasmic aggregation is that autophagy is more efficient in the cytoplasm, thus the nucleus is the more vulnerable of the cellular compartments to polyQ toxicity (Iwata et

al., 2005). Another possibility is that localization of toxic aggregate species may vary between the disorders. Therefore, in the search for common mechanisms, researchers must still keep the individual proteins in mind.

### **1.1.3 Distinguishing between the polyglutamine disorders - protein context**

When comparing the polyQ disorders, one must take into consideration that other than the polyQ tract, none of the disease proteins share any sequence similarity. Therefore, as witnessed by the commonalities among the polyQ diseases, the glutamine expansion itself plays a major role in aggregation formation and the correlated pathogenesis. However, the affected proteins must also strongly modulate the particular pathogenic mechanisms for the individual disorders. The greatest evidence for the involvement of other protein sequences in polyQ toxicity is the specificity of the neuronal subsets affected in each of the diseases (Table 1.1). For example in SCA1, cerebellar Purkinje cells are the prominent site of pathology (Genis et al., 1995; Robitaille et al., 1995) whereas in SBMA it is the spinal motor neurons that are lost (Kennedy et al., 1968). Hence much of the current research on the topic has focused on regions outside of the polyQ stretch, examining how specific sequences and domains as well as any resultant covalent modifications of the proteins affect the disease processes. As first predicted, some of these studies have resulted in common themes for all of the polyQ disorders, but some are perhaps relevant only to the individual diseases and cell-type specificity.

#### ***1.1.3.1 Fragments versus whole protein- caspase cleavage***

The early stages of research that noted the importance of the influence of outside sequences on polyQ pathology began with the topic of caspase cleavage. At least seven of the nine reported polyQ proteins are substrates for caspases, the cysteine protease cell death “executioners” (Ellerby et al., 1999a; Young et al., 2007). Initial studies found that regionally specific caspase cleavage of htt formed toxic, truncated fragments and was imperative for aggregation and cytotoxicity (Wellington et al., 1998; Ellerby et al., 1999a; Wellington et al., 2000). Similar findings were also made for the AR (Ellerby et al., 1999b) and atrophin1 (Ellerby et al., 1999a). This led to the conclusion that an

expanded glutamine peptide isolated from an intact protein is more toxic than when it is within the intact protein, arguing that sequences outside the glutamine stretch may dampen the deleterious effect of the expanded polyglutamine tract (Wellington and Hayden, 2000; Zoghbi and Botas, 2002).

However, animal models utilizing truncated fragments have not been able to replicate some key features of the disorders. For example, a mouse model expressing an amino terminal human htt with an expanded polyQ of 120 showed widespread htt inclusions but no clinical evidence of neuronal dysfunction or degeneration. In contrast, a mouse expressing the full-length htt protein with the same polyQ length and the same level of huntingtin expression formed inclusions that were toxic (Slow et al., 2005). Expression of a full-length AR in mouse models is also imperative for replicating the neuronal degeneration seen in SBMA (Adachi et al., 2001; McManamny et al., 2002). These models provide evidence for the complex nature of the polyQ pathogenic mechanisms. Although N-terminal fragments produced by caspase cleavage of the mutant proteins appear to be a prerequisite for toxicity and to represent another common step in the pathogenesis of the protein aggregation diseases (Tarlac and Storey, 2003), their presence alone is not sufficient to entirely recapitulate the diseases in animal models. Thus, researchers have delved further into investigating sequences neighboring the polyQ stretches in order to determine their role in diminishing or enhancing the toxicity seen in human patients.

#### ***1.1.3.2 Cis-acting modulators of polyglutamine toxicity***

Apart from the generation of toxic protein fragments, scientists are finding that other regions such as particular domains, other amino acid runs, or even unspecified sequences also contribute to toxicity in an undefined manner. One of the first studies to provide evidence that a region other than the polyQ influenced disease pathology demonstrated that the AXH domain of ataxin1 participated in protein aggregation. The AXH domain (ataxin1/HBP1) is similar in structure to the high mobility group (HMG) box transcription factor HBP1 (HMG box-containing protein-1) and plays a role in transcriptional repression of ataxin1. Interestingly, this region underwent a  $\beta$ -enriched structural conformation when isolated *in vitro*. Moreover, the study found that deletion of

this site or replacement with its HBP1 homolog significantly reduced aggregation in an SCA1 cell model (de Chiara et al., 2005).

The effect of other amino acid runs on polyQ toxicity has also very recently come under investigation. The htt protein, for example, contains a proline-rich region immediately following the polyQ expansion. When wild-type or mutant derivatives of htt are expressed in a yeast system, neither protein form results in cell death. However, deletion of the proline-region was found to unmask the toxicity of htt with an expanded polyQ region (Dehay and Bertolotti, 2006). A similar study found that a FLAG-epitope (DYKDDDK) at the amino or carboxy terminus of the htt exon I unmasked the toxicity of an otherwise benign polyQ protein, whereas the endogenous polyproline region carboxy-terminal to the amplified polyQ tract was demonstrated to convert toxic proteins into non-toxic ones (Duennwald et al., 2006). Experimentally poly- or oligo-proline tracts placed at the carboxy-termini but not the amino-terminal region of polyQ polypeptides change the conformation and decrease the rate of aggregate formation of these proteins (Bhattacharyya et al., 2006). Proline regions are also found at the carboxy-termini of the polyQ regions in atrophin1 and the AR. While the proline region of atrophin1 has been found to be involved in the binding of interaction partners in a polyQ dependent manner (Okamura-Oho et al., 2003), any effects of the small proline stretch of the AR on polyQ toxicity have yet to be investigated.

An example of undefined outside sequences influencing polyQ toxicity has been demonstrated by the ability of the co-chaperone CHIP (C-terminus of Hsc-70 interacting protein) to protect against polyQ-induced neurodegeneration. CHIP is an E3 ligase that connects chaperones to the ubiquitin-proteasome machinery, which is responsible for protein quality control by degrading misfolded proteins such as the polyQ proteins and aiding in the refolding of nonnative proteins. CHIP has been shown to interact with the polyQ expanded mutants of ataxin3, htt (Jana et al., 2005), ataxin1, and most recently the AR (Adachi et al., 2007). Overexpression of CHIP was shown to ameliorate toxicity in a *Drosophila* model of SCA1 and also in a “protein context” manner. The researchers found that CHIP overexpression had no effect on an isolated polyQ tract of 127 but was again effective when the polyQ tract was in the context of a htt backbone (Al-Ramahi et

al., 2006). Therefore, it is again seen that the surrounding framework is crucial for polyQ pathology and the modulation of that pathology.

### ***1.1.3.3 Phosphorylation of the polyglutamine proteins***

Moving away from the discussion of specified regions and the protein backbones as a whole, recently mutations of specific amino acids outside the polyQ stretches that are sites for protein modifications have been shown to positively or negatively influence aggregate formation and toxicity of proteins such as the AR and ataxin1 (Emamian et al., 2003; Thomas et al., 2004). The main focus of these studies has been the phosphorylation of the various polyQ disease-causing proteins. To date, several phosphorylation pathways including the insulin growth factor-1/Akt (IGF-1/Akt) pathway and the mitogen-activated protein kinase (MAPK) pathways have been implicated in the polyQ disease mechanisms. Again the htt protein was one of the first to be shown to be directly affected by phosphorylation, in this case by the serine/threonine pro-survival kinase Akt at htt serine 421. Akt is activated downstream of the IGF-1 receptor and phosphoinositide 3-kinase (PI3K) in the IGF-1/Akt signaling pathway, a stimulator of cell growth and proliferation as well as an inhibitor of apoptosis. Activation of the IGF-1/Akt pathway was shown to result in phosphorylation of htt, which was essential for the resultant neuroprotective effects, increased cell survival, and decrease in intranuclear inclusions (Humbert et al., 2002). Positive effects of activating the IGF-1 pathway in cell models of SBMA have also been recently elucidated (Palazzolo et al., 2007). However, activation of Akt has been found to have quite the opposite effect on ataxin1, the protein responsible for SCA1. Researchers have found that Akt phosphorylation of ataxin1 serine 776 is an important step in the pathogenesis of the protein containing a polyQ expansion (Chen et al., 2003; Emamian et al., 2003).

The MAPK pathways have not only been shown to direct phosphorylation of some of the polyQ proteins but also in turn to be upregulated by polyQ expanded mutant forms of the same proteins (LaFevre-Bernt and Ellerby, 2003; Apostol et al., 2006; Schilling et al., 2006). The superfamily of MAPKs comprises three major signaling pathways: the extracellular signal-regulated protein kinase 1 and 2 (ERK1/2) cascade, the c-Jun NH2-terminal kinase or stress-activated kinase (JNK/SAPK) cascade, and the p38

family of kinases cascade (reviewed in (Robinson and Cobb, 1997). ERK1/2 signaling, which preferentially regulates cell growth and differentiation, is affected by both mutant htt and mutant AR. Activation of the ERK1/2 pathway by an AR containing an expanded polyQ region and a coupled phosphorylation at the N-terminus of the AR has been reported to be required for polyQ toxicity (LaFevre-Bernt and Ellerby, 2003). In contrast, activation of the ERK1/2 pathway by mutant htt is associated with cell survival. Instead, in the case of htt with a pathological polyQ stretch, it is the activation of the JNK/SAPK pathway that functions mainly in response to stress signals from inflammation or apoptosis that is associated with pathogenesis (Apostol et al., 2006). Although three ERK1 consensus sites have been identified in htt (Schilling et al., 2006), the effect of phosphorylation of these specific sites is unknown. In this same vein there are many phosphorylation sites and other sites of covalent modification whose influence on the various polyQ proteins has yet to be fully described. In a review on the role of protein context in the polyQ disorders, it was suggested that “all roads lead to a critical serine phosphorylation” (La Spada and Taylor, 2003). This statement accurately summarizes the idea that although understanding individual protein context is imperative to understanding the pathogenic mechanisms of the separate polyQ diseases, unifying themes can be extracted from very specific studies.

## **1.2 Spinal and bulbar muscular atrophy as a model for polyglutamine disorders**

As can be witnessed by many of the aforementioned studies regarding aggregation and protein context, Huntington's disease is the most common as well the most actively studied of the rare polyQ disorders. Therefore, many of the initial findings that are relevant to all of the polyQ diseases were first found in models of Huntington's. Despite this fact, using Huntington's as a polyQ disease model has its disadvantages. One major drawback is the lack of knowledge pertaining to the functional characterization of the wild type htt protein. Research has found roles for htt as an antiapoptotic protein (Leavitt et al., 2001) as well as a transcription factor (Gauthier et al., 2004), but many gaps have yet to be filled, especially in regards to how an expanded polyQ region alters wild type huntingtin function. A lack of information pertaining to the native function of the proteins involved in the spinocerebellar ataxias also exists in the polyQ field. The one true exception to this scenario is the AR whose expanded polyQ stretch results in SBMA. The well-characterized properties of the AR make SBMA an attractive disease to study as a model for the polyQ disorders, and thus the particulars of SBMA and its associated protein will be discussed further in the following sections.

### **1.2.1 Kennedy's Disease- the first polyQ disorder**

X-linked spinal and bulbar muscular atrophy (SBMA), or Kennedy's disease, was first described in 1966 in a scientific abstract by William R. Kennedy, M.D. Two years later in 1968, a full report followed describing a sex-linked recessive trait that resulted in "progressive proximal spinal and bulbar muscular atrophy of late onset" (Kennedy et al., 1968). For the next 20 years, any information regarding the disease described as a slowly progressive motor neuronopathy came from clinical studies of the rare patients. The sex-linked aspect of the disease meant that only males were afflicted, and the late-onset manifestation of symptoms was typically between the ages of 30-50 years. Patients were found to exhibit proximal and facial-bulbar muscle weakness, atrophy, and consistent fasciculation (or muscle "twitching") occurring especially about the lips, chin, and tongue. Hand tremors and debilitating muscle cramps were also reported (Stefanis et al., 1975). Other manifestations were present in the form of endocrine abnormalities, which

included gynaecomastia, impaired spermatogenesis, reduced fertility, and testicular atrophy (Arbizu et al., 1983). In post-mortem examinations, it was revealed that the number of motor neurons in the spinal anterior horns as well as the facial and hypoglossal nuclei were severely reduced, and those that remained were atrophic (Fig 1.2) (Harding et al., 1982).

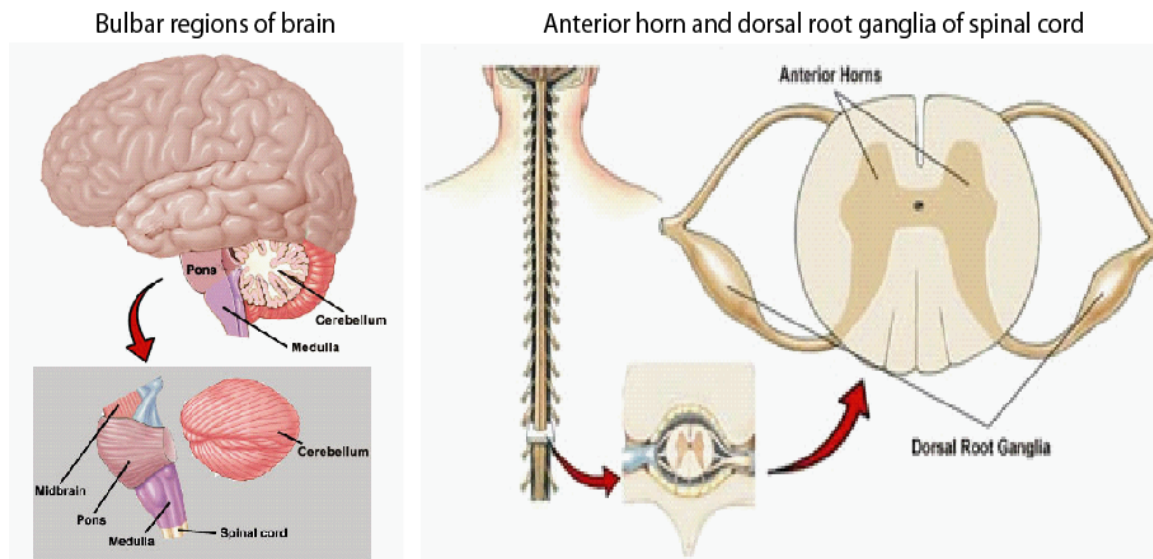


**Figure 1.2 Neuronal regions affected in SBMA** from <http://www.stanford.edu/group/hopes/rltdsci/trinuc>

Finally in 1991 a breakthrough in the research of patient samples occurred, identifying the cause of the disease as a CAG-repeat expansion in the first exon of the androgen receptor (AR) gene located on the long arm of chromosome Xq13-21 (La Spada et al., 1991). Disease onset was found to occur when this CAG stretch contained more than 40 glutamine residues as opposed to the normal range of 9 to 34 glutamine residues. This was the first case in which a disease had been linked to an expansion mutation of a polyglutamine region, and it kick-started basic research of SBMA. The novel mutational discovery also soon led to the identification of the genes for Huntington’s and SCA1 (Banfi et al., 1994; Cha and Dure, 1994), resulting in a full explosion of basic science research for the newly designated “polyQ disorders”. Especially in this early period, as scientists were first beginning to analyze the neuronal dysfunction and protein aggregation associated with the polyQ proteins, studying SBMA was gainful due to the fact that: (1) the wild type AR was a protein whose physiological

functions had been extensively researched, and (2) functional properties of the AR allowed for easy manipulation of neurotoxicity in a laboratory setting.

### **1.2.2 The Androgen Receptor – a unique polyQ protein**

A member of the nuclear receptor superfamily, the AR is a ligand-inducible transcription factor that falls into the categorical subgroup of the steroid/thyroid hormone receptor family (Mangelsdorf et al., 1995). The role of the AR is to mediate the action of the sex steroid hormones known as androgens. Androgens play critical roles in the sexual development of both males and females but are especially crucial for the male phenotype as key players in male sexual differentiation, development and maintenance of male secondary characteristics, and the initiation and maintenance of spermatogenesis (George and Wilson, 1994). Androgens act on a wide range of target tissues that include those closely associated with sexual development as well as the vascular system, central nervous system, gastrointestinal tract, immune system, skin, kidney, and lung (Wierman, 2007). In addition, androgens are central in the development of age-related pathologies in men such as development of benign prostate hyperplasia and prostate cancer (Dehm and Tindall, 2007). Onset of SBMA can also be counted among these age-related pathophysiological events. In fact, the higher levels of circulating androgens in men is a central reason as to why females that are homozygous for SBMA display little to no symptoms. The prominent androgens in the aforementioned developments are testosterone and its metabolite 5 $\alpha$ -dihydrotestosterone (DHT). DHT is produced from testosterone in the male urogenital tract and peripheral tissues by two isoenzymes of 5 $\alpha$ -reductase (Russell and Wilson, 1994). An increased binding affinity for the AR makes DHT the more potent of the two androgens.

In order to understand the action of androgens such as DHT, the structure of the AR must be taken into consideration (Fig. 1.3). The 110 kDa AR protein is structurally similar to its steroid receptor family members, which include the glucocorticoid, estrogen, mineralocorticoid, and progestin receptors. The modular structure of the AR includes a variable N-terminal domain (NTD) harboring AR transcriptional activation function (AF-1), a highly conserved central DNA binding domain (DBD), a short hinge region, and a highly conserved C-terminus containing the AR ligand binding domain

(LBD) and AF-2 coactivator binding surface (Bain et al., 2007). Other characteristic features include three homopolymer tracts of glutamine, glycine, and proline in the NTD and a critical nuclear localization signal (NLS) located at the junction of the DBD and hinge regions. Three dimensional structures of peptides from the LBD, which consists of up to 12  $\alpha$  helices that form a pocket for ligand capture, and AF-2 regions as well as the AR DBD have been resolved using X-ray crystallography (Matias et al., 2000). The AR N-terminal domain, which encompasses the AF-1 as well as the infamous polyQ region, is unstructured in solution and thus has been resistant to structural determination by crystallization.

In the classical model of AR subcellular dynamics, also referred to as the genomic action of the androgen receptor, the unliganded AR is confined in a multi-heteromeric inactive complex in the cytoplasm. This complex consists of members of the heat shock family of chaperones such as Hsp70 and Hsp90 and high molecular weight immunophilins and aids in giving the AR a ligand accessible conformation (Pratt and Toft, 1997). Upon binding of a ligand such as DHT, the last  $\alpha$  helix of the LBD shifts to provide a key interaction interface. The composition of the AR/chaperone complex is also altered, allowing exposure of the NLS and subsequent translocation to the nucleus. There it interacts with DNA as a homodimer at androgen response elements (AREs) found in the regulatory regions of target genes. The resulting complex is able to recruit coactivators through the ligand-dependent transactivation function (AF-2) of the LBD and the autonomous activation function (AF-1) of the NTD and thus activate transcription of the specific target genes (Zhou et al., 1994; Jenster, 1998; Dehm and Tindall, 2007). The amino acid repeat regions of the NTD have additionally been reported to affect this process. AR transcriptional activity has been shown to be inversely correlated with the length of the polyQ stretch *in vitro* (Kazemi-Esfarjani et al., 1995) while complete deletion of the polyglycine region severely hampers transactivation activity (Gao et al., 1996). Outside of its transcription factor status, the AR may also regulate events in the cytoplasm by participating in rapid/non-genomic signaling cascades (Freeman et al., 2005). However, it is the binding of ligand and nuclear translocation that is the essential method of action for SBMA pathology; and therefore the AR is unique among the polyQ

proteins in its dependence on ligand activation (Takeyama et al., 2002; Chevalier-Larsen et al., 2004; Katsuno et al., 2004).

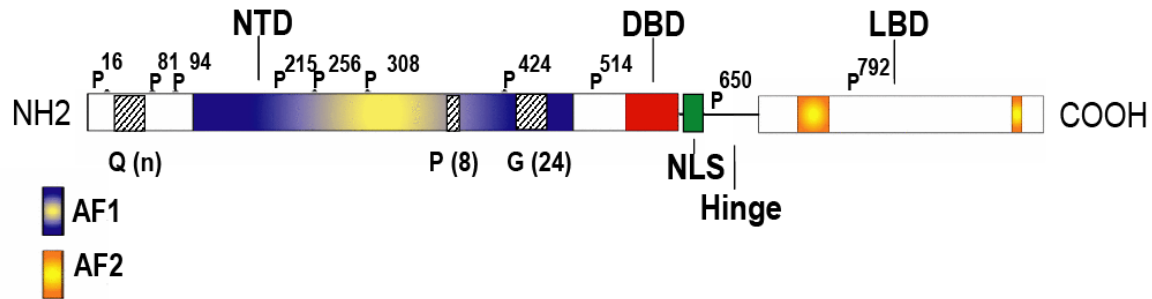


Figure 1.3 Androgen receptor structural domains and phosphorylation sites

### 1.2.2.1 Manipulating the AR in SBMA models – ligand binding, nuclear localization, and transcriptional activity

The ligand inducible properties of the AR have been used advantageously to study the specific disease mechanisms of SBMA as well as general toxic properties that are applicable for all of the polyQ disorders. With the ability to modulate the introduction of ligand to cell or animal model systems, induction of aggregation and toxicity and detrimental effects on particular cellular processes have been able to be examined in a controlled manner. For example, researchers have utilized androgen agonists and antagonists in conjunction with AR constructs of specific domains to determine the importance of nuclear translocation in the onset of SBMA. Using a *Drosophila* model of SBMA, one group found that using androgen antagonists such as hydroxyflutamide and bicalutamide that suppress the transactivation function of the mutant AR but still allow nuclear translocation resulted in an aggravated phenotype (Takeyama et al., 2002). In addition, an N-terminal fragment of the AR containing an expanded polyQ stretch and NLS region but no DBD or LBD was sufficient to induce neurodegeneration in the fly model. These results suggested that the presence of the polyQ AR in the nucleus is a major factor for induction of toxicity. As nuclear localization is also a common theme among the polyQ disorders, having a clearly defined scenario for the AR also makes

SBMA a good model to examine the molecular mechanisms of polyQ toxicity in the nucleus.

Once a polyQ protein such as the AR is in the nucleus, one of the logical candidates for the progression of polyQ toxicity is an interference with gene transcription. In fact, a functional commonality of the polyQ proteins is that each functions at some level of transcriptional regulation, either directly or indirectly through intracellular signaling (Truant et al., 2007). Again, because the AR is itself a transcription factor whose presence in the nucleus can be modulated by hormone induction, SBMA models are ideal to study abnormal interactions with coactivator or corepressor molecules. The most obvious change for the polyQ expanded AR is its own suppressed transcriptional activity, as previously mentioned, that includes altered mediation by coactivators such as members of the group of the 160-kDa nuclear receptor (p160) coactivators and ARA24 (Hsiao et al., 1999; Irvine et al., 2000). However, the presence of the polyQ stretch also alters other transcriptional pathways. One such abnormal interaction is the sequestration into nuclear inclusions of cAMP-responsive element binding protein (CREB)-binding protein (CBP), a transcriptional coactivator that is involved in numerous signaling cascades (McCampbell et al., 2000). This sequestration, which interferes with CREB and CBP-dependent transcription, was first discovered in SBMA and was subsequently found to apply to most if not all of the polyQ disorders (Steffan et al., 2000; Nucifora et al., 2001; Stenoien et al., 2002). Another change in interaction has been reported to occur in relation to AR/c-Jun mediated transcription. The AR and c-Jun interact normally to regulate each other's transcriptional activity, and the polyQ stretch disrupts this interaction (Grierson et al., 1999). c-Jun acts as a mediator of cell survival and apoptosis and is part of the c-Jun NH2-terminal kinase (JNK) pathway, which responds to cellular stress and has also been associated with Huntington's, SCA7, and DRPLA (Liu, 1998; Okamura-Oho et al., 2003; Merienne et al., 2007).

#### ***1.2.2.2 Manipulating the AR in SBMA models – mutations of sites of covalent modifications***

Between the events of ligand binding of the AR and activation of transcription of target genes, several post-translational modifications such as acetylation and

phosphorylation of the receptor occur (Fu et al., 2000; Gioeli et al., 2002; Lieberman et al., 2002). As previously discussed, covalent modifications of the polyQ proteins have been shown to have profound effects on the pathogenic mechanisms of the polyQ disorders. SBMA is no exception; and moreover, the AR has the distinct advantage over the other polyQ proteins in that many of these acetylation and phosphorylation sites are already well characterized in the wild type context of the protein. An example is given by the ligand-dependent acetylation of the AR at lysines 630, 632, and 633. Acetylation of these sites, which are located next to the NLS on the carboxy-terminal side, has been associated with enhanced p300 coactivator binding and the regulation of transcription of certain target gene promoters (Fu et al., 2003) Mutation of these sites to alanine in the wild type AR resulted in disruption of ligand-dependent nuclear translocation, a marked increase in aggregation upon hormone treatment, and inhibition of proteasome function (Thomas et al., 2004). Each of these features was reminiscent of the polyQ expanded AR, suggesting that decreased acetylation of the AR containing a glutamine expansion may contribute to SBMA pathology.

The AR has been shown to be a phosphoprotein whose phosphorylation status changes after exposure to androgens (van Laar et al., 1990; van Laar et al., 1991). Compounded with the fact that most of these phosphorylation sites are located in the polyQ-containing NTD (Fig 1.2), it seems intuitive that phosphorylation could play an important role in the molecular mechanisms of SBMA. Specific phosphorylation sites that have been utilized in mutational studies thus far include Akt phosphorylation consensus sites at serine 215 and 792 (Palazzolo et al., 2007) as well as a MAPK phosphorylation consensus site at serine 514 (LaFevre-Bernt and Ellerby, 2003). In the case of AR phosphorylation due to the IGF-1/Akt pathway, overexpression of Akt has been shown to result in a destabilization of the receptor (Lin et al., 2002); and more specifically, Akt phosphorylation at serine 215 was previously shown to be associated with an inhibition of wild type AR mediated transcription (Taneja et al., 2005). In a recent study, Akt was also shown to phosphorylate the AR containing a polyQ expansion. Furthermore, mimicking phosphorylation at Akt serine sites 215 and 792 by substitution with aspartate residues resulted in reduced ligand-binding, nuclear translocation, and transcriptional activity of both the wild type and mutant AR. These effects also

corresponded with a reduced toxicity for the AR containing the polyQ expansion, suggesting that the IGF-1/Akt signaling pathway could be utilized for developing therapeutic targets. As briefly mentioned in an earlier section, the ERK1/2 pathway has also been implicated in SBMA. Disruption of ERK1/2 signaling using a specific inhibitor was found to reduce polyglutamine cell death and was also correlated with a change in AR phosphorylation (LaFevre-Bernt and Ellerby, 2003). This alteration in phosphorylation status was contributed to a change in phosphorylation at the MAPK consensus site serine 514. Substitution of this serine with an alanine residue again resulted in a reduction of polyQ toxicity as well as a reduction in associated caspase cleavage products. Unlike the serine 215 and 792 sites, how the phosphorylation status at serine 514 effects the wild type AR was not investigated.

### ***1.2.2.3 Manipulating the AR in SBMA models – utilizing model system to full potential***

Current research has yielded several separate studies for the individual polyQ disorders that have revealed the significance of protein context and have demonstrated that manipulating neighboring sequences or domains of the polyQ proteins can greatly affect toxicity. Unfortunately, many of these studies have been narrowly focused and have not thoroughly examined effects on both wild type and polyQ expanded proteins. Studies involving covalent modifications have also tended to focus on global changes in aggregation and toxicity, without further classification of different types of aggregate species. Additionally, all of these studies were carried out in cell culture systems and have not been confirmed in animal models. In the case of the AR, where many sites of covalent modifications have yet to be characterized in the context of the polyQ stretch, there are several uninvestigated prospects that could yield much insight into the mechanisms of SBMA and the polyQ disorders as a group. These include: (1) investigation of characterized sites of covalent modification in wild type and polyQ backgrounds, (2) careful consideration to differences in aggregate species and toxicity, and (3) utilization of animal models.

### **1.3 Animal models of the polyglutamine disorders**

Mouse and *Drosophila* models have now been created for most of the polyQ disorders. While these models have not been utilized to examine some of the subtleties involved in the importance of protein context for the polyQ disorders, they have enabled the field to advance in areas such as interacting partners that convey selective neuronal vulnerability (Sopher et al., 2004), characterization of toxic aggregate species (Li et al., 2007), and potential therapeutic strategies (Pandey et al., 2007). However, recapitulating certain key aspects of the diseases has proven challenging. In the next sections, the difficulties, advantages, and disadvantages of the different types of models will be discussed with an emphasis on models for SBMA.

#### **1.3.1 Mouse models**

The first polyQ mouse model was created in 1995 in order to replicate the disease symptoms observed in SCA1. This model was created using a full length ataxin1 with glutamine stretches of 30 and 82 amino acids, and ataxin1 expression was driven by a Purkinje cell-specific promoter (Burrigh et al., 1995). While this model was quite successful in mimicking many aspects of SCA1, morphological changes of the Purkinje cells did not exactly correlate with those seen in the human disease; and researchers were also still uncertain whether expression of the full-length protein was necessary for pathogenesis. These first particular dilemmas became common obstacles for the creation of reliable polyQ mouse models. The mouse models of Huntington's, SCA3, and SBMA that soon followed therefore experimented with many different approaches to solve these problems. These approaches included testing the toxicity of truncated fragments versus full-length protein, working with different neuronal specific promoters, and experimenting with different levels of expression and polyQ lengths (Yamada et al., 2007). To date, mouse models have been created for all of the polyglutamine disorders except SCA6 and SCA17.

### ***1.3.1.1 Mouse models of SBMA***

The earliest mouse models of SBMA were not as successful as the first SCA1 mouse model in recapitulating aspects of the human disease. The first model, established in the same year as the SCA1 model, used a neuron specific promoter to drive human AR cDNA with a glutamine region of 44 amino acids, a common length in SBMA patients (Bingham et al., 1995). This model surprisingly did not exhibit any neurological defects and also lacked the generational repeat instability seen in families afflicted with SBMA. Two other early models also failed to demonstrate neurological phenotypes in mice up to two years of age despite being able to reproduce repeat instability (La Spada et al., 1998) or having higher expression levels and a longer polyQ length of 65.

The next two attempts to replicate SBMA in mouse models utilized truncated fragments rather than the full-length AR. One group created a model system using a truncated AR with a polyQ stretch of 112 driven by the widely expressed prion protein promoter or the neurofilament-light chain promoter, which exhibits a more limited expression pattern (Abel et al., 2001). A second group developed a mouse using the AR promoter to drive expression of a polyQ tract of 239 glutamines, an exaggerated size over what is seen in human patients (Adachi et al., 2001). Both models effectively reproduced neurological symptoms, which included gait abnormalities and muscle weakness. Neuronal nuclear inclusions were also found to be present throughout the brain and spinal cord. Severity and onset of symptoms varied with the expression patterns of the promoters as well as the length of the polyQ tracts. A major drawback to both models, however, was the lack of motor neuronal specificity as well as gender specificity. These particular aspects seemed to require components present in the full-length receptor.

The most recent group of transgenic models have all expressed the full-length AR but with different levels and patterns of expression and to varying degrees of success. The first of these full-length models used an AR with 97 glutamines under the control of the cytomegalovirus (CMV) enhancer and the chicken  $\beta$ -actin promoter (Katsuno et al., 2002). These mice exhibited characteristic signs of muscle atrophy and neuronal intranuclear inclusions, and symptoms were enhanced in male mice. However, there was an absence of neuronal cell death. A similar scenario of neuronal inclusions but lack of cell death was also evident in mice expressing a 112 polyQ AR driven by the prion

promoter (Chevalier-Larsen et al., 2004). Oddly enough, the opposite development was seen in two other mouse models. Mice expressing an AR with 120 glutamines under the control of the CMV promoter experienced neuronal loss and muscular atrophy but showed a lack of inclusion formation (McManamny et al., 2002). The most recently published model took advantage of heterologous yeast artificial chromosome (YAC) transgenesis in order to express an AR containing 100 glutamines at near endogenous levels, under control of endogenous AR regulatory elements (Sopher et al., 2004). This model recapitulated key elements of motor neuronal specific cell death, muscle pathology, and gender specificity. However, these mice also failed to exhibit nuclear inclusions.

A mouse model that fully recapitulates all of the essential neuropathological aspects of SBMA, or any of the other polyQ disorders, has yet to be established. Nevertheless, the models have brought information to the field; including the knowledge that clinical onset of symptoms is not clearly dependent upon neuronal death. Rather, the phenotypes in mice lacking neuronal death may be due to increased neuronal dysfunction (Merry, 2005; Yamada et al., 2007). Additionally, the models have highlighted the idea that neuronal intranuclear inclusions may be cytoprotective and that pathology may be more directly linked to toxic intermediary structures. A recent study did indeed find that soluble oligomeric species underlined the pathology of the AR112 prion promoter mouse model (Li et al., 2007). The difficulties in producing accurate models, and especially in reproducing neuronal death, suggests that pathogenesis in the models is related to mutant protein levels and the amount of time a neuron is exposed to the mutant polyQ protein. It is possible that the approximate two year life span and aging process of the mouse may not be sufficient time for mouse neurons to acquire an amount of toxic intermediates and cellular damage that is comparable to that seen in the decades-long human process (Yamada et al., 2007). Therefore alternative approaches have also been sought to model the polyQ diseases.

### **1.3.2 Invertebrate models –*Drosophila* and *C. elegans***

After initial efforts were made to mimic the polyQ disorders in mice, scientists experimented with invertebrate model systems to explore if other models could prove

successful where the mouse models were facing difficulties. Invertebrate models have a distinct advantage over their mammalian counterparts due to rapid reproductive cycles and short life spans (Fig 1.4), which allow rapid construction of different transgenic models and quick evaluation of pathological phenotypes as well as experimental therapeutic interventions. Yet another advantage is the ability to perform nonbiased screens for suppressors or enhancers of polyQ toxicity. To date, both *Drosophila melanogaster* (fruit fly) and *Caenorhabditis elegans* (nematode) models have been utilized to model human neurodegenerative diseases, including the polyQ disorders. Models of Alzheimer's disease in *Drosophila* and *C. elegans* preceded work on the polyQ disorders and gave substantial evidence that these animal systems could be used to model such age-related disorders (Luo et al., 1992; Link, 1995).

The first *Drosophila* model of a polyQ disorder directed expression of an N-terminal htt fragment to the fly eye using the eye specific expression construct pGMR (glass multimer reporter) (Jackson et al., 1998). The fly eye was specifically employed because of its proven viability as a genetic system for investigation of cellular processes, especially those associated with cell death (Wolff et al., 1997). The *Drosophila* eye is a highly regular and organized structure of around 800 individual units and any morphological disruption of this organization can be clearly visualized. This first study demonstrated that a polyQ expanded htt could induce age-related cell death by apoptosis and cause the formation of inclusions in neurons of the fly eye. The many *Drosophila* models that have followed have opted for the GAL4-UAS expression system (Fig. 1.4) in which a promoter (or enhancer) directs expression of the yeast transcriptional activator GAL4 in a specific pattern and GAL4 in turn directs transcription of the GAL4-responsive UAS target gene in an identical pattern. Using this more flexible approach, investigators have been able to direct polyQ expression to the eye photoreceptors to look again at neurodegeneration in the eye, pan-neuronally to examine survival and behavioral effects, and to other types of cells to examine cell type specificity (Warrick et al., 1998). Another interesting aspect of using the GAL4-UAS system is that it provides an additional amplification step, leading to higher levels of expression of the particular polyQ construct. This results in an earlier onset of pathogenesis for these models in comparison to the first model produced by Jackson, et al. Fly models using the GAL4-

UAS system have thus far been created for Huntington's, SBMA, DRPLA, SCA1, SCA2, SCA3, and SCA7. In addition, expression of polyQ tracts alone has been shown to be sufficient to induce pathogenesis in *Drosophila* (Marsh et al., 2000).

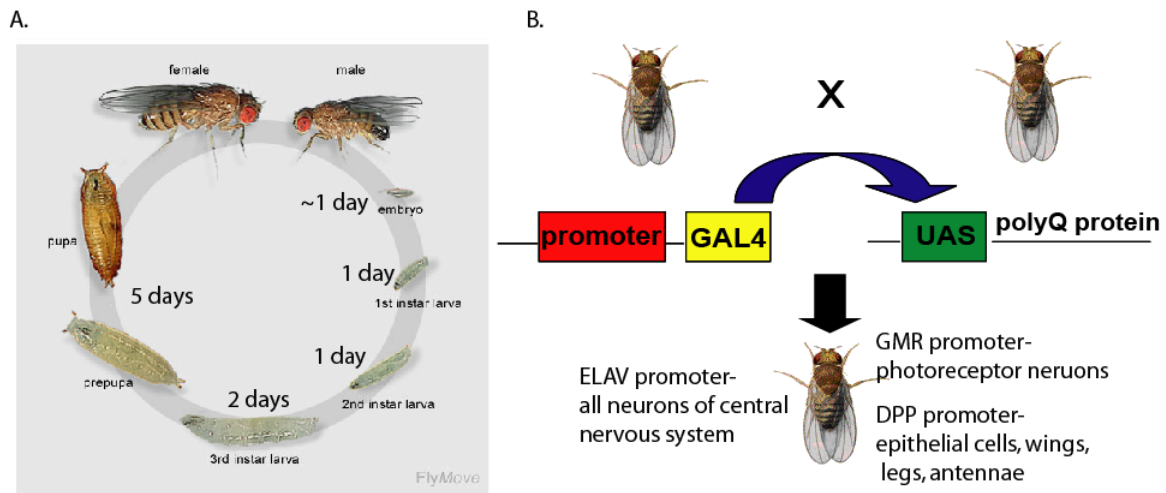


**Figure 1.4 *Drosophila* model system** (A) Life cycle of *Drosophila melanogaster* (Weigmann et al., 2003) (B) GAL4-UAS system in *Drosophila*

With models existing only for Huntington's and isolated polyQ tracts, *C. elegans* have not been used quite as extensively as *Drosophila* to model the polyQ disorders. Nevertheless, the existing models have proven to be valuable to the field. One distinct advantage of the *C. elegans* model is the ability to precisely identify specific neurons and follow their development or survival throughout the animal's lifetime. Utilizing such methods, researchers found that neurons expressing a polyQ htt fragment exhibited functional impairment prior to aggregate formation, neurodegeneration, and cell death (Faber et al., 1999). The relative ease of visualization of the nematode's structure has also allowed for investigation of protein aggregates; their influence on toxicity; and in turn, the influence of molecular chaperones on aggregate formation (Satyal et al., 2000). More recent studies have used the nematode to examine potential drug therapies (Voisine et al., 2007) as well as roles of protein interaction partners (Parker et al., 2007).

Both *Drosophila* and *C. elegans* have been proven as sound model systems with their ability to replicate the aggregate formation, neurotoxicity, and behavioral

characteristics of the polyQ disorders. A recent study has also demonstrated that *Drosophila* polyQ models reproduce features of human CAG repeat instability, another central aspect of the polyQ disorders (Jung and Bonini, 2007). With this in mind, the *Drosophila* system perhaps has the advantage over *C. elegans* in that: (1) scientists have been utilizing *Drosophila* in genetics for about fifty years longer resulting in a model system that is therefore more widespread and (2) *Drosophila* have a more complex nervous system and behavioral paradigm with a development that is more similar to mammals.

### ***1.3.2.1 Modeling SBMA in Drosophila***

For SBMA in particular, *Drosophila* models have been able to recapitulate key aspects of the polyQ disorder. The first SBMA fly models appeared almost simultaneously in 2002. The first model (Takeyama et al., 2002) expressed a full length human AR containing a stretch of 52 glutamines in the fly eye and clearly demonstrated for the first time that pathology was dependent upon ligand-induced nuclear translocation. The second model (Chan et al., 2002) used quite a different approach, expressing only an N-terminal fragment of the AR with a polyQ region of 112 to demonstrate aggregation and neurodegeneration. More importantly, this study showed that increased chaperone activity alleviated degeneration while disruption of proteasome activity resulted in enhanced neurodegenerative phenotypes. The most recent addition to the SBMA models has also used *Drosophila* to investigate aspects of the ubiquitin-proteasome system involved in the disease (Pandey et al., 2007). By directing expression of a full-length AR with 121 glutamines to the fly eye, this study showed that proteasome impairment was associated with ligand-induced toxicity. Furthermore, it was found that expression of histone deacetylase 6 (HDAC6), a microtubule-associated deacetylase that interacts with polyubiquitinated proteins, alleviated toxicity by promoting compensatory autophagy of the aberrant protein. Therefore, regulation of HDAC6 may be a possible therapeutic approach for intervening with the neurodegeneration process.

As seen in the SBMA models discussed above, some of the essential reasons for use of polyQ animal model systems are the ability to further elucidate the mechanisms of the disorders *in vivo* through manipulation of cellular pathways and possible interaction

partners, investigation of *in vivo* aggregate formation, and use of this information for the screening and testing of compounds to alter aggregate formation and toxicity ((Furutani et al., 2005; Desai et al., 2006; kQi et al., 2007; Latouche et al., 2007).

## **1.4 The path to therapy- therapeutic compounds for inhibiting polyglutamine toxicity**

All paths of research of the polyQ disorders eventually lead to the question, “How can this research benefit those suffering from the rare disorders?” In this respect, both mouse and *Drosophila* models have been critical in the screening and testing of various potential therapeutic agents. As is the case with many of the aforementioned studies, some findings have been applicable in only the context of a specific protein and disease, such as the AR and SBMA. However, a few tested treatments have been aimed at the common aspects of the diseases and have thus been found appropriate for multiple polyQ disorders.

### **1.4.1 SBMA specific therapies**

The unique aspect of SBMA being a ligand-induced polyQ disorder also means that the disease has a unique therapeutic target, the AR ligand testosterone. This is evident in the full-length polyQ AR *Drosophila* models in that no neurodegeneration is seen in the absence of hormone administration. Mouse models have been used to demonstrate that deprivation of androgens result in a vast improvement over the pathological phenotype. The elimination of androgens by surgical castration of an SBMA male mouse with an AR of 112 glutamines resulted in a partial recovery of motor function. Neurofilament heavy chain levels, which were reduced in the SBMA model, were also partially restored (Chevalier-Larsen et al., 2004). An alternative to surgical castration is the use of leuprolin as a therapeutic compound. Leuprolin is a lutenizing hormone-releasing hormone agonist that reduces testosterone levels from the testis; essentially it is an agent for chemical castration. In a mouse model expressing a full-length AR with a polyQ stretch of 97 residues, administration of leuprolin rescued motor dysfunction and nuclear aggregation of the mutant AR in male mice (Katsuno et al., 2003). Although androgen ablation therapy shows much promise as a method for treating SBMA, the treatment comes with many drawbacks for the patient. Surgical or even chemical castration is not something to be taken lightly as both sexual function and fertility are highly affected. Therefore, researchers are continually seeking out other possible therapeutic targets for SBMA.

Another specific target for SBMA therapy came to light when Sopher et al., published a mouse model that implicated altered expression of vascular endothelial growth factor (VEGF) in the motor neuronal death that is characteristic of the disease (Sopher et al., 2004). VEGF is important in the maintenance of motor neuronal health and survival; and its expression is regulated by the transcriptional cofactor CBP, whose function has been shown to be disrupted in the polyQ disorders by sequestration along with other transcriptional regulators into the mutant protein aggregates (Nucifora et al., 2001). A recent study found that the synthetic chemical compound 5-hydroxy-1,7-bis(3,4-dimethoxyphenyl)-1,4,6-heptatrien-3-one (ASC-J9), a compound loosely based on a component of the spice curcumin, was able to disrupt the interaction of the mutant AR with AR coregulators in the aggregate species in an SBMA mouse model (Yang et al., 2007). This not only led to a decrease in aggregation but also to an increase in the expression of the VEGF isoform VEGF164, the mouse equivalent of isoform VEGF165 in humans. Motor impairment was also greatly improved. These results point to an alternative SBMA treatment that eliminates the side effects of altering serum testosterone levels. Other alternatives may also be found in treatments that are appropriate for more general polyQ targets.

#### **1.4.2 General polyQ inhibitors**

Many therapeutic strategies have concentrated on suppressing protein aggregation or inhibiting neuronal apoptosis in a particular polyQ disorder. Because such themes are common to the polyQ diseases as a group, these strategies have proven to be generally applicable. For example, upregulation of heat shock proteins and molecular chaperones such as Hsp40 and Hsp70 that play critical roles in protein folding has been shown to inhibit toxicity in several different models (Chai et al., 1999; Cummings et al., 2001; Adachi et al., 2003). Inhibition or modulation of the function of Hsp90, which regulates the activity, turnover, and trafficking of many proteins, has also been shown to reduce aggregation and ameliorate the toxic phenotypes of SBMA and Huntington's (Sittler et al., 2001; Thomas et al., 2006a). Neuronal death has been tackled by investigating ways to inhibit caspase-associated cell death (Sanchez et al., 1999) and testing various agents with neuroprotective properties such as lithium chloride, basic fibroblast growth factor

(FGF-2), humanin, glial cell-line derived neurotrophic factor (GDNF), and estrogen (Darrington et al., 2003; McBride et al., 2003; Jin et al., 2005; Kariya et al., 2005; Watase et al., 2007). Another method that encompasses reducing both aggregation and cell death has been to target transcriptional dysregulation, which is believed to be a major cause of neuronal dysfunction in the polyQ disorders.

#### ***1.4.2.1 HDAC inhibitors***

Histone deacetylases (HDAC) and histone acetyl transferases (HAT) work in conjunction to modify chromatin by removing or adding acetyl groups to histones and thereby inhibiting or activating transcription, respectively (Marks et al., 2001). In the polyQ disorders, the HAT activity of transcriptional regulators such as CBP is disrupted due to recruitment into polyQ aggregates (Kazantsev et al., 1999). This interference with the transcriptional machinery results in cell death that is directly associated with the decreased histone acetylation (McCampbell et al., 2001). Correcting this imbalance of acetylation/deacetylation with administration of HDAC inhibitors has been found to greatly reduce polyQ toxicity in *Drosophila* and mouse models (Hockly et al., 2003; Agrawal et al., 2005).

Specific HDAC inhibitor compounds that have been tested for the polyQ disorders include suberoylanilide hydroxamic acid (SAHA) and sodium butyrate. SAHA is a hybrid polar compound that inhibits HDAC1 and HDAC3 and causes hyperacetylation of histone H4 (Richon et al., 1998). With SAHA's ability to cross the blood-brain barrier, administration of the compound was able to improve motor impairment in a Huntington's mouse model (Hockly et al., 2003). However, major drawbacks to the use of SAHA are its insolubility in aqueous solution and the potential lethal toxicity of the compound. An alternative to SAHA is the less toxic HDAC inhibitor sodium butyrate, a short-chain fatty acid that is produced in the colonic lumen as a consequence of microbial degradation of dietary fibers (Joseph et al., 2004). Sodium butyrate has shown potential therapeutic benefits of reduced toxicity and motor improvement in *Drosophila* models of Huntington's and SCA7 as well as mouse models of SBMA and DRPLA (Steffan et al., 2001; Minamiyama et al., 2004; Ying et al., 2006; Latouche et al., 2007). However, as noted in the study of the SBMA mouse model, the

dosage range of sodium butyrate that yields these benefits is very narrow; thus making dosage determination for clinical studies potentially problematic.

#### ***1.4.2.2 Melatonin as a candidate polyglutamine inhibitor***

Although there have been a few success stories of therapeutic compounds performing well in animal models, a smooth path to clinical trials is rarely imminent. This is especially true for novel synthetic compounds that may show toxic side effects. Therefore, instead of reinventing the wheel, an alternative method is to examine compounds that have been through clinical testing for other purposes and are known to be safe for human patient administration. An example of such a candidate inhibitor for the polyglutamine disorders is melatonin. Melatonin, a hormone secreted mainly by the pineal gland in humans, plays a central role in the circadian cycle and is also well-recognized as a powerful antioxidant. It has been marketed as a general health supplement in the United States since 1993 (Lewis and Clouatre, 1999) and has been studied for the treatment of cancer, immune disorders, cardiovascular diseases, depression, seasonal affective disorder, and sexual dysfunction (Waldhauser et al., 1993; Sewerynek, 2002; Shiu, 2007). However, it is melatonin's role as a free radical scavenger and general antioxidative protectant that researchers first recognized may be beneficial for several neurodegenerative disorders.

Production of melatonin declines in a physiological-age dependent manner, and this reduction in melatonin levels has been associated with the oxidative stress and degenerative changes that occur with aging (Srinivasan, 1997). Moreover, such oxidative damage has been implicated as a major factor in age-associated disorders such as Alzheimer's, Parkinson's, and the polyglutamine disorders (Markesbery, 1997; Goswami et al., 2006; Lavoie et al., 2007). A major source of oxidative damage in these disorders is due to mitochondrial dysfunction. Melatonin has been found to be a potent antagonist of mitochondrial radical formation, thus demonstrating neuroprotective benefits. In addition to its antioxidant role, melatonin has also been shown to have antifibrillogenic actions that can disrupt  $\beta$ -amyloid toxicity (Matsubara et al., 2003; Cheng and van Breemen, 2005). These properties give melatonin much potential as an inhibitor of polyQ toxicity.

## 1.5 Aims

For the group of debilitating neurodegenerative diseases known as the polyglutamine disorders, there is still much to be discovered on the path to effective therapies. Previous studies have shown that much can be learned from investigation of the individual diseases. Utilizing the disorder spinal and bulbar muscular atrophy as a model for polyQ toxicity due to the unique properties of its associated polyQ protein, the androgen receptor; the aim of this work was to further investigate how specific sites neighboring the polyQ region affect aggregation and toxicity in both expanded polyQ and wild type situations. A further point to be addressed was how any alterations in aggregate species correlated with differences in toxic properties exhibited in a *Drosophila* model of SBMA. Lastly, the ability of the HDAC polyQ inhibitor sodium butyrate to affect the varied toxic properties brought about by the mutation of neighboring sites was investigated in conjunction with investigating the therapeutic potential of melatonin.

## 2.0 MATERIALS AND METHODS

### 2.1 Materials

#### 2.1.1 Chemicals and consumables

Name	Source
Acrylamide	Roth, Karlsruhe
Agar (strands)	Probio GmbH, Eggenstein
Agarose	Peqlab, Erlangen
Ampicillin	Roth, Karlsruhe
Ammonium Persulfate (APS)	Roth, Karlsruhe
5 $\alpha$ -Androstan-17 $\beta$ -ol-3-one (DHT)	Sigma-Aldrich Chemie, Steinheim
Bovine Serum Albumin (BSA)	PAA Laboratories GmbH, Pasching
Apple Juice	Various sources
Bacto-Agar	Otto Nordwald GmbH, Hamburg
Bacto-Trypton	Roth, Karlsruhe
Beer Yeast	Probio GmbH, Eggenstein
Bromophenol blue	Sigma-Aldrich Chemie, Steinheim
Chloroform	Merck, Darmstadt
Cornmeal	Friedrichstal Mühle, Stutensee
Dimethylsulfoxide (DMSO)	Fluka, Neu Ulm
Dithiothreitol (DTT)	Gibco, Invitrogen, Karlsruhe
DNA Marker 1kb	PeqLab, Erlangen
Dulbecco's Modified Eagle Medium	Gibco, Invitrogen, Karlsruhe
Ethylenediamine Tetraacetic Acid (EDTA)	Roth, Karlsruhe
Ethanol (EtOH)	Roth, Karlsruhe
Ethidium Bromide	Roth, Karlsruhe
Glycylglycerine	Roth, Karlsruhe
Glycine	Roth, Karlsruhe
Glycerol	Roth, Karlsruhe
Glucose	Roth, Karlsruhe
Hydrogen Chloride (HCl)	Merck, Darmstadt
Isopropanol, Propan-2-ol	Merck, Darmstadt
D-Luciferin <i>Firefly</i>	Biosynth AG, Staad
Magnesium Chloride	Roth, Karlsruhe
Magnesium Sulfate	Roth, Karlsruhe
Melatonin	Sigma-Aldrich Chemie, Steinheim
Methanol (MeOH)	Roth, Karlsruhe
$\beta$ -Mercaptoethanol	Roth, Karlsruhe
Milk Powder	Saliter, Obergünzburg
Mowiol 40-88 (Polyvinyl alcohol)	Sigma-Aldrich, Taufkirchen
Nipagin (Methyl-p-Hydroxybenzoate)	Sigma-Aldrich, Taufkirchen
1X and 10X Phosphate Buffered Saline (PBS) - /- Ca <sup>2+</sup> and Mg <sup>2+</sup>	Gibco, Invitrogen, Karlsruhe
Penicillin/Streptomycin	Gibco, Invitrogen, Karlsruhe

Phenol	Roth, Karlsruhe
Potassium Chloride	Merck, Darmstadt
Protein marker	PeqLab, Erlangen
Rotisol	Roth, Karlsruhe
Saccharose	Roth, Karlsruhe
Sodium Acetate	Roth, Karlsruhe
Sodium Butyrate	Sigma-Aldrich Chemie, Steinheim
Sodium Chloride	Roth, Karlsruhe
Sodiumdodecylsulfate (SDS)	Roth, Karlsruhe
Sodium Hydroxide	Roth, Karlsruhe
Sodium Hypochlorite Solution	Roth, Karlsruhe
Sugar Syrup	Grafschafter Krautfabrik, Meckenheim
Tetramethylethylenediamine (TEMED)	Roth, Karlsruhe
Tris-Base	Roth, Karlsruhe
Tris-HCl	Roth, Karlsruhe
Triton X-100	Sigma-Aldrich, Taufkirchen
Trypsin	Difco, Detroit
Tween 20	Roth, Karlsruhe
Voltalef Halocarbon Oil	Lehmann and Voss and Co., Hamburg
Yeast (fresh)	Various sources
Yeast extract	Gibco, Invitrogen, Karlsruhe

### 2.1.2 Enzymes

All restriction endonucleases and other modifying enzymes were purchased from Invitrogen GmbH (Karlsruhe, Germany), New England Biolabs (Beverly, USA) or Promega (Mannheim, Germany).

### 2.1.3 Plasmids and constructs

#### Reporter gene and expression-plasmids for transient transfection in cells:

Name	Description
<b>pG13MMTV</b>	Encodes the firefly luciferase gene under the control of the mouse mammary tumour virus (MMTV) long terminal repeat cloned as a BamHI/BglIII fragment from the plasmid pHCwtCAT (Kaspar et al., 1993)
<b>Renilla-tk-luc</b>	Vector containing cDNA encoding <i>Renilla</i> luciferase. Used as internal control. Obtained from Promega. (Mannheim, Germany)
<b>pSG5-ARwt</b>	Expression plasmid with the cDNA of the human wild type androgen receptor. The receptor contains a polyglutamine region of 22 amino acids.
<b>pSG5-ARQ77</b>	Expression plasmid with the cDNA of the human androgen receptor with an expanded polyglutamine region of 77 amino acids.
<b>pSG5-ARwt MAPk/423 Ala (ARQ22dm)</b>	Expression plasmid with the cDNA of the human androgen receptor with polyglutamine region of 22 amino acids. Serines 424 and 514 are mutated to alanine.
<b>pSG5-ARQ77 MAPk/423 Ala (ARQ77dm)</b>	Expression plasmid with the cDNA of the human androgen receptor with expanded polyglutamine region of 77 amino acids. Serines 424 and 514 are mutated to alanine.

ARQ22 and ARQ77 were obtained by subcloning the respective AR sequence into the expression vector pSG5 as previously described (Becker et al., 2000). Serine residues at positions 424 and 514 were exchanged into alanines by the Quikchange mutagenesis method (Stratagene., La Jolla, CA) to generate ARQ22dm and ARQ77dm expression vectors.

### Vectors and expression-plasmids for *Drosophila* injection:

Name	Description
p $\Delta$ 2,3	Helper-plasmid for P-element vector
pUAST	P-element vector with white eye gene that acts as a marker for successful incorporation into the <i>Drosophila</i> genome
pUAST-ARwt	<i>Drosophila</i> P-element plasmid containing cDNA of the human wild type androgen receptor. The receptor contains a polyglutamine region of 22 amino acids.
pUAST-ARQ77	<i>Drosophila</i> P-element plasmid containing cDNA of the human androgen receptor with an expanded polyglutamine region of 77 amino acids.
pUAST-ARwt MAPk/ 423 Ala (ARQ22dm)	<i>Drosophila</i> P-element plasmid containing cDNA of the human androgen receptor with polyglutamine region of 22 amino acids. Serines 424 and 514 are mutated to alanine.
pUAST-ARQ77 MAPk/ 423 Ala (ARQ77dm)	<i>Drosophila</i> P-element plasmid containing cDNA of the human androgen receptor with expanded polyglutamine region of 77 amino acids. Serines 424 and 514 are mutated to alanine.

Each of the AR sequences (ARQ22, ARQ22dm, ARQ77, and ARQ77dm) was cloned into the *Bam*HI/*Bgl*II site of the P element vector pUAST (Brand and Perrimon, 1993).

#### 2.1.4 Bacteria and eukaryotic cells

##### Bacterial cells

Name	Genotype
<i>E. coli</i> DH 5 $\alpha$ (for cloning)	F <sup>-</sup> , end A1, hsd R17 (r <sub>k</sub> <sup>-</sup> , m <sub>k</sub> <sup>+</sup> ), sup E44, thi-1, $\lambda$ -, rec A1, gyr A96, relA1

##### Eukaryotic cell lines

Name	Description
COS7	Simian kidney cell line: androgen receptor deficient. COS7 cells were cultivated in DMEM supplemented with 10% fetal bovine serum (FBS) unless otherwise indicated.

### 2.1.5 *Drosophila melanogaster* lines

Name	Description (Source)
<i>w<sup>1118</sup></i>	<i>Drosophila</i> line used for injections. Expresses gene for white eyes. (Bloomington <i>Drosophila</i> Stock Center)
<b>ELAV-Gal4</b> ( <i>embryonic lethal, abnormal vision</i> )	Used for crossing experiments. Pan-neural expression. (Bloomington <i>Drosophila</i> Stock Center)
<b>GMR-Gal4</b> ( <i>glass multimer reporter</i> )	Used for crossing experiments. Expression in photoreceptor neurons. (Bloomington <i>Drosophila</i> Stock Center)

### 2.1.6 Antibodies

#### Pre-immune sera

Rabbit and goat pre-immune sera were obtained from VECTOR Laboratories Inc., CA, U.S.A..

#### Primary antibodies

Name	Description (Source)
<b>anti-AR 44</b>	Rabbit polyclonal antibody against aa 543-557 of the human androgen receptor.
<b>anti-AR F39.4.1</b>	Mouse monoclonal antibody against aa 301-320 of the human androgen receptor (BioGenex)
<b>anti-AR (C-19)</b>	Rabbit polyclonal antibody against the C-terminus of the human androgen receptor (Santa Cruz Biotechnology Inc.)
<b>anti-AR (N-20)</b>	Rabbit polyclonal antibody against the N-terminus of the human androgen receptor (Santa Cruz Biotechnology Inc.)
<b>anti-ERK 2 (D-2)</b>	Mouse monoclonal antibody against the C-terminus of the human ERK 2 Map kinase p42 (Santa Cruz Biotechnology Inc.)
<b>anti-Polyglutamine-Expansion Diseases Marker (1C2)</b>	Mouse monoclonal antibody that recognizes polyglutamine stretches greater than 37 aa.
<b>anti-<math>\alpha</math> Tubulin (H-300)</b>	Rabbit polyclonal antibody against aa 149-448 of human $\alpha$ Tubulin

**Secondary antibodies**

All secondary antibodies HRP conjugated were purchased from DAKO Diagnostika GmbH, (Hamburg, Germany). All secondary fluorescently labeled antibodies were purchased from Jackson Immuno Research (USA).

## 2.2 Methods

### 2.2.1 DNA - cloning techniques

#### 2.2.1.1 DNA fragmentation with restriction enzymes

One unit of an enzyme is defined as the amount of enzyme required to completely digest 1 $\mu$ g of Phage Lambda ( $\lambda$ ) DNA in one hour. For the preparation and digestion of DNA for cloning, 10 units of the necessary enzyme were used per  $\mu$ g of DNA. A mixture of DNA, enzyme, and the appropriate buffer were left to incubate at the required temperature (usually 37°C) for a period of 3 hours to overnight. The volume of the reaction was such that the final volume consisted of only up to ten percent glycerol from the enzyme and buffer solutions. For the analysis of fragment size and the isolation of fragments after digestion, the DNA fragments were separated by agarose gel electrophoresis.

#### 2.2.1.2 Separation of DNA fragments by agarose gel electrophoresis

The separation and analysis of DNA fragments was performed on a horizontal agarose gel consisting of 1-2% agarose, depending on the expected size of the fragments. The amount of agarose for the desired gel concentration was dissolved by boiling in 1 X TAE buffer. After the solution cooled to an approximate temperature of 60°C, ethidium bromide was added for an end concentration of 0.4 $\mu$ g/ml. The solution was then poured into a horizontal gel chamber to solidify, and a comb was placed near the top to provide slots for the samples to be loaded. The 1 X TAE buffer was poured over the hardened gel and samples were mixed with DNA sample buffer and loaded in the gel. A 1kb DNA standard ladder was also loaded in the first lane of the gel. The gel was run with 80-100V. Separation of the fragments was visualized under a UV-Transilluminator and then photographed.

Buffers	Composition
TAE	0.04 M Tris pH 7.2, 0.02 M sodium acetate, 1 mM EDTA
DNA sample buffer	5 mM EDTA, 50% glycerol, 0.01 g bromophenol blue

#### ***2.2.1.3 DNA extraction from agarose gel***

The band of an isolated DNA fragment was identified under UV-light and removed from the gel with a scalpel and placed in a 1.5 ml Eppendorf tube. The DNA was then extracted using the manufacturer's instructions from an Easy-Pure kit (Biozym Diagnostik GmbH, Oldendorf, Germany). The tube was filled to the top with SALT-buffer and incubated at 55°C on a shaker for 5 minutes. The solution was vortexed and 9µl BIND was added and mixed by inverting the tube. After a 5 minute incubation at room temperature (RT), the mixture was centrifuged briefly at 12000 rpm. The supernatant was disposed, and the pellet was resuspended in 1ml of WASH. The mixture was incubated at room temperature for 5 minutes and again briefly centrifuged at 12000 rpm. The supernatant was disposed and the pellet was centrifuged again in order to pipette off any remaining liquid. The pellet was dried for several minutes and then eluted with 25µl H<sub>2</sub>O. After 5 minutes incubation, the new mixture was centrifuged for 1 minute at 12,000 rpm, and the DNA supernatant was pipetted into a new 1.5 ml Eppendorf tube.

#### ***2.2.1.4 Ligation of DNA fragments into plasmid vectors***

DNA content of fragments to undergo the ligation reaction was checked by running both the vector and insert on an agarose gel. The appropriate combination for ligation was approximately 3-4X the amount of insert for 1X the amount of vector (~50-100ng). The correct ratio of DNA fragments were combined with 1.5µl T4-DNA-Ligase and 1 µl 10 X Ligase Buffer for a total reaction volume of 10 µl and allowed to incubate overnight at 16°C.

#### ***2.2.1.5 Transformation of bacteria***

A volume of 5 µl of ligation mixture or 20-40 ng plasmid-DNA was given to 50 µl of DH5- $\alpha$  competent cells, and the mixture was incubated on ice for 30 minutes. After a 90 second heat shock at 42°C and then 2 minutes on ice, 450 µl SOC-Medium was added to the bacteria and allowed to incubate on a shaker at 37°C for at least 45 minutes. The suspension was spread onto selective agar plates, and the plates were incubated overnight at 37°C. Bacteria with recombinatorial DNA were identified by restriction enzyme analysis of DNA prepared from a mini-preparation.

<b>Buffers</b>	<b>Composition</b>
SOC-Medium	2% bacto-tryptone, 0.5% yeast extract, 10mM NaCl, 2.5mM KCl, 10mM MgCl, 10mM MgSO <sub>4</sub> , 20mM glucose

## **2.2.2 Preparation of recombinant plasmid DNA from transformed bacteria**

### ***2.2.2.1 Mini-preparation of plasmid DNA***

Single bacterial colonies were picked, inoculated in 3 ml of LB medium containing the appropriate antibiotic and grown overnight under constant shaking at 37°C. 1.5 ml of these cultures were transferred to a fresh vial and the bacteria were collected as a pellet by centrifugation at 12000 rpm (centrifuge Eppendorf 5417 R) for 10 min at RT. Briefly, the bacterial pellet was resuspended in 150 µl of solution P1 containing RNase A, from the MaxiPrep Kit (Qiagen) and left for 5 min at RT. Then 300 µl of solution P2 were added and the mixture was incubated for 5 min on ice. After addition of 225 µl of solution P3 followed by vortexing, the lysate was again left for 5 min on ice. After centrifugation at 12000 rpm for 10 min at 4°C, 400 µl of the supernatant were collected and transferred to a fresh tube containing 1 ml of ice-cold ethanol. Incubation for 30 min at -80°C allowed for the precipitation of nucleic acids. The plasmid DNA pellet was collected by centrifugation at 12000 rpm for 10 min at 4°C and was washed once with 70% ethanol. The resulting pellet was air-dried and resuspended in 50 µl of H<sub>2</sub>O.

### ***2.2.2.2 Maxi-preparation of plasmid DNA***

Plasmid DNA was prepared on a large scale using the Qiagen Plasmid Maxi Kit (Qiagen) following the manufacturer's instructions. A volume of 200-250 ml of LB medium supplemented with the appropriate antibiotic was inoculated with 1.5 ml of the remaining mini-preparation and incubated with shaking (220 rpm) at 37°C overnight until the bacteria had reached a stationary growth phase. The bacteria were pelleted by centrifugation in a fixed angle rotor at 6000 rpm (centrifuge Hermle ZK 401) for 5 min and the pellet resuspended in 10 ml solution P1. Following 5-10 min incubation at RT, the cells were lysed by addition of 10 ml solution P2. Once the solution had taken an opaque appearance, the mixture was neutralized with 10 ml of solution P3 and the entire

content inverted gently to aid the mixing of the solutions. After an additional 10 min on ice, the cell wall fragments and the bacterial chromosomal DNA were sedimented by centrifugation at 7500 rpm for 30 min at 4°C (centrifuge Hermle ZK 401). The retained supernatant was then added directly to a pre-equilibrated (15 ml Buffer QBT) Qiagen-tip 500 column and entered the resin by gravity flow. The QIAGEN-tip 500 was then washed twice with 30 ml of Buffer QC, and the plasmid DNA was eluted in 15 ml of Buffer QF. The DNA was then precipitated by adding 11 ml of isopropanol to the DNA fraction. The samples were then centrifuged for 30 min (centrifuge Beckman Coulter) and washed in 5 ml 80% ethanol before being re-suspended to a final concentration of 1-3 mg/ml in TE buffer and stored at -20°C.

<b>Media and Buffers</b>	<b>Composition</b>
LB Medium	10 g tryptone, 5 g yeast extract, and 10 g NaCl for 1 l (autoclaved before use)
Buffer P1 (Resuspension Buffer)	10 mM EDTA, 50 mM Tris-HCl pH 8.0, and 400 mg/ml RNase A
Buffer P2 (Lysis Buffer)	200 mM NaOH, 1% SDS
Buffer P3 (Neutralization Buffer)	3 M Na acetate, pH 4.8
Buffer QBT (Equilibration Buffer)	700 mM NaCl, 50 mM MOPS pH 7.0, 15% isopropanol (v/v), 0.15% Triton X-100 (v/v)
Buffer QC (Wash Buffer)	1 M NaCl, 50 mM MOPS pH 7.0, 15% isopropanol (v/v)
Buffer QF (Elution Buffer)	125 mM NaCl, 50 mM Tris-HCl pH 8.5, 15% isopropanol (v/v)
TE buffer	10 mM Tris-HCl, 1 mM EDTA pH 8.0

### ***2.2.2.3 Phenol/chloroform extraction of plasmid DNA***

To remove unwanted protein contaminants from nucleic acid solutions an equal volume of Tris-buffered phenol and chloroform at a ratio of 1:1 (v/v) was added and the mixture was vortexed. The two phases were separated by centrifugation at 12000 rpm for 10 min. The upper aqueous nucleic acid-containing phase was transferred to a fresh reaction tube and subjected to a further round of extraction with phenol/chloroform (1:1, v/v).

#### ***2.2.2.4 Ethanol precipitation of plasmid DNA***

In order to recover nucleic acids from solution, the salt concentration was brought to 200 mM by adding 1/10 of the original solution volume of 3 M Na-acetate (pH 4.8-5.0) and 2.5 volumes of cold ethanol. After 30 min to overnight incubation at -20°C or 30 min at -80°C, the precipitate was centrifuged at 12000 rpm for 15 min. The pellet was washed with 80% ethanol, centrifuged for another 3 min to remove the salt, and then dried. DNA was resuspended in H<sub>2</sub>O.

#### ***2.2.2.5 Determination of nucleic acid concentration***

The concentration of nucleic acids was determined by measuring their optical density (OD) at 260 and 280 nm. An OD<sub>260</sub> = 1 is equivalent to 50 µg/ml double stranded DNA. A ratio of OD<sub>260</sub>/OD<sub>280</sub> ranging from 1.8 to 2.0 indicates an acceptable purity of the nucleic acid.

### **2.2.3 Cell culture**

#### ***2.2.3.1 Passaging of cells***

COS7 cells were maintained at 37°C in an incubator (Forma Scientific, Labortect GmbH, Göttingen, Germany) in 5% CO<sub>2</sub> and 95% air humidity. All cells were grown in Petri dishes or flasks (Greiner, Frickenhausen, Germany) of varying sizes depending on the application. The cells were allowed to grow until a confluence of 80- 90% had been reached, whereupon the cells were subsequently split by trypsinization and re-seeded at a lower density. Trypsin treatment of cells was performed by removal of the culture medium from the cells, followed by one wash with 1X phosphate buffered saline (PBS). After removal of PBS, 0.25% trypsin was applied to the cells and the cells incubated at 37°C until they became detached. Fresh medium was then directly applied and the cells re-plated at the desired density in new Petri dishes.

#### ***2.2.3.2 Freezing and thawing of cells***

To prepare cells for long term storage, logarithmically growing cells were trypsinized and collected by centrifugation at 800-1500 rpm. The medium was removed

and the cells resuspended in culture medium with 10-50% FCS and 10% DMSO and placed in 1 ml aliquots in cryovials. After incubation on ice for 1 hour, the cells were placed at -80°C for 16-24 h before finally being stored in liquid nitrogen. To re-propagate cells, the vials were removed from the liquid nitrogen and placed at 37°C.

### ***2.2.3.3 Transient transfections***

FuGene6™ transfection reagent was used according to the manufacturer's instructions. Proliferating cells were sub-cultured the day before transfection, allowing cells to reach 50-80% confluency on the day of the experiment. For a 35 mm culture dish, 3-6 µl of FuGene6™ reagent were diluted in serum-free medium to a total volume of 100 µl and incubated at room temperature for 5 min. The diluted FuGene6™ solution was then added dropwise to a second sterile tube containing 1-2 µg of DNA and incubated at room temperature for 15 min. The mixture was finally transferred to the cells dropwise and by gentle swirling to ensure an even distribution. For AR transactivation studies, typically 1.2 µg of the desired reporter plasmid, 0.3 µg of renilla luciferase construct as an internal control, and 0.5 µg of an AR expression vector were transfected. 24 h after transfection the cells were treated either with vehicle alone or vehicle containing 10<sup>-7</sup> M dihydrotestosterone (DHT) for another 20 h. Then the cells were harvested for the luciferase measurements. For protein localization and aggregation experiments the cells were transfected with 1.5-3 µg of the AR expression vector(s). The cells were treated with hormone 36 h after transfection for 3 h. For all transfection experiments the cells were kept in the DMEM medium without phenol red and containing 3% charcoal treated FCS (CCS) to remove residual steroids.

### ***2.2.3.4 Analysis of gene expression through luciferase activity test***

#### **Measurement of firefly luciferase activity**

After transfection, cells were in culture for at least 24-48 h to allow expression of the transfected reporter gene. Typically they were kept in 6-well plates. Cells were then washed twice in PBS without Ca<sup>2+</sup> and Mg<sup>2+</sup>. PBS was then removed and the cells harvested in 300 µl 1X lysis buffer (Passive Lysis Buffer, Promega, Mannheim,

Germany). The cells were kept on ice for 10 min and occasionally rocked to distribute the buffer evenly and favour the detachment of the cells from the plates. The cell lysates were pipetted up and down several times, collected with a rubber policeman, and finally transferred to pre-cooled vials. 100 µl of cell lysate were transferred to a reading tube, and 350 µl of assay buffer and 100 µl of luciferin assay solution were then added by autoinjection. Luciferase activity was measured by use of a luminometer (Berthold, Wildbad, Germany).

<b>Buffers</b>	<b>Composition</b>
Assay buffer	1mM DTT, 1 mM ATP in glycyglycine buffer
Glycyglycine buffer	25 mM glycyglycine, 15 mM MgSO <sub>4</sub> and 4 mM EGTA
Luciferin assay solution	1mM luciferin; stock solution: 0.28 mg/ml

#### **Measurement of Renilla luciferase activity**

100 µl of cell lysates were mixed with 500 µl of coelenterasin buffer together with substrate solution. Luminescence was measured by use of a luminometer (Berthold, Wildbad, Germany).

<b>Buffers</b>	<b>Composition</b>
Coelenterasin buffer	0.1 M KPi-buffer, 0.5 NaCl, 1 mM EDTA, pH 7.6
kKPi-buffer	0.2 M KH <sub>2</sub> PO <sub>4</sub> and 0.2 M K <sub>2</sub> HPO <sub>4</sub> , pH 7.6
substrate solution	25 nM end concentration coelenterazine, Byosinth AG, Gstaad, Switzerland

#### **2.2.3.5 Immunofluorescence**

##### **Preparation of the paraformaldehyde solution**

To make a 10% stock solution 20 g of paraformaldehyde crystals were dissolved in 80 ml of water and heated up to 60°C. To facilitate the dissolving of paraformaldehyde

several drops of NaOH were added. After the crystals were dissolved the solution was cooled down, mixed with 100 ml of 2x PBS, aliquotted, and stored at -20°C.

### **Preparation of polyvinyl alcohol mounting medium**

20 g polyvinyl alcohol was mixed with 80 ml of 1 X PBS and stirred overnight with a magnetic stirrer at a temperature of 60°C. 50 ml of glycerin was added, and the solution was stirred until uniform. Several crystals of thymol were added as a preservative. The mixture was filtered and stored upside down in an airtight container.

### **Immunofluorescent staining**

For immunofluorescence experiments, COS7 cells were seeded into 6-well plates at a density of  $2 \times 10^5$  cells per well with a sterile coverslip put into every well. The next day the cells were transfected with the FuGene6™ transfection reagent and 24 h after transfection treated with either the vehicle or  $10^{-7}$  M DHT for up to 3 h. After treatment, the cells were washed 2 times with PBS and fixed for 20 min with 3% paraformaldehyde (in PBS). To remove the paraformaldehyde ions the cells were then incubated for 15 min in 50 mM  $\text{NH}_4\text{Cl}$  (in PBS) and finally permeabilized in 0,1% Triton-100 (in PBS) for 5 min. Afterwards the cells were washed 2 times with PBS and blocked for 1 h with PBS supplemented with 3% FCS (PBS-3%FCS).

After the blocking, PBS-3%FCS was removed and 150  $\mu\text{l}$  of the primary antibody solution (1:50 AR F39.4.1) in PBS-3%FCS was pipetted directly onto the coverslip and incubated for 1h. Then the cells were washed 3 times with PBS-3%FCS and covered with 150  $\mu\text{l}$  of the secondary antibody (1:200 Cy3 anti-mouse) for another 30-60 min. The cells were then washed 3 times with PBS.

Finally the coverslips were taken from the 6-well plate and rinsed in  $\text{dH}_2\text{O}$ . The water drops were removed, and the coverslip was placed onto the glass slide with a drop of fluorescence mounting medium with the cell covered side facing downwards. Then the slides were dried for 30-60 min at room temperature and stored in a dark place at 4°C.

## 2.2.4 *Drosophila* methods

### 2.2.4.1 *Culturing of fly stocks*

Fly stocks were kept at 25°C in polystyrene tubes with ceaprene stoppers (Greiner Bio-One) on standard fly-food medium. Every three to four weeks, fly stocks were placed in new tubes with fresh stock food.

### 2.2.4.2 *Preparation of fly food*

For large quantities of stock food, 80 g of agar strands were soaked overnight in 10 l H<sub>2</sub>O. The next day, the H<sub>2</sub>O and agar was boiled at 100°C in a pressure cooker. Once the agar was completely in solution, the temperature was turned down to 90°C. Then 1 l of sugar syrup was added while continuously stirring. In a separate container, 165 g beer yeast and 815 g cornmeal were dissolved in 3.3 l H<sub>2</sub>O. The mixture was then added to the cooker and allowed to boil for 5-10 min at 100°C. The mixture was then allowed to cool for 15 min until the temperature reached 65°C. Finally, 20 ml of 10% Nipagin (20 g in 200 ml EtOH) was added and a pump was used to fill the small, medium, and large sizes of polystyrene tubes.

For food containing sodium butyrate, the above recipe was made on a 1/10 scale. A 500 mM solution of sodium butyrate was made with H<sub>2</sub>O, and 200 ml was added to 130 ml H<sub>2</sub>O plus the 16.5 g beer yeast and 81.5 g cornmeal. This mixture was added to the cooker after the addition of sugar syrup, just as in the original protocol.

In order to make normal or sodium butyrate fly food containing EtOH, DHT, and/or melatonin, the recipe was again used on a 1/10 scale. Typically, 300 ml of food was used for each hormone/inhibitor combination. The amounts added were as follows for 300 ml:

Type of food	Amounts added
EtOH	6 ml 80% EtOH
DHT	3 ml 10 <sup>-1</sup> M DHT and 3 ml 80% EtOH
Melatonin	3 ml 1M Melatonin and 3 ml 80% EtOH
Melatonin/DHT	3 ml 1 M Melatonin and 3 ml 10 <sup>-1</sup> M DHT

Some crosses were performed on apple-agar plates. 8.25 g of agar-agar was dissolved in 300 ml dH<sub>2</sub>O in a 500 ml bottle and autoclaved. This solution could be stored at room temperature until needed. The agar was then microwaved until melted and 10 g sucrose and 100 ml apple juice were added. The mixture was then cooled to 65°C and 0.6 g Nipagin dissolved in 4 ml ethanol were added. The apple-agar solution was then added to small bacterial plates (Greiner Bio-One) and allowed to cool before stored at 4 °C.

#### ***2.2.4.3 Injections for germ-line transformation***

##### **Injection mix purification**

5 µg of the pΔ<sub>2,3</sub> helper plasmid (10kb) was added to approximately 2 times more (molar ratio) of the P transgene of interest (i.e. pUAS<sub>t</sub>-ARQ22, pUAS<sub>t</sub>-ARQ77, etc). The volume was adjusted to 100 µl with dH<sub>2</sub>O. 100 µl of (1:1) Phenol/Chloroform was added and mixed by finger tapping. The mixture was centrifuged for 5 min, 14000 rpm at 4°C. 90 µl of the supernatant was put in a fresh eppendorf and 9 µl of 3M Sodium Acetate pH 4.8 was added. 225 µl of 100% cold EtOH was added, and the mixture was allowed to precipitate for at least 60 min at -80°C. The mixture was then spun down for 30 min, 14000 rpm at 4°C, washed with 500 µl 80% EtOH and centrifuged again for 5 min. The pellet was then allowed to dry for 30 min under a fume hood. After drying, the DNA pellet was resuspended in 37 µl of dH<sub>2</sub>O. 1 µl was saved to examine the quality/ratio of the injection mix while the other 36 µl were stored at -20°C.

##### **Quality/ratio controls**

1 µl from the injection mixture was used for a digestion with the restriction enzyme EcoRI. A complete digestion yielded two bands of approximately 3.5 and 6.8 kb corresponding to the two fragments from the pΔ<sub>2,3</sub> vector, as well as two bands corresponding to the pUAS<sub>t</sub>-AR plasmid used (approximately 8.4 kb and 3.6 kb). The correct ratio of pUAS<sub>t</sub>-AR to pΔ<sub>2,3</sub> vector was no less than 3:1.

### Injection mix preparation

4  $\mu$ l of 10X injection buffer was added to the stored 36  $\mu$ l DNA mix, and 4x10  $\mu$ l aliquots were made of the resulting “injection mix” and stored at -20°C. 100  $\mu$ l of sterile 1X injection buffer was also prepared with dH<sub>2</sub>O and stored at -20°C.

Buffers	Composition
10X Injection buffer	0.1M Sodium Phosphate Buffer pH 6.8, 5mM KCL
1 M Sodium Phosphate Buffer pH 6.8	4.97 ml 1M Na <sub>2</sub> HPO <sub>4</sub> and 5.03 ml 1M NaH <sub>2</sub> PO <sub>4</sub> in 100 ml dH <sub>2</sub> O

### Injection procedure

At least two full large containers of *w<sup>1118</sup>* flies were put in a large container with a 10 cm apple-agar plate and yeast paste at 25°C at least 18 h before the time of injection. Several hundred flies were needed to produce enough eggs/embryos, and females produced eggs best when they were about one week old and well fed. Flies also tended to lay more eggs when kept in the dark. On the day of injection, the apple-agar plate was changed at least twice in the morning and checked after 30 min each time to ensure that the flies were laying a sufficient amount of embryos. The apple-agar plate was replaced again, and the flies were allowed to lay eggs for 30-40 min. While the flies were allowed to lay eggs, the injection mix was thawed and centrifuged to pellet any dust particles or insoluble material. From then on, the injection mix was kept on ice. After 30-40 min of egg-laying, the apple-agar was plate was taken in order to collect the laid embryos and was replaced with a fresh plate.

The rest of the injection procedure took place in a room maintained at 18°C. The embryos were collected from the apple-agar plate using a small paintbrush and transferred to a small sifting basket with a mesh bottom that was partially submerged in water. After a sufficient amount of embryos were transferred, excess water was removed by blotting the basket briefly on absorbent paper. Next, the embryos were dechorionated for 3-5 min in 1.8% bleach (sodium hypochlorite solution). In order to keep the bleaching time as short as possible, the process was monitored under a dissecting scope. The embryos were then rinsed several times with water, aiding the removal of the chorions.

The dechorionated embryos were transferred by paintbrush to a slice of apple-agar (5 x 50 mm) on a resting microscope slide. Now, the embryos could be lined up in a row using a small dissecting needle. The embryos were oriented so that the anterior end was close to the near edge of the agar slice. Usually, 80-100 embryos were placed in the same direction, close together but not touching. The row of embryos was transferred to a coverslip (24 x 64 mm) with a 5-mm wide strip of double-sided tape along one edge. The coverslip was lowered carefully on the embryos so that the posterior end of the embryos pointed outward when attached to the tape and were set back approximately 0.5 mm.

Before injection, the embryos were briefly dried in order to reduce hydrostatic pressure. Optimal drying time depended on the humidity and temperature of the room (18°C) as well as the state of the silica gel crystals used for drying. Older silica gel obtains a pinkish color and requires a longer drying time. Therefore, embryos were dried for 5-7 min and then covered with a thin layer of Voltalef halocarbon oil to prevent further drying. The coverslip with embryos was placed on a slide also using oil and adjusted into the slide holder for the microscope (Olympus).

While embryos were drying, the injection needle (Injection Needle Femtotips, Eppendorf) was loaded with 2 µl injection mix using microloader tips (Eppendorf). The injection needle was carefully placed in the holder of the injection apparatus (Leitz) and brought into focus under the microscope. The injection needle was brought backwards as the slide with the embryos was brought into focus. The needle was then moved forwards so it was positioned slightly above the coverslip and oil. As the needle was brought into the oil, it was tested for suitable DNA flow through the needle tip. The tip was then used to puncture the posterior end of the embryos, and the DNA mix was injected using an Eppendorf Microinjector 5242. From egg collection to injection of embryos, the procedure took no more than 1.5 h. Any embryos that were deemed too old and had already begun the nucleation process were destroyed using the injection needle.

### **Establishment of transgenic lines**

After injection the embryos were kept at 18°C in oil until hatching (2-3 days). Newly hatched larvae were placed in standard stock fly food to develop. After eclosion, adult flies were backcrossed with three *w<sup>1118</sup>* flies of the appropriate sex, making sure that

any transgenic or  $w^{1118}$  females were virgins. Because the pUAS<sub>t</sub> vector contains a copy of the mini-white<sup>+</sup> gene, any flies in the F1 generation that contained the transgene would have yellowish to orange eyes. These F1 generation flies were taken and backcrossed again with  $w^{1118}$  flies. Any F1 flies with red eyes were avoided as they most likely contained multiple copies of the transgene. Usually, 3-4 backcrosses were sufficient to establish a homozygote transgenic line.

#### **2.2.4.4 Genetic crosses**

The Gal4/UAS system was utilized to express genes of interest (i.e. ARQ22, ARQ77, etc.) in specific tissues of *Drosophila melanogaster*. To summarize, in any given “driver” fly line, a promoter (enhancer) directs expression of the yeast transcription factor GAL4 in a specific pattern. GAL4 then directs transcription of the Gal4-responsive (UAS) target gene in an identical pattern. GMR-GAL4 (glass multimer reporter) and ELAV-GAL4 (embryonic lethal abnormal vision) lines were used to direct expression of the AR in the photoreceptor neurons and throughout the central nervous system, respectively. To cross flies, virgin female flies were collected from the desired GAL4 line. Typically 8-10 virgin females were crossed with 3-4 males from the desired UAS-AR line. Depending on the experiment, crosses were either made on standard medium, medium containing hormone and/or inhibitors, or apple agar plates.

#### **2.2.4.5 Scanning electron microscopy**

Flies of the correct age and phenotype were anesthetized with CO<sub>2</sub>, and heads were separated from the bodies. Freshly collected heads were then transferred stepwise to 100% ethanol (1 h each in 30%, 50%, 70%, 90%, 95%).

For microscopy, three heads of each phenotype were mounted on an aluminum stub using double stick carbon tape. Samples were then introduced into the chamber of the sputter coater (Balsers) and coated with a very thin film of gold/palladium before SEM examination.

#### 2.2.4.6 Immunohistochemistry

Wandering third-instar larvae were dissected in Ringer solution, separating the CNS. Brains were fixed in 1 ml 0.5 PBT + 4% formaldehyde for 1 h. The brains were then washed in PBT (5/5/15/30 min) and transferred stepwise to 100% methanol (5 min 30%, 5 min 70% MeOH in Ringer solution). The samples were then stored at -20°C in 100% MeOH overnight.

The next day the brains stored in 100% MeOH were transferred stepwise back to Ringer solution (5 min 70%, 5 min 30% MeOH). The brains were then washed extensively (5/15/15/30/30/60 min) with PBT and blocked for 1 h in 0.5 PBT + 5% goat serum. The blocking solution was then exchanged and primary antibodies were added (1:1000 Draq5 and 1:200 AR C-19). The brains were incubated overnight, rotating at 4°C.

After overnight incubation, the supernatant was discarded, and the brains were washed extensively (5/5/15/30/60 min) with 0.1 PBT. The brains were blocked in 0.5 PBT + 5% goat serum for 1 h. The blocking solution was exchanged and fluorescently labeled secondary antibody was added (1:200 anti-rabbit-Cy2). The brains were incubated for 1.5 h at room temperature in the dark or overnight at 4°C. Finally they were washed in 0.1 PBT (5/15/15/30 min) and mounted in Mowiol. Slides were kept in a dark cool place to dry and eventually stored at 4°C.

<b>Buffers</b>	<b>Composition</b>
0.1 PBT	0.1% (v/v) TritonX100 in PBS
0.5 PBT	0.5% (v/v) TritonX100 in PBS
Ringer	182 mM KCL, 46mM NaCl, 3 mM CaCl <sub>2</sub> , 10mM Tris
Mowiol	24 ml glycerol, 9.6 g Mowiol, 24 ml H <sub>2</sub> O, 48 ml 0.2M Tris-HCl pH 8.5

#### 2.2.4.7 Locomotion analysis

Transgenic fly lines were crossed with ELAV-GAL4 flies on standard medium. Once crosses were producing a sufficient amount of viable eggs, crosses were transferred to apple-agar plates containing yeast paste. After 72 hours, first instar larvae were

collected from the agar and yeast paste, washed, and placed back on the apple agar plates. The first-instar larvae were then collected and placed in stock food containing the following hormone and inhibitor combinations:

- 10<sup>-3</sup>M DHT + equivalent volume of 80% ethanol
- 10<sup>-2</sup>M melatonin + one volume 80% ethanol
- 100 mM sodium butyrate + one volume 80% ethanol
- 2 volumes 80% ethanol
- 10<sup>-3</sup>M DHT + 10<sup>-2</sup>M melatonin
- 10<sup>-3</sup>M DHT + 100 mM sodium butyrate

After 72 hours, wandering third-instar larvae were placed individually in the center of a 10 cm dish containing a flat layer of 0.7% agar on an evenly illuminated light box emitting infrared light (Lee et al., 2004). Movement of the larvae was recorded and analyzed using Noldus EthoVision version 3.1.16. The recording time was 2.5 minutes or until the larvae reached the edge of the agar, which was outside the recording arena. Parameters analyzed by the EthoVision program included velocity, angular velocity, and mean turn angle.

#### ***2.2.4.8 Survival analysis***

Transgenic fly lines were crossed with ELAV-GAL4 flies on standard medium. Once crosses were producing a sufficient amount of viable eggs, crosses were transferred to apple agar plates containing yeast paste. After 36 hours, eggs were collected from the agar and yeast paste, washed, and placed back on apple agar plates until hatching. Directly after hatching, larvae were placed in stock food containing the following combinations of hormone and inhibitors:

- 10<sup>-3</sup>M DHT + equivalent volume of 80% ethanol
- 10<sup>-2</sup>M melatonin + one volume 80% ethanol
- 100 mM sodium butyrate + one volume 80% ethanol
- 2 volumes 80% ethanol
- 10<sup>-3</sup>M DHT + 10<sup>-2</sup>M melatonin
- 10<sup>-3</sup>M DHT + 100 mM sodium butyrate

Larvae were placed at a rate of 50 larvae per food vial. The percentage of larvae surviving to pupation and eclosion was then calculated.

## **2.2.5 Methods for work with protein from cells and *Drosophila***

### **2.2.5.1 Preparation of protein lysates**

#### **Preparation of protein lysates from COS7 cells**

Cells at 80-90% confluency, typically grown in a 6-well or 10 cm plate, were washed twice with ice-cold PBS, collected in 1 ml PBS, spun down for 3 min at 4000 rpm at 4°C, resuspended in 100 µl of PBS + protease inhibitor cocktail, and lysed with 3 freeze-thaw cycles. Then the lysates were centrifuged for 10 min at 12000 rpm at 4°C, and the supernatants were taken and stored at -80°C. Alternatively, after collection of cells in 1 ml PBS, cells were lysed with NP40 lysis buffer, and whole cell lysates were stored at -20°C.

<b>Buffers</b>	<b>Composition</b>
NP40 lysis buffer	150 mM NaCl, 50 mM Tris-HCl pH 8.0, 5 mM EDTA pH 8.0, 1% NP40

#### ***Drosophila* lysates**

Flies of the correct age and phenotype were collected and snap frozen by putting them in an eppendorf tube on dry ice. Working on dry ice, 50 heads were separated from bodies using forceps and a razor blade (Wilkinson-Sword) and placed in a tube on dry ice. 50 µl RIPA buffer was added, and heads were crushed using a glass rod. The homogenized mixture was sonified with 3 x 10 s pulses (Bioruptor) and then centrifuged for 5 min at 4°C, 13000 rpm (centrifuge Eppendorf 5417 R). The supernatant was transferred to a fresh tube, and the head pellet was resuspended in 50 µl RIPA. The sonification and centrifugation steps were repeated, and the supernatant was added to the previous. When necessary, lysates were stored at -20°C.

<b>Buffer</b>	<b>Composition</b>
RIPA buffer	50 mM Tris HCl pH 7.6, 1% Triton, 0.5% NaDOC, 150 mM NaCl, 0.1% SDS, 2 mM EDTA + 1:200 protease inhibitor cocktail

### ***2.2.5.2 Determination of protein concentration***

The Bradford assay was used to determine the protein concentration of cell and *Drosophila* lysates. 0.5 µl lysate sample was mixed with 250 µl of 1X Bradford reagent (Bio-Rad) in an eppendorf tube. As a protein standard, 250 µl 1X Bradford reagent was mixed with increasing amounts of 1 µg/µl BSA solution (e.g. 0, 2, 4, 6) where the BSA had been diluted in the appropriate lysis buffer. 200 µl of each solution was transferred into an ELISA plate, and the optical density (OD) was measured immediately at 600 nm.

The standard curve was determined by using the results obtained from the BSA dilutions in the equation,  $y=ax + b$ .

“y” = amount of protein in µg

“x” = the OD reading.

“a” = slope of the line

“b” = origin on y axis

### ***2.2.5.3 Separation of proteins by SDS polyacrylamide gel electrophoresis***

Usually 10% SDS-Polyacrylamide gels were used. The Penguin Doppelgelsystem P9DS apparatus (Peqlab, Erlangen, Germany) was used to cast the gel. 20 ml of resolving gel were poured and overlaid with Rotisol. After polymerization, Rotisol was washed off with deionized water. 10 ml of stacking gel were then added and allowed to polymerize. The gel was fixed within the gel tank and 1X Laemmli buffer (running buffer) was poured over the gel. The desired amounts of cell or *Drosophila* lysate were mixed 1:1 in 2X SDS sample buffer, boiled at 95°C for 5 min, and loaded by lane onto a SDS-PAGE. Samples were run into the stacking gel at 80V, and then run at 150V for approximately 3 hours or 40V overnight.

<b>Buffers and gel solutions</b>	<b>Composition</b>
10% SDS-Polyacrylamide gel	9.9 ml acrylamide/bis-acrylamide 30:0.8, 11.7 ml 1 M Tris-HCl pH 8.8, 8.4 ml bi-distilled H <sub>2</sub> O, 150 ml 20% (w/v) SDS, 300 ml 10% APS, 15 ml TEMED
Stacking gel (5% SDS-polyacrylamide)	7.3 ml bi-distilled H <sub>2</sub> O, 1.68 ml acrylamide/bis-acrylamide, 0.69 ml 1 M Tris-HCl, pH 6.8, 56 ml 20% SDS; 45 ml 10% APS and 15 ml TEMED
1X Laemmli buffer	25 mM Tris, 200 mM glycine, 0.1% (w/v) SDS
2X SDS sample buffer (50 ml)	28.74 ml H <sub>2</sub> O, 6.26 ml Tris-HCl pH 6.8, 10 ml 20% SDS, 5 ml β –Mercaptoethanol, a few grains of bromophenolblue

#### **2.2.5.4 Western blotting**

After proteins were separated by SDS-PAGE, they were electrically transferred onto Immobilon membrane (Millipore, type PVDF, pre-soaked in methanol) at 250-300 mA for at least 6 hours in transfer buffer. Immunoblotting was performed according to individual instructions for each antibody. Typically, in order to reduce unspecific binding of the antibodies to the membrane, the blot was incubated in blocking solution at RT for 1 h with shaking. For detection of proteins of interest the membrane was incubated in blocking solution containing the appropriate primary antibody (optimal working dilution was determined empirically) at room temperature for 3h or 4°C overnight. After 3 washes of 5 min each in PBST, the membrane was incubated 1 hour in blocking solution containing a 1:2000 dilution of HRP-conjugated secondary antibody. Once the membrane had been washed 3 times for 5 min each, detection of specific proteins was achieved by enhanced chemiluminescence using ECL Western blotting detection reagents as recommended by the manufacturer (Amersham, Braunschweig, Germany) and exposure to ECL Hyperfilm (Amersham, Braunschweig, Germany) .

<b>Buffers</b>	<b>Composition</b>
Transfer buffer	25 mM Tris, 190 mM glycine, 20% (v/v) methanol, and 0.05% (w/v) SDS
Blocking solution	1x PBS, 0.05% Tween, 3-5% milk powder
PBST	1x PBS, 0.05% Tween
<b>Primary Antibodies</b>	<b>Dilutions</b>
anti- AR F39.4.1	1:1000
anti- AR (N-20)	1:200
anti-ERK 2 (D-2)	1:3000
anti-Polyglutamine-Expansion Diseases Marker (1C2)	1:5000
anti- $\alpha$ - Tubulin (H-300)	1:200

#### ***2.2.5.5 Stripping of the Western blot membranes***

To allow more than a single use of Western blot membranes, the membranes were incubated with a stripping solution at 50°C for 30 min with shaking. The membranes were then washed five times for 5 min in 1X PBS without Ca- and Mg-.

<b>Buffers</b>	<b>Composition</b>
Stripping Solution	62.5 mM Tris, pH 6.8, 2% SDS, 0.75% 2-mercaptoethanol

#### ***2.2.5.6 Filter trap analysis of aggregates***

##### **Filter trap**

Transfected COS7 cells were harvested and lysed in NP40 lysis buffer. For larvae analysis, third-instar larvae were homogenized in RIPA buffer. Total protein concentration was measured using the Bio-Rad Bradford assay. Equal protein amounts of cell or larval lysate were brought to a concentration of 2% SDS/ 50mM DTT, boiled for 3 min, and applied to a 0.22  $\mu$ m cellulose acetate membrane (Schleicher and Schuell) that

had been washed three times with 0.1% SDS, 10 mM Tris pH 8.0, 150mM NaCl in a slot blot apparatus. Samples were gently vacuumed, and the membrane was washed twice more with the same wash buffer. Insoluble AR protein was analyzed using anti-AR antibody, (1:200 AR N-20) (Santa Cruz Biotechnologies).

### **Dot blot**

To demonstrate equal AR expression in transfected cells, dot blot analysis was performed by applying 1 µg of protein lysate to a nitrocellulose membrane (Hybond-C pure). The membrane was allowed to dry and then probed with anti-AR antibody, AR N-20.

### **2.2.5.7 Immunoprecipitation**

#### **Preparation of protein A sepharose beads**

An amount corresponding to 300-500 µl of Protein A Sepharose beads were mixed with 10 ml TE in a 15 ml Falcon tube. The beads were shaken for 2 h at 4°C and then centrifuged for 3 min at 2000 rpm. Beads were washed twice with TE and resuspended in 3 volumes TE for a 25% bead slurry.

<b>Buffers</b>	<b>Composition</b>
TE buffer	10 mM Tris-HCl, 1 mM EDTA pH 8.0

#### **Immunoprecipitation of protein**

*Drosophila* lysates were freshly prepared in RIPA buffer with added inhibitors. Lysates were brought to a volume of 950 µl with RIPA buffer + inhibitors. Primary antibody (50 µl AR44) was added, and the mix was incubated overnight, rotating at 4°C.

The next day 100 µl 25% Protein A Sepharose bead slurry was added to the lysate/antibody mix and incubated for 3 h, rotating at 4°C. Mixes were then centrifuged for 1 min at 4°C, 14000 rpm. The resulting bead pellet was washed five times by vortexing with 500 µl RIPA + inhibitors. Beads were kept on ice during washes. Bead

pellets were resuspended in 40-50  $\mu$ l of 2X sample buffer, boiled at 95°C, and loaded onto SDS-PAGE. Samples were further analyzed by Western blotting.

<b>Buffers</b>	<b>Composition</b>
RIPA + inhibitors	50 mM Tris HCl pH 7.6, 1% Triton, 0.5% NaDOC, 150 mM NaCl, 0.1% SDS, 2 mM EDTA , 1 mM Na <sub>3</sub> VO <sub>4</sub> , 50 $\mu$ M ZnCl <sub>2</sub> , 1:200 protease inhibitor cocktail
2X SDS sample buffer	28.74 ml H <sub>2</sub> O, 6.26 ml Tris-HCl pH 6.8, 10 ml 20% SDS, 5 ml $\beta$ –Mercaptoethanol, a few grains of bromophenolblue

## **3.0 RESULTS**

### **3.1 Mutation of distinct serine residues at the N-terminus of the AR**

For the polyglutamine (polyQ) disorders, the details of the various pathways which begin with the presence of the polyQ stretch and lead to the misfolding of the affected proteins and death of specific subsets of neurons are still largely unknown. Several recent studies have shown that protein modification or sequences outside the amplified polyQ stretch exert significant effects on the disease progression (LaFevre-Bernt and Ellerby, 2003; Okamura-Oho et al., 2003; Thomas et al., 2004; Luo et al., 2005; Duennwald et al., 2006). Therefore candidate amino acid residues neighboring the polyQ stretch of the androgen receptor (AR) were identified and subsequently investigated as to whether alterations of these sites would affect the properties of this protein that are characteristic of polyQ cytotoxicity.

#### **3.1.1 Two possible phosphorylation sites shown *in vitro***

As an attribute of being a steroid hormone receptor, the AR is dependent upon phosphorylation for its normal functional activity as a transcription factor (Lin et al., 2001). In general, phosphorylation is also known to bring about conformational changes of proteins associated with neurodegeneration (Buee et al., 2000). Due to the fact that all of the polyQ proteins exhibit both gain-of-function features as well as undergo conformational changes in the disease processes (Ross, 2002), it is very likely that phosphorylation of the proteins through the various signalling cascades plays a significant role in the aggregation and toxicity of the polyQ disorders. In the specific case of SBMA, the MAPK/ERK signalling pathway has been implicated in the disease mechanisms. Previous studies have shown that a mutation at serine 514, a putative site of phosphorylation by a proline directed serine kinase at the N-terminus of the AR, blocked cell death induced by an AR with an amplified polyQ stretch (LaFevre-Bernt and Ellerby, 2003). In an *in vitro* kinase assay performed by Dr. Sigrun Mink, a former member of the lab, it was confirmed that the N-terminal amino acid sequence 360-557 of the AR is phosphorylated by the proline directed serine kinase ERK (Fig. 3.1A). Although the levels were reduced in comparison to the normal ERK phosphorylation substrate, basic

myelin protein (MBP), amino-terminal fragments of the nuclear receptor coactivator p300 or dihydrofolate reductase (DHFR) proteins that were used as negative controls were not phosphorylated (Fig. 3.1A). Next, in attempt to localize which serine residues were responsible for the demonstrated phosphorylation by ERK, Dr. Mink analyzed the effect on *in vitro* phosphorylation of an alanine substitution of the known ERK consensus site at serine 514. Contrary to published data (Yeh et al., 1999), an alanine substitution at serine 514 did not abolish the *in vitro* phosphorylation by ERK2 (Fig. 3.1B). Therefore the nearby serine 424, which shares a similar sequence to the ERK consensus sequence, was also substituted with an alanine residue. Only with the simultaneous substitution of serines 514 and 424 by alanine residues was phosphorylation blocked. An exchange of serine 424 alone was also not enough to abolish the *in vitro* phosphorylation (Fig. 3.1B). Interestingly, serine 424 is one of five serine residues [16, 81, 256, 308 and 424] at the N-terminus of the AR that shows an increased phosphorylation in the presence of androgen (Gioeli et al., 2002; Yang et al., 2005).

Because simultaneous mutations at serines 424 and 514 were able to block *in vitro* phosphorylation of the AR by ERK and ERK signalling has been implicated in SBMA and Huntington's (LaFevre-Bernt and Ellerby, 2003; Apostol et al., 2006), it was deemed plausible that a double mutation of these sites may also effect the conformation of the AR as well as the polyQ aggregation and toxicity associated with SBMA. These mutations were therefore introduced into the full length AR with a polyQ stretch of 22 or with an amplified polyQ tract of 77, termed ARQ22dm and ARQ77dm respectively, for determination of structural alterations.

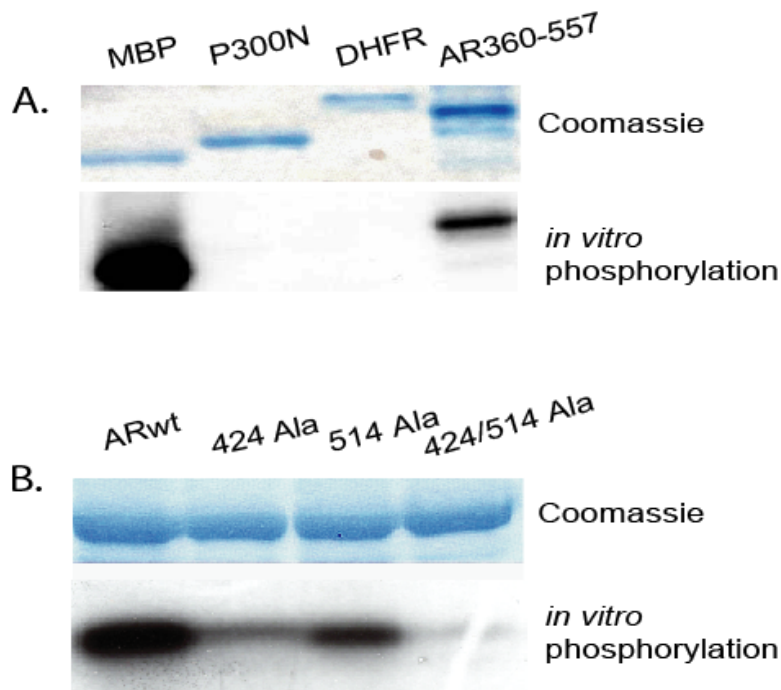


**Figure 3.1 *In vitro* MAP Kinase ERK2 phosphorylation of the region 360-536 of the AR reveals two possible phosphorylation sites**

The region between amino acids 360 -536 of androgen receptor can be phosphorylated by ERK2 *in vitro*. Purified proteins were incubated with recombinant ERK2 in the presence of [ $\gamma$ - $^{32}$ P] ATP, separated by SDS page and visualized by autoradiography. Duplicate gels were stained with Coomassie blue to demonstrate equal loading (upper panels). (A) An *in vitro* phosphorylation assay shows MAP kinase phosphorylation of AR(360–536). AR(360-536) was used as a substrate for the phosphorylation reaction together with myelin basic protein (MBP) as a positive control and dihydrofolate reductase (DHFR) protein fragment and the amino terminal portion of p300 (amino acids 551-753) as negative controls. (B) Mutated AR(360–546) fused to GST is phosphorylated by ERK2. GST-fusion proteins of the AR(360-536) as well as the 360–546 sequence with the serine residues at position 424 or 514 or both exchanged for alanine residues were used as substrates for *in vitro* phosphorylation reactions. Shown is the autoradiograph of the phosphorylation analysis.

### 3.1.2 Conformational changes induced by substitution of serine residues 424 and 514

In the polyQ disorders, one important step in the pathogenic mechanisms is accepted to be a misfolding or conformational change from the “wild type” structure of the polyQ proteins. The consequences of this misfolding include changes in protein-protein interactions, changes in homeostasis, and aggregate formation (Paulson et al., 2000). It is likely that any mutation of the protein that would have an effect on polyQ toxicity, especially mutations of sites for covalent modifications, would affect the structure of the protein. Hence, the first step in examining the effects of mutating AR serines 424 and 514 on possible aggregation and polyQ toxicity was to investigate local conformational changes in the AR N-terminal region brought about by the mutations. Demonstrating sensitivity of a protein to proteases has been shown to be one method of determining alterations in folding in a polyQ disease model (Gidalevitz et al., 2006). Additionally, limited proteolytic digestion has been successfully used by other investigators to demonstrate conformational changes in the AR and other nuclear receptors (Allan et al., 1992; Neuschmid-Kaspar et al., 1996; Lazennec et al., 1997). Therefore, a limited proteolytic digestion of the AR was performed in collaboration with Dr. Liubov Shatkina, a former member of the lab.

The four variants of the AR (ARQ22/wild type, ARQ22dm, ARQ77, and ARQ77dm) were synthesized *in vitro* and radiolabeled with [<sup>35</sup>S] methionine so the receptors could later be visualized by fluorography. The receptors were then subjected to digestion by the serine protease trypsin, a commonly used protease in proteomics experiments for digestion of proteins into peptides. Trypsin was also the protease of choice for detecting structural alterations in the AR in previous studies (Neuschmid-Kaspar et al., 1996; Reid et al., 2002). Digestion with trypsin was able to demonstrate distinct differences in the digestion patterns of ARQ22 and ARQ77 as well as between their cognate mutants (Fig. 3.2). A comparison of ARQ22 and ARQ22dm or ARQ77 and ARQ77dm showed two clear differences. First, although the digestion patterns for ARQ77 and ARQ77dm were similar, an upward shift was exhibited by the fourth and fifth bands (marked with asterisks) in the ARQ77dm pattern. These distinct protease digestion fragments ran at 55kDa and 60kDa on the polyacrylamide gel, thus being larger fragments than the corresponding fourth and fifth bands of the ARQ77. Second, the

ARQ22dm and ARQ77dm proteins were highly sensitive to protease digestion such that they were fully digested by 30 min of incubation with the trypsin solution. The ARQ22 and ARQ77 proteins were relatively resistant to the tryptic digestion (Fig. 3.2). These results indicated that the two serine mutations did indeed produce an alteration in the structure of the AR.

With this first experimental step clarified, the mutated receptors were then used in a cell culture model to examine the effect of the amino acid substitutions on properties of the AR associated with SBMA and polyQ toxicity in general. These altered properties are namely nuclear localization and the subsequent transactivation function of the receptor as well as aggregate formation and toxicity following treatment with androgen.

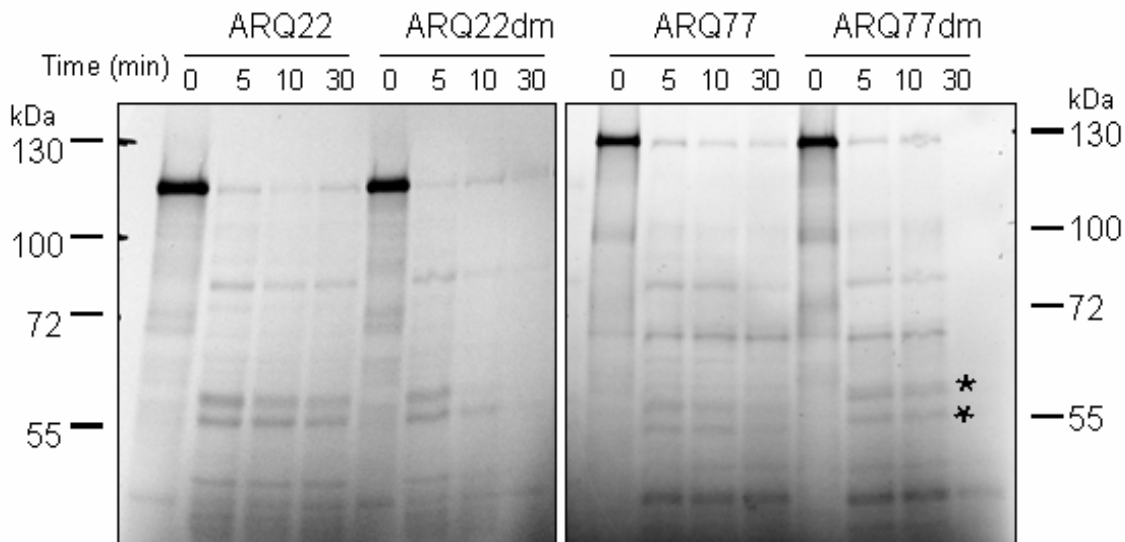


**Figure 3.2 Mutation of serine residues 424 and 514 leads to conformational changes in wild type AR and an AR with an extended polyQ stretch**

ARQ22, ARQ22dm, ARQ77 and ARQ77dm were *in vitro* transcribed and translated in a TNT coupled reticulocyte lysate system of Promega in the presence of [<sup>35</sup>S] methionine. The *in vitro* synthesized receptors were incubated at room temperature in the presence of trypsin (2.5 µg/ml) for the indicated time periods. The reactions were terminated by the addition of denaturing gel loading dye and the products were fractionated on an 8% SDS-polyacrylamide gel. The gels were dried and the radioactive peptides visualized by fluorography. The pictures demonstrate the fragment pattern generated from the androgen receptors loaded with agonist. The asterisks indicate the position of migration of the 55 and 60 kDa fragments generated from ARQ77dm.

## **3.2 Cell culture model used to investigate *in vivo* effects of serine site mutations**

In order to characterize the four structurally diverse AR variants, the receptors were transiently expressed in COS7 cells, an African green monkey kidney fibroblast-like cell line that is AR deficient. This cell line was chosen due to its reliable transfection efficiency and because of its proven ability to act as a model for the different polyQ disorders (Ho et al., 2001; Nozaki et al., 2001; Bailey et al., 2002; Chou et al., 2006).

### **3.2.1 Mutation of serine 424 and 514 residues affects nuclear localization and transactivation by the AR**

The localization of the polyQ proteins to the nucleus has been deemed a key aspect in polyQ pathogenesis (Klement et al., 1998; Saudou et al., 1998; Diamond et al., 2000). As a ligand-activated transcription factor, the AR is dependent on androgen binding for relocation from the cytoplasm to the nucleus. Therefore, models of SBMA are also dependent on the ligand binding that leads to nuclear localization for aggregation and toxicity to occur. Another aspect closely linked to this nuclear translocation is the alteration of transcriptional activity in polyQ affected neurons. Several reports have indicated the polyQ proteins in disruption of transcription (Riley and Orr, 2006). In the case of the polyQ expanded AR in SBMA, the AR itself is known to exhibit altered transcriptional activity (Thomas et al., 2006b). Hence, an initial way to characterize the effects of mutating serine sites 424 and 514 in the wild type and polyQ AR was to examine changes in cytoplasmic-nuclear transport as well as differences in transactivation by the receptors following hormone treatment.

### ***3.2.1.1 Accumulation of AR in nucleus altered with AR mutants***

To view changes in the compartmentalization of the AR, the wild type and mutated AR expression vectors were transiently transfected in COS7 cells. Cells were then treated with the androgen 5 $\alpha$ -dihydrotestosterone (DHT) for varying time points up to 2.5 h to allow for redistribution. After harvesting and fixation of the cells, staining with an AR antibody that was then followed by a fluorescently labelled secondary antibody allowed for visualization of the subcellular distribution of the AR. All immunofluorescence experiments were performed in collaboration with Dr. Shatkina.

The cytoplasmic-nuclear localizations of the receptors were grouped into four categories as illustrated in Fig. 3.3A, and the statuses of the AR variants were thus able to be compared at the different time points. First noted was a marked delay and decrease in nuclear accumulation of ARQ77 compared to ARQ22 as previously reported (Becker et al., 2000) (Figs. 3.3B and C). Surprisingly, when compared with the wild type ARQ22, the ARQ22dm also showed a lag in nuclear accumulation at 30 min and 1.5 h after treatment with DHT (Fig. 3.3D; \* $p \leq 0.05$ ). The reverse effect was observed in the cytoplasmic-nuclear transport of ARQ77dm when compared with its ARQ77 counterpart in that there was an increase in the percentage of cells exhibiting a nuclear distribution, especially after 30 min and 1.5 h of DHT treatment (Fig. 3.3E; \*  $p \leq 0.05$ ). The majority of transfected cells containing each of the AR constructs showed nuclear staining after 2.5 h of hormone treatment.

From these experiments it could not be determined whether a true delay in nuclear transport was occurring or rather an increase in fast nuclear export of the receptor. In either scenario, it was reasoned that the presence or lack thereof of the AR in the nucleus may affect transcriptional activity and other facets of polyQ pathogenicity.

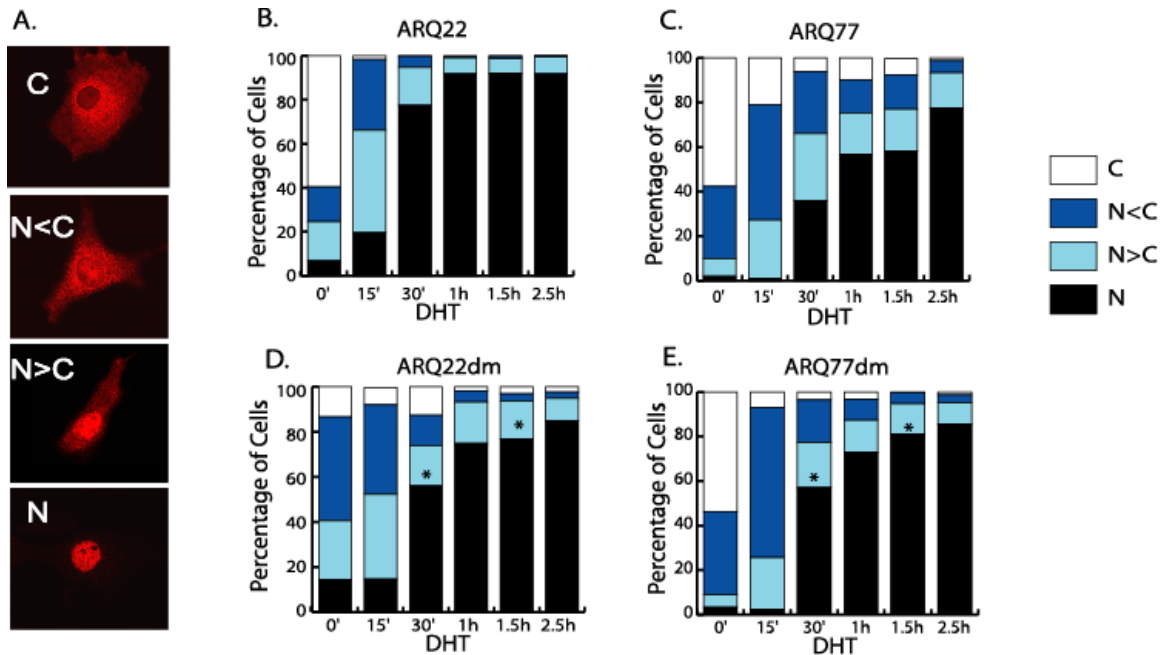


**Figure 3.3 Kinetics of cytoplasmic-nuclear transport is altered after mutation of serine residues 424 and 514**

COS7 cells were transiently transfected with 1.5  $\mu\text{g}$  ARQ22, ARQ22dm, ARQ77 or ARQ77dm expression vector. Approximately 48 h after transfection, the cells were treated either with vehicle or  $10^{-7}\text{M}$  DHT for the indicated time periods, harvested, and stained with a mouse monoclonal anti-AR antibody F39.4.1 followed by an anti-mouse antibody labeled with a fluorescent dye Cy3. The cells were visualized with a LSM 510 inverted Zeiss confocal microscope. (A) Subcellular localization of the AR proteins was determined by the percentage of positive stained cells and was categorized into the four indicated stages. The bar charts show the percentage of cells at each stage for (B) ARQ22, (C) ARQ77, (D) ARQ22dm, and (E) ARQ77dm after control and hormone treatment for the indicated time periods. For each AR construct, at each time point, 200-250 cells were analyzed in three different experiments. The results show the average values of these analyses and the results of ARQ22dm and ARQ22 as well as ARQ77dm and ARQ77 were compared by t-test  $*p \leq 0.05$

### 3.2.1.2 Transactivation by wild type AR affected by polyQ stretch and serine mutations

As demonstrated by the nuclear localization assay, treatment of the AR with DHT leads to accumulation of the AR in the nucleus. Once in the nucleus, the AR binds to androgen responsive elements (AREs) of DNA and regulates gene transcription. In order to determine whether the differences seen in the kinetics of nuclear localization translated into differences in transcriptional activity of the AR constructs, a luciferase-reporter gene assay was utilized to measure the transactivation activity by the wild type and mutated AR expression vectors. Each of the AR constructs were transiently transfected in COS7 cells in conjunction with a reporter plasmid containing the firefly luciferase gene under the control of the mouse mammary tumor virus (MMTV), whose long-terminal repeat (LTR)-promoter contains hormone responsive elements. Therefore, any hormone-dependent gene regulation through the AR would lead to production of luciferase, which emits light with interaction of its cognate substrate luciferin. Transactivation activity by the AR could thus be quantified by adding luciferin substrate to cell lysates and using a luminometer to measure light production. Additionally, a *Renilla* luciferase reporter construct was co-transfected as an internal control. A comparison of firefly luciferase activity to *Renilla* luciferase activity yielded the relative luciferase/transactivation activity for each experiment.

The most obvious disparity in transcriptional activity by the four receptors was due to the presence of the polyQ expansion. Not only did the ARQ77 background demonstrate lower basal activity in comparison to the receptors containing a polyQ stretch of 22 (Fig. 3.4A) but the fold induction was also considerably reduced (Fig 3.4B). This result corroborated the inverse correlation between polyQ length and transactivation by the AR that has been previously reported (Irvine et al., 2000; Thomas et al., 2006b). As for the effect of the serine site mutations, the ARQ22dm showed a significant decrease in basal activity in comparison to the wild type ARQ22 (Fig. 3.4A; \* $p \leq 0.05$ , \*\* $p \leq 0.005$ ). This decrease in basal activity also meant an overall decrease in transcriptional activity following treatment with DHT, a pattern similar to that of the toxic polyQ AR. However, the presence of the serine mutations resulted in an increase in fold-induction for the ARQ22 background (Fig. 3.4B), demonstrating this particular

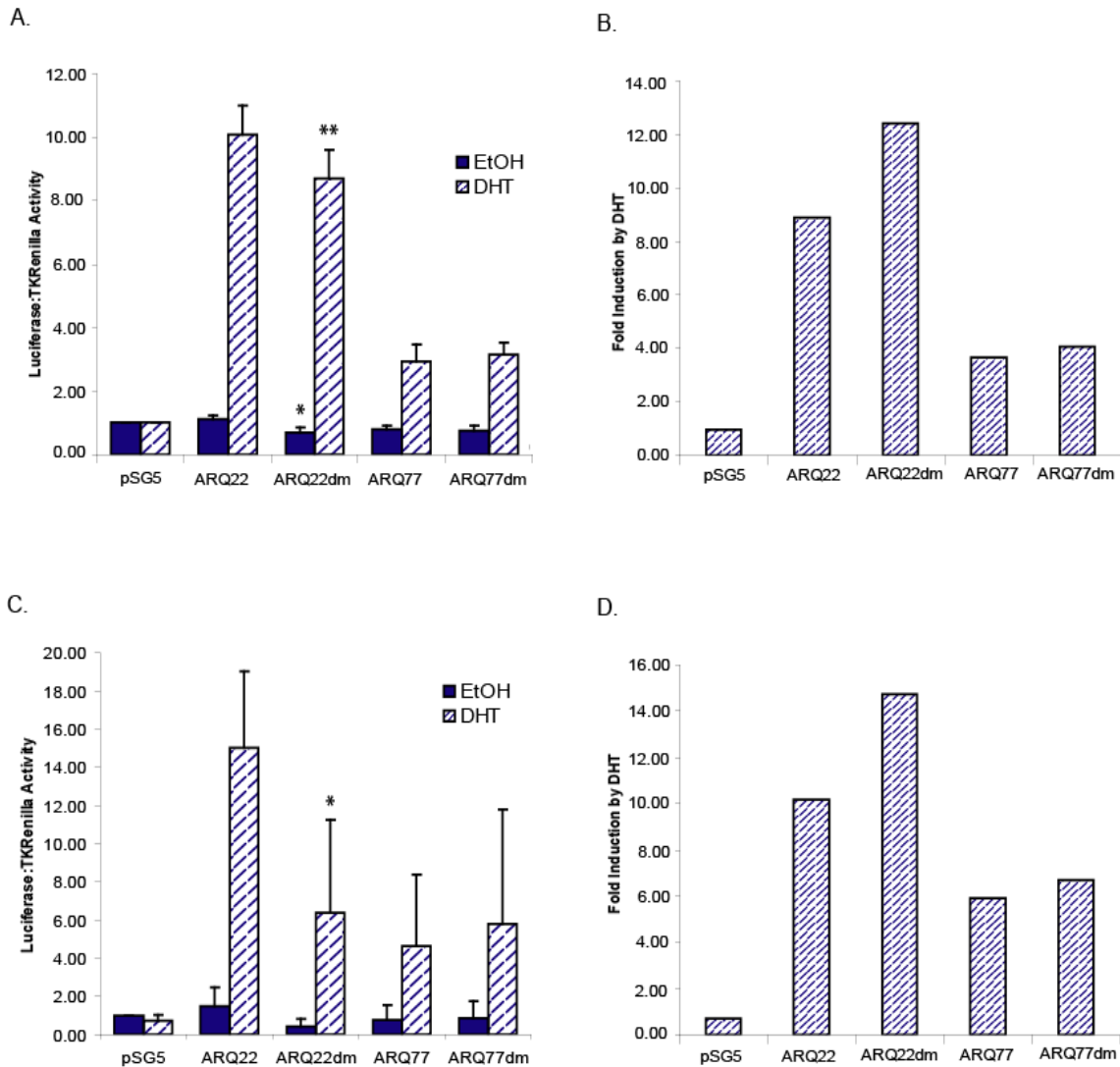


**Figure 3.4 Transactivation by the AR is altered in mutant variants**

COS7 cells were transiently transfected with 0.5  $\mu\text{g}$  pSG5 vector, ARQ22, ARQ22dm, ARQ77 or ARQ77dm expression vector, 0.3  $\mu\text{g}$  TKRenilla, and 1.2  $\mu\text{g}$  MMTV or Probasin. Approximately 24 h after transfection, cells were treated either with vehicle or  $10^{-7}\text{M}$  DHT for 16 h. Cells were then harvested and assessed for luciferase activity. TKRenilla activity was used as an internal control. (A) Relative luciferase activity using the MMTV promoter was lower for the ARQ22dm in comparison to ARQ22. (B) However, the ARQ22dm shows a higher fold induction. The fold induction by DHT was calculated based on the mean relative luciferase activities. (C) The probasin promoter revealed the same trend of lower transcriptional activity. (D) Fold induction values for the probasin promoter were similar to that of the MMTV. \* $p < 0.05$ , \*\* $p < 0.005$ ; Error bars represent standard deviation.

receptor's unique properties. There were no significant differences in activity with and without hormone treatment between the ARQ77 and ARQ77dm constructs.

As an alternative to the MMTV promoter, which responds not only to androgens and glucocorticoids but also mineralocorticoids and progestins through inverted repeat glucocorticoid responsive elements (GREs) (Ham et al., 1988), the probasin promoter was also used to assess changes in hormone-dependent transcriptional activity. The probasin gene codes for a rat prostate protein and is regulated *in vitro* (Dodd et al., 1983) and *in vivo* by androgens (Rennie et al., 1993). Androgen induction of expression of the probasin gene is mediated by two direct repeat androgen receptor binding sites and thus exhibits strong AR-specific regulation. Use of the probasin promoter did indeed lead to an increase in androgen responsiveness (compare Figs. 3.4 A and B with C and D). However, the overall depiction of transactivation was not so different from the MMTV results (Figs. 3.4C and D). With the probasin promoter, the overall activity of the ARQ22dm was again significantly reduced in comparison to the wild-type ARQ22 (Fig. 3.4C; \*  $p \leq 0.05$ ), and the increase in fold induction by the ARQ22dm was reproduced. Also, the serine mutations again did not affect the lower basal transcriptional activity or fold inductions seen in the ARQ77 background (Figs. 3.4C and D).

With alterations in nuclear localization (ARQ22dm and ARQ77dm) and transcriptional activity (ARQ22dm) established, it was deemed necessary to further explore how the serine site mutations altered the wild type and toxic polyQ AR properties. Therefore, the AR variants' propensity to form the aggregates that are characteristic of the polyQ disorders was explored.

### **3.2.2 Mutation of serines 424 and 514 affects the formation of intracellular inclusions by the AR**

A major defining feature of the polyQ disorders is the formation of polyQ protein aggregates. The complex biochemical process of aggregation encompasses everything from soluble monomers and oligomeric intermediates to small protofibrils and finally insoluble fibrillar aggregates (Ross, 2002). A large body of research has thus revolved around characterization of aggregate species and the role that these different species play in the polyQ disease mechanisms. Because aggregation is believed to originally stem from an altered conformational structure of the polyQ protein due to the presence of the polyQ stretch, it follows that other structural alterations would produce deviations in the aggregation pathway. Indeed, several studies have shown that alterations in covalent modifications can globally increase or inhibit aggregation of the polyQ proteins (Humbert et al., 2002; Emamian et al., 2003; Fei et al., 2007). To take the premise one step further, the wild type and conformationally diverse AR variants were tested for their ability to form inclusions in the cell; and these aggregates were characterized by kinetics, structure, localization, and solubility.

#### ***3.2.2.1 Inclusions differ in structural type and kinetics of formation***

In order to visualize cellular inclusions produced by the four AR constructs, immunofluorescence studies were performed in collaboration with Dr. Shatkina. Because nuclear localization of the AR is required for aggregation and toxicity in SBMA, the time course necessary for AR nuclear translocation was chosen to observe inclusion formation. The AR expression vectors were transiently transfected in COS7 cells, and the cells were treated with DHT for varying time points up to 2.5 h to allow for redistribution. The cells were then harvested, fixed, and stained with an AR antibody followed by a fluorescently labelled secondary antibody. Confocal microscopy was utilized to image the formed inclusions.

A number of cells expressing the receptors showed intracellular inclusions. The inclusions formed by each of the AR constructs differed in size, structure, and localization. The aggregates were characterized as being cytoplasmic or nuclear (C or N)

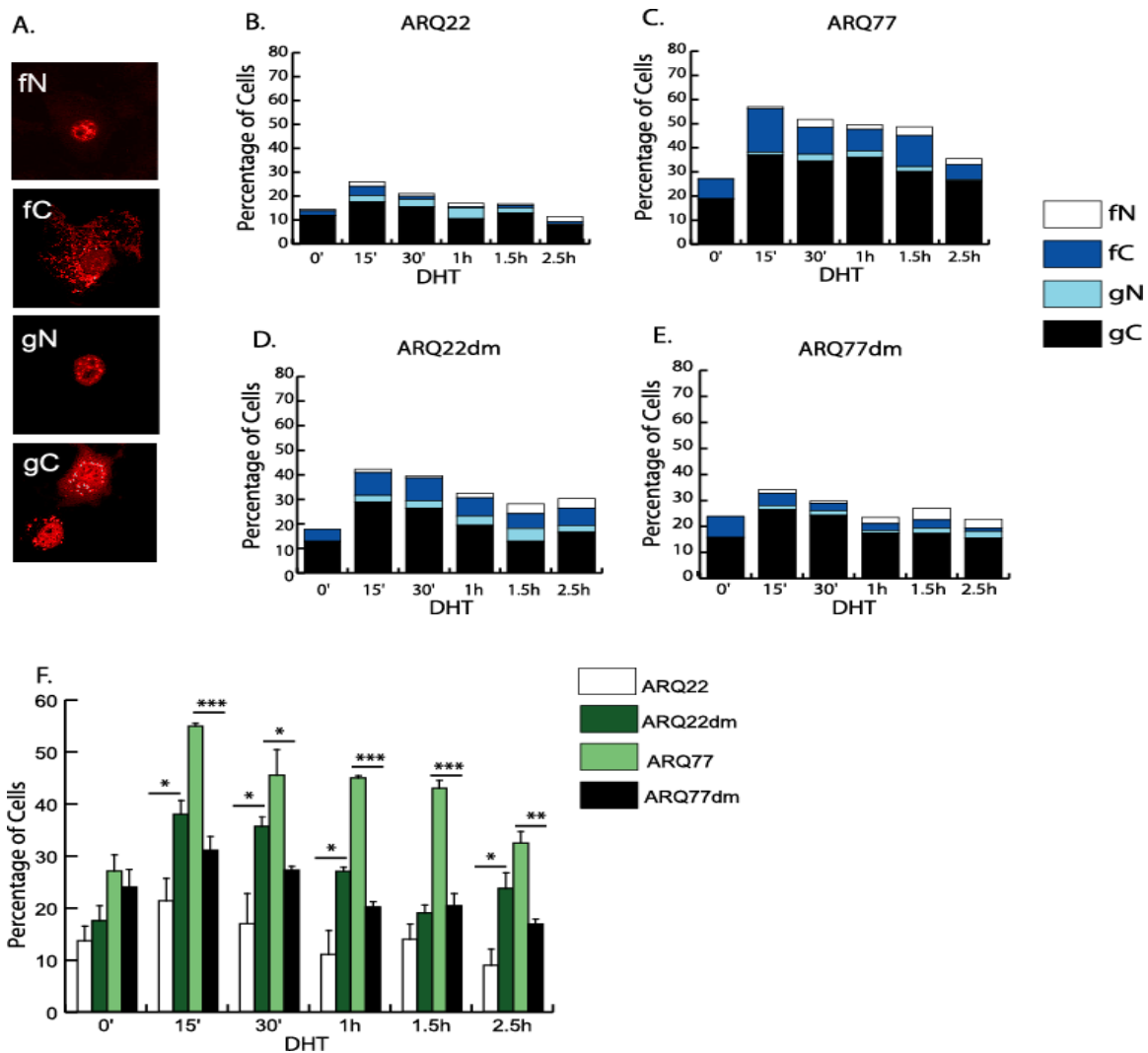


**Figure 3.5 Mutation of serine 424 and 514 alters kinetics of formation of intracellular inclusions**

COS7 cells were transiently transfected with 1.5  $\mu$ g ARQ22, ARQ22dm, ARQ77 or ARQ77dm expression vector. Approximately 48 h after transfection, the cells were incubated on ice for 1 h, thereafter treated either with vehicle or  $10^{-7}$ M DHT at 37°C for the indicated time periods, harvested, and stained with a mouse monoclonal anti-AR antibody F39.4.1 followed by an anti-mouse antibody labeled with the fluorescent dye Cy3. The cells were visualized with a LSM 510 inverted Zeiss confocal microscope. Intracellular inclusions were determined by the percentage of positively stained cells containing AR inclusions after control treatment and incubation with the hormone. (A) Intracellular inclusions were categorized by type and localization: fibrous nuclear (fN), fibrous cytoplasmic (fC), globular nuclear (gN), or globular cytoplasmic (gC). The bar charts show the percentage of cells for each category for (B) ARQ22, (C) ARQ77, (D) ARQ22dm, and (E) ARQ77dm after control treatment and incubation with hormone. For each AR construct at each time point 200-250 cells were analyzed in three separate experiments. (F) Total cytoplasmic aggregation was quantified and ARQ22dm and ARQ77dm were compared by t-test to ARQ22 and ARQ77 respectively. \* $p < 0.05$ , \*\* $p < 0.001$ , \*\*\* $p < 0.0005$

as well as being either of a diffuse, fibrous nature, or large and globular structures (f or g) (Fig. 3.5A). On the whole, no significant differences in inclusions in the nucleus among the AR constructs were detected (Figs. 3.5B-E). The majority of the inclusions seen in this and earlier experiments performed in the lab appear to be localized in the cytoplasm. Both the cytoplasmic fibrous and globular inclusions (fC and gC) were significantly increased in ARQ22dm expressing cells but decreased in ARQ77dm expressing cells in comparison to ARQ22 and ARQ77, respectively (Fig. 3.5 compare panels B with D and C with E). The overall quantification of the results showed that after 15 min of hormone treatment, cells with the ARQ77 showed a marked increase in intracellular inclusions (Fig. 3.5F). As this receptor moved into the nucleus, the number of cells with inclusions decreased but was still significantly higher than the ARQ22 cells. The mutation of the two serine residues had different effects on the receptors. In comparison to the wild type ARQ22, the ARQ22dm showed an increase in the percentage of cells with inclusions over the 2.5 h time-course of hormone treatment. In the ARQ77 background, the double mutation (ARQ77dm) reduced the intracellular inclusions throughout the 2.5 h treatment with DHT (Fig. 3.5F).

These results demonstrated that the mutation of AR serine sites 424 and 514 could either globally inhibit (ARQ77) or increase (ARQ22) inclusion formation, depending on the length of the polyQ stretch. More specifically, the inhibition or increase affected cytoplasmic inclusions and was fairly constant over the time course after an initiation at 15 min. The next step in differentiating between the AR wild type situation and the demonstrated aggregation processes of the mutant AR variants was to examine the solubility of the inclusions.

### ***3.2.2.2 Both polyQ stretch and presence of serine mutations affect solubility of inclusions***

One of the first diagnostic markers for the polyQ disorders was the presence of detergent-insoluble aggregated polyQ protein in post-mortem tissue (DiFiglia et al., 1997). An often used method to assay for the presence of aggregates has thus been to test the solubility of tissue or cellular fractions in the detergent sodium dodecyl sulphate (SDS), a denaturing agent that disrupts non-covalent bonds in the proteins. Two

particular assays used to analyze the solubility of cellular inclusions are the filter retardation assay and SDS-PAGE-western blot analysis of polyQ cellular lysates. In the filter retardation assay, the intracellular inclusions are trapped on cellulose acetate membrane as SDS-insoluble aggregates (Heiser et al., 2002) while SDS-PAGE-western blot analysis allows detection of SDS-insoluble aggregated protein that remains in the SDS-PAGE stacking gel (Merry et al., 1998).

For the filter retardation assay, COS7 cells were transfected with the different AR expression vectors and treated up to 2.5 h with DHT to analyze inclusion solubility over the time course required for nuclear translocation. Cellular lysates were applied to a cellulose acetate membrane and vacuumed through, leaving any insoluble material behind. AR aggregates were then visualized by probing the membrane with an AR antibody and utilizing chemiluminescence detection. Insoluble material in both ARQ77 and ARQ77dm transfected cells were detected throughout the time course of the experiment (Fig. 3.6A; upper panel). In the case of the ARQ22 and ARQ22dm expressing cells, insoluble material was only detected in ARQ22dm transfected cells at the earliest time points of DHT treatment (15min – 1 h). In contrast no significant insoluble material was identified for the ARQ22 expressing cells (Fig. 3.6A; upper panel). All four receptor variants were expressed to a similar level as determined by dot blot analysis of the same lysates (Fig. 3.6A; lower panel).

As aggregation is a dynamic process, it was also desirable to examine the solubility of inclusions after longer time points. Intriguingly, after a lengthy 72 h of hormone treatment, insoluble material could only be detected in lysates of cells expressing ARQ77 and ARQ77dm (Fig. 3.6B). A comparable result was also obtained by SDS-PAGE-western blot analysis of lysates of transiently transfected COS7 cells treated for 16 h with DHT or vehicle (Fig. 3.6C). Again, the receptor variants were expressed to similar levels as determined by immunoblot assays (Fig. 3.6C; lower panel).

From the above results, it seems that the ARQ22dm transfected cells that had previously been scored as showing an increase in intracellular inclusions in the immunofluorescence assay appear to contain receptor aggregates that are insoluble only at time points up to 1 h as determined in the filter retardation assay. It is therefore likely that these aggregated proteins are only transiently formed and decrease with time, or their

state of solubility changes with time. It also follows that these ARQ22dm inclusions structurally differ from those produced from the receptors with the ARQ77 background. Assays to determine the structure of the aggregates are thus necessary to fully distinguish between the AR variants.

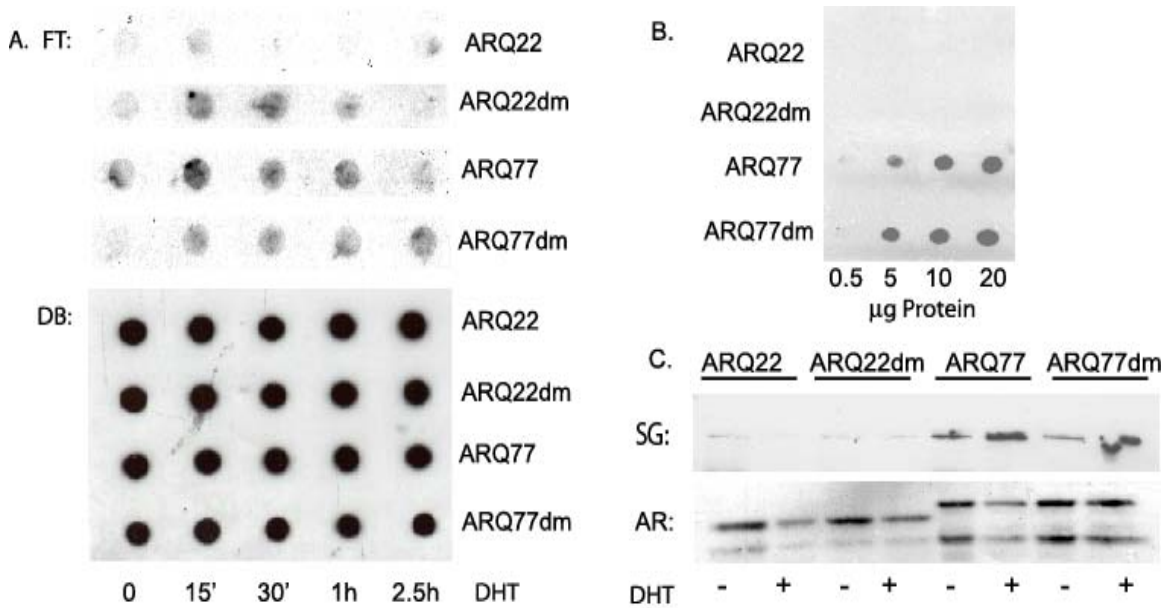


**Figure 3.6 Differences in aggregate formation due to mutations at serine residues 424 and 514**

Filter retardation assays were performed to determine the solubility of aggregates formed by AR constructs. COS7 cells were transiently transfected and induced with vehicle or  $10^{-7}$ M DHT for the indicated time points. Cells were harvested and lysed in NP-40 lysis buffer. Protein concentration and AR expression were determined by Bradford assay and subjected to Western blot or dot blot analysis, respectively. Protein samples were diluted in 2% SDS/ 50mM DTT and loaded on a cellulose acetate membrane. Insoluble material was trapped on the membrane after application of a vacuum. (A) FT: filter trap assay using 5 µg protein from ARQ22, ARQ22dm, ARQ77, and ARQ77dm transfected cells after control treatment and incubation with hormone. DB: Dot blot analysis of 1 µg protein of cell lysates used for the filter retardation assay demonstrates an approximately equal amount of AR expression. (B) Filter trap assay using 0.5, 5, 10, and 20 µg protein from ARQ22, ARQ22dm, ARQ77, and ARQ77dm transfected cells after control treatment and incubation with hormone for 72 h (C) Western blot analysis of whole cell lysates after 16 h hormone treatment demonstrating aggregates in the stacking gel of a 4% stacking/ 12.5% running, SDS-polyacrylamide gel

### 3.2.2.3 1C2 antibody preferentially recognizes expanded polyQ region

In an attempt to further characterize differences in aggregation and conformation of the AR due to the polyQ stretch and/or the serine site mutations, 1C2 immunoreactivity was examined. The 1C2 antibody is thought to recognize an epitope, which is associated with toxicity, formed by misfolded proteins with long glutamine tracts (Trottier et al., 1995). For the purpose of distinguishing between the wild type and AR variants in this work, it was found that using equal amounts of the AR variants in immunoblot assays and staining them with the 1C2 antibody only identified the extended polyQ stretches in the ARQ77 and ARQ77dm proteins. The 1C2 antibody was unable to distinguish between more subtle structural alterations or changes in toxic properties (Fig. 3.7). Thus more robust models that measure possible toxic effects of the ARQ22dm as well as changes in toxicity of the ARQ77dm were needed to clarify the alterations in nuclear localization, transcription, and inclusion formation and solubility that were evident in the cell culture model.

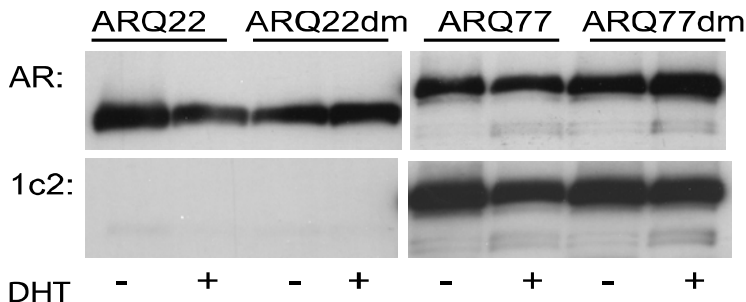


**Figure 3.7 Serine mutations do not alter 1C2 reactivity**

COS7 cells were transiently transfected and induced with vehicle or  $10^{-7}$ M DHT. Whole cell lysates were used for western blot analysis with AR F39.4.1 (1:1000) and 1C2 (1:5000) antibodies. The equally loaded lysates on the gel show that the 1C2 antibody preferentially recognizes the ARQ77, regardless of the presence of the serine site mutations.

### **3.3 *Drosophila* model of SBMA used to analyze effects of serine site mutations**

*Drosophila* have been successfully used to model human neurodegenerative diseases such as Parkinson's pathology as well as polyQ expansion disorders such as SCA3, Huntington's disease, and SBMA (Warrick et al., 1998; Feany and Bender, 2000; Fortini and Bonini, 2000; Takeyama et al., 2002). Each of these models have utilized a GAL4-UAS expression system in which a transgenic *Drosophila* line containing the yeast transcriptional activator GAL4 under the control of a specific promoter (or enhancer) is crossed with a second transgenic line containing the gene of interest under the control of the GAL4-responsive UAS target gene (Phelps and Brand, 1998). This allows for expression of the gene of interest (the polyQ proteins) in specific tissues according to the type of promoter/enhancer used. Using this *Drosophila* expression system, Takeyama et al., 2002, demonstrated neuronal degeneration upon hormone treatment through ectopic expression of the AR with an amplified polyQ stretch in the fly eye. A similar approach to analyze the potentially toxic properties of the mutant AR variants was employed by creating four transgenic AR lines by microinjection of ARQ22, ARQ22dm, ARQ77, and ARQ77dm constructs. Through crosses with GAL4 transgenic lines, the constructs were expressed in the photoreceptor neurons of the eye under the control of the *glass multimer reporter* (GMR) or throughout the central nervous system under the control of the pan-neuronal embryonic lethal abnormal visual system (ELAV) promoter. As in previous SBMA *Drosophila* models (Takeyama et al., 2002), ingestion of DHT during the larval stages of development was sufficient to induce toxicity. The chosen hormone concentrations were also in the range of those previously used (Takeyama et al., 2002; Pandey et al., 2007).

#### **3.3.1 Conformational changes induced by mutation of serines 424 and 514 in *Drosophila***

In order to verify that the *Drosophila* system could accurately model the toxic effects of the AR variants, it was confirmed that the initial results of structural alteration seen *in vitro* could also be validated in the animal model. Transgenic flies were first crossed with ELAV-GAL4 flies in order to have AR expression in the central nervous

system. Then, in the same vein as the limited proteolytic digestion of the *in vitro* translated receptors, a partial tryptic digest on lysates made from the AR-expressing *Drosophila* was performed. Although there were no clear differences in the pattern of digestion between the ARQ22 and ARQ22dm or the ARQ77 and ARQ77dm, the receptors containing the serine site mutations did show a greater resistance to the tryptic digestion (Fig. 3.8). Therefore, despite differences in pattern and digestion resistance in comparison to the *in vitro* translated receptors, it was verified that the serine site mutations also seemed to alter the AR structure in the *Drosophila* model.

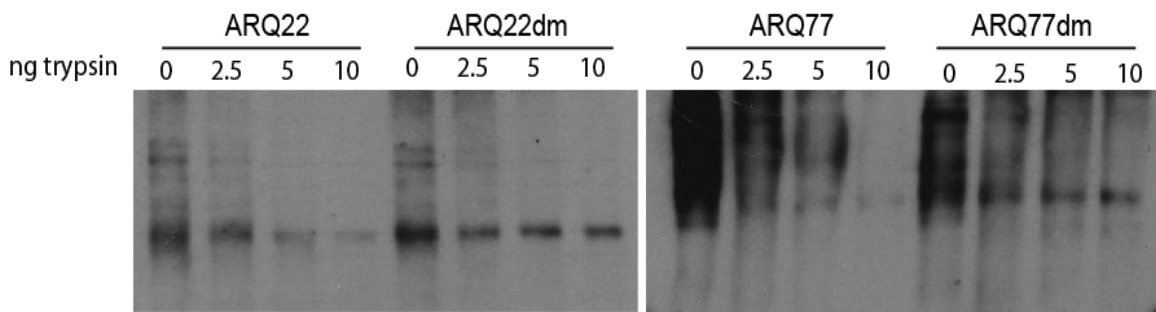


**Figure 3.8 Mutation of serine residues 424 and 514 leads to conformational changes in androgen receptors expressed in *Drosophila***

AR fly lines and ELAV-GAL4 flies were crossed on normal stock medium. Lysates were made from adult progeny, and the protein concentrations were determined by Bradford assay. 20  $\mu$ g of lysate was used for each trypsin concentration. The digestion reaction was carried out for 15 min at room temperature before being stopped by the addition of denaturing gel loading dye. The products were then fractionated on an 8% SDS-polyacrylamide gel and were visualized by western blot analysis using AR antibody (N-20).

### **3.3.2 Mutations of serines 424 and 514 affect nuclear accumulation and aggregation of the AR in a fly model of SBMA**

In an effort to corroborate results seen in cell culture as well as further validate the AR *Drosophila* model, *in vivo* nuclear localization and aggregation of the AR in the four transgenic lines were examined. The immunofluorescence and filter retardation assays from cell culture experiments were thus adapted for *Drosophila* tissues and protein lysates.

### 3.3.2.1 Mutant AR demonstrates altered nuclear localization in fly lines

To observe changes in compartmental distribution of the AR, immunohistochemical analysis was performed on the brains of transgenic third instar larvae treated with and without hormone. Experiments were performed utilizing both the GMR and ELAV drivers, both of which allowed for discernible AR expression in the eye imaginal discs. Flies expressing the GMR driver and AR constructs were allowed to grow on stock food without or with  $10^{-3}$ M DHT for the time period between hatching and the wandering third instar larval stage, while flies expressing the ELAV driver were only treated for 72 h due to the toxic effects on survival. Once the larvae reached the third instar stage, brains were fixed and stained for AR expression for viewing with confocal microscopy. Both the ELAV (not shown) and GMR drivers (Fig. 3.9A) produced similar results when employed to examine neurons expressing the AR constructs in the eye imaginal discs of third instar larvae. Equal expression of the AR constructs in the fly lines was demonstrated by western blot analysis (Fig. 3.9B).

In the GMR flies treated with or without hormone, the ARQ22 receptor showed a tendency towards nuclear localization (Fig. 3.9A); however, the effect was more pronounced upon DHT treatment (Fig. 3.9A see higher magnification yellow overlay color). ARQ22dm, ARQ77, and ARQ77dm expressing neurons in the eye imaginal discs all showed a propensity for the receptor to cluster in the cytoplasm after hormone treatment (Fig. 3.9A). For each of these three lines, although some nuclear localization was evident only after DHT treatment, there appeared to be a lack of nuclear accumulation, which was not evident in the ARQ22 larvae. Although this assay did not allow for discrimination between the ARQ22dm, ARQ77, and ARQ77dm, these *in vivo* results paralleled the reduced nuclear accumulation seen in cell culture experiments. The next verification of polyQ pathogenesis was to test for the presence of aggregates as well as additional structural features of the AR variants in the fly lines.

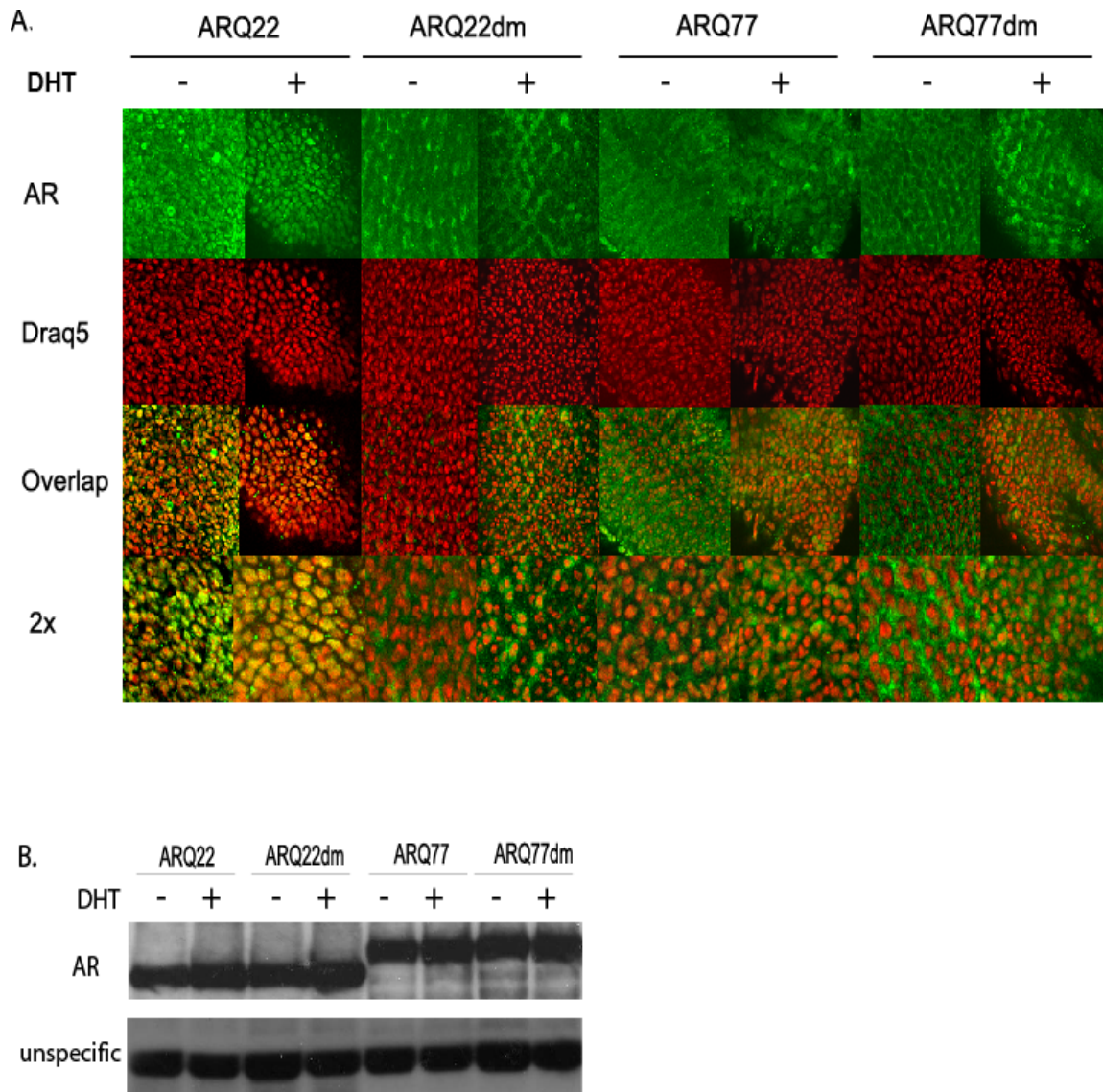


**Figure 3.9 Nuclear localization of AR in *Drosophila***

AR fly lines and GMR-GAL4 flies were crossed on medium containing vehicle (ethanol) or  $10^{-3}$ M DHT and progeny were allowed to feed until the third instar wandering larval stage. (A) Brains were dissected from larvae, fixed, and stained with AR C-19 and Draq5 for nuclear staining, followed by an anti-rabbit antibody labelled with Cy2. Cells of the eye imaginal disc were visualized with an LSM 510 inverted Zeiss confocal microscope. (B) Lysates were made from adult flies of the same crosses used for immunofluorescence in order to demonstrate equal AR expression levels.

### 3.3.2.2 Aggregation and 1C2 recognition in fly lines comparable to cell model

Because misfolding and aggregation of the mutant polyQ proteins is such a central theme in the polyQ disorders, it is important to establish disease models that can reproduce this feature. Therefore, aggregation of the AR driven by ELAV in third instar wandering larvae was examined by adapting the filter retardation assay used in the cell culture model (Fig. 3.10A). Two days after hatching, the transgenic larvae were placed on medium containing  $10^{-3}$ M DHT or vehicle for a total of 72 hours. By this time the larvae had reached the third instar stage of development and were then homogenized for protein extracts for aggregation analysis. As with the results of the filter retardation assay using lysate from cultured cells, larvae treated with DHT generated insoluble AR protein in the ARQ22dm, ARQ77, and ARQ77dm lines, in comparison to larvae treated with vehicle alone. However, ARQ77 larvae also showed slight levels of insoluble aggregate formation without hormone treatment. Any aggregation seen in the ARQ22 larvae treated without or with  $10^{-3}$ M DHT appeared to be negligible.

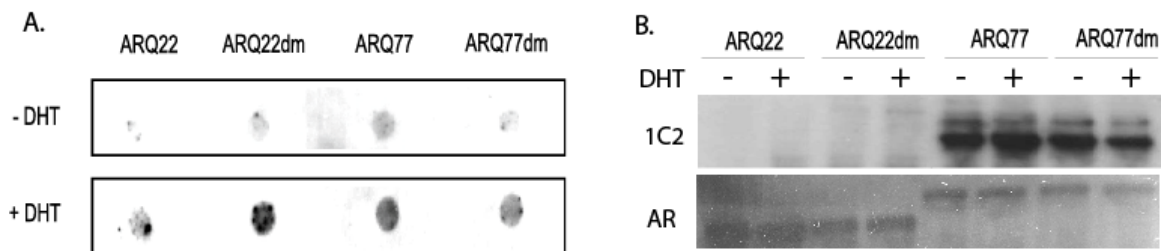


**Figure 3.10 Aggregation and conformation of AR in transgenic *Drosophila***

(A) Aggregation was assessed using the filter trap assay. Third instar larvae treated without and with hormone were homogenized in 2  $\mu$ l RIPA/larvae. Samples were then prepared as described for cell lysates. Protein concentrations of the larval lysates were measured by Bradford assay and 50  $\mu$ g were loaded on the cellulose acetate membrane. (B) GMR-GAL4 flies were crossed with the AR transgenic flies on medium with  $10^{-3}$ M DHT or vehicle. Extracts were produced from heads of 50 adult progeny. *Drosophila* lysates were immunoprecipitated using the AR44 antibody. Western blot analysis was then used to demonstrate that the 1C2 antibody preferentially recognizes the ARQ77 also in *Drosophila*, regardless of the presence of the serine site mutations.

In a second attempt to associate a particular structural conformation with the levels of aggregation, 1C2 immunoreactivity was also tested on *Drosophila* extracts from adult flies treated with and without hormone. However, again staining of the *Drosophila* extracts was only observed for the ARQ77 and ARQ77dm samples as shown in the cell culture experiments (Fig. 3.10B). Lysates prepared from both ELAV and GMR crosses yielded identical results.

The combined results regarding nuclear accumulation and aggregation together with the differences in basic AR conformation, all properties closely associated with polyQ toxicity, substantiated the cell culture data in an *in vivo* model and demonstrated that the *Drosophila* model was a reliable system. Therefore, the fly model was used to directly measure the differences in toxicity due to the serine site mutations.

### **3.3.3 Neurodegeneration occurs in fly lines expressing AR with mutations at serine residues 424 and 514**

A frequently used assay to directly gauge toxicity in *Drosophila* models of the polyQ disorders is to ectopically express the polyQ protein of interest in the eye of the fly and then score the flies for degeneration and morphological disruption of the eye (Jackson et al., 1998; Bonini, 1999; Takeyama et al., 2002). To examine neurodegeneration in the present *Drosophila* model, flies demonstrating similar expression levels of the AR under the control of the photoreceptor expressed GMR promoter (Fig. 3.11B) were treated without or with  $10^{-3}$ M DHT for the 5-day time period between hatching and pupation. After eclosion, fly eyes were preliminarily examined by light microscopy (LM) and then scanning electron microscopy (SEM) (Fig. 3.11A). Compound eyes of flies expressing ARQ22 and ARQ22dm looked normal even at higher image magnification (Fig. 3.11A). Flies expressing ARQ77 and ARQ77dm showed very slight deformations in the absence of hormone (Fig. 3.11A). Ingestion of DHT resulted in disruption of eye morphology for flies expressing ARQ77 as previously reported (Takeyama et al., 2002). DHT treatment also resulted in disruption of eye morphology for those flies expressing ARQ77dm and ARQ22dm but to somewhat reduced levels in comparison to ARQ77 flies (Fig. 3.11A). In contrast, the presence of DHT did not affect the eye morphology of the wild type ARQ22 transgenic flies.

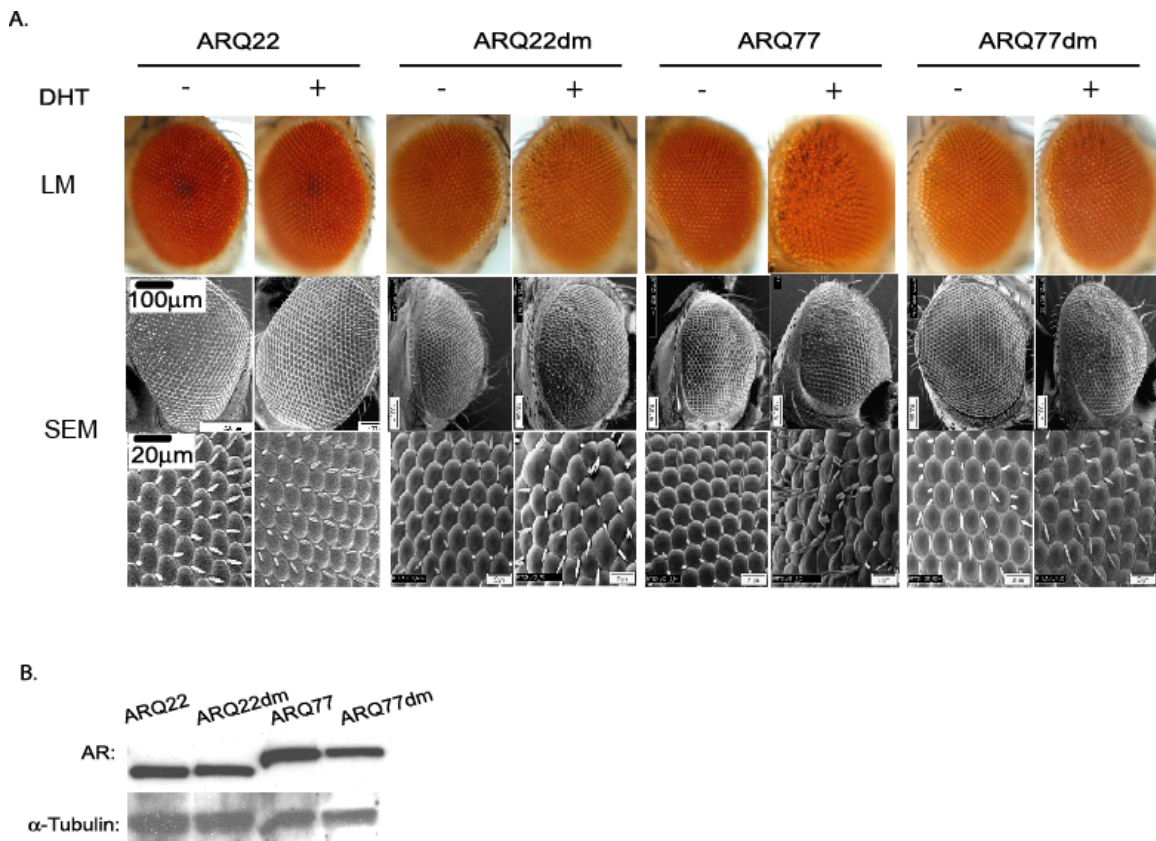


**Figure 3.11 Ligand-induced degeneration of photoreceptor neurons in flies containing amplified polyQ stretch and serine 424/514 mutations**

AR fly lines and GMR-GAL4 flies were crossed on medium containing vehicle (ethanol) or  $10^{-3}$ M DHT and progeny were allowed to feed for 5 days after hatching and before pupation. After eclosion of progeny, heads were collected and examined by light microscopy (LM). Afterwards, heads were fixed in increasing concentrations of ethanol for SEM analysis. (A) LM and SEM of the compound eyes of transgenic flies with and without DHT treatment. (B) Immunoblots with 20  $\mu$ g lysate of the transgenic fly heads using anti-AR antibody and an anti-  $\alpha$ -tubulin antibody.

While the demonstrated differences in toxicity by introduction of the serine site mutations in the ARQ22 background were definitive, the slight differences between the ARQ77 and ARQ77dm were not as clear using the qualitative neurodegeneration assay. For this reason, a set of quantitative behavioral and survival experiments were designed to measure pathogenicity.

### **3.3.4 Mutation of serine residues 424 and 514 affects locomotion and survival of fly lines expressing ARQ22 and ARQ77**

Neuronal expression of polyQ proteins has been reported to cause defects in larval development in polyQ *Drosophila* models (Lee et al., 2004). These defects can result in manifestations of behavioral abnormalities as well decreased rates of survival. The following locomotion and survival assays were hence used to assess toxic defects in larval development due to the presence of the polyQ stretch and/or the serine site mutations in the AR transgenic fly lines.

#### ***3.3.4.1 Locomotion assay demonstrates subtle differences between AR mutant lines***

In order to better quantify differences in pathogenicity in the four fly lines, the transgenic flies expressing the AR under the control of the pan-neuronal ELAV promoter were used to monitor differences in locomotion and behavior. Larvae were allowed to develop for three days before hormone treatment due to toxic effects on survival. A set number of larvae were then transferred to medium without or with  $10^{-3}$ M DHT. After approximately 48 h of treatment, the then wandering third instar larvae were placed in the center of an agar plate that was evenly illuminated by a light box; and the larvae were monitored for 2.5 min using Noldus software for behavioral analysis. The Noldus program allowed for assessment of speed of motion and angular velocity. Angular velocity of the larvae was defined as change in direction of movement per unit time and was used to quantify the subtle directional changes of movement of the larvae.

The wild type situation for the locomotion assay was demonstrated by the ARQ22 larvae. On average, when a larva from this group was placed on the agar plate, it moved in a relatively straight path to the edge of the plate at a rate of approximately 0.16 mm/s. Hormone treatment was expectedly shown to have no significant effect on the speed or angular velocity for the ARQ22 larvae (Figs. 3.12A and B). The tendency to make an overall direct path was also not modified by administration of hormone (Fig. 3.12C). In the context of the ARQ22 background, mutation of the two serine sites resulted in a significant reduction in locomotor speed upon hormone treatment ( $***p < 0.0005$ ; Fig. 3.12A). An increase in angular velocity provided further evidence for defects of the central motor pattern generator in the ARQ22dm larvae (Fig. 3.12B) as did the pattern of

the overall path of the larvae (Fig. 3.12C). As anticipated, larvae expressing the ARQ77 and treated with hormone demonstrated great deficits in locomotor speed and patterning (Figs. 3.12A, B, C). The hormone treated ARQ77dm larvae also showed difficulty in movement in comparison to the wild type ARQ22 larvae, but there was a small but significant improvement in comparison to ARQ77 larvae (\* $p < 0.05$ ; Figs. 3.12A, B, C). These results gave the first significant evidence of changes in toxicity levels attributable to the AR mutations at serines 424 and 514.

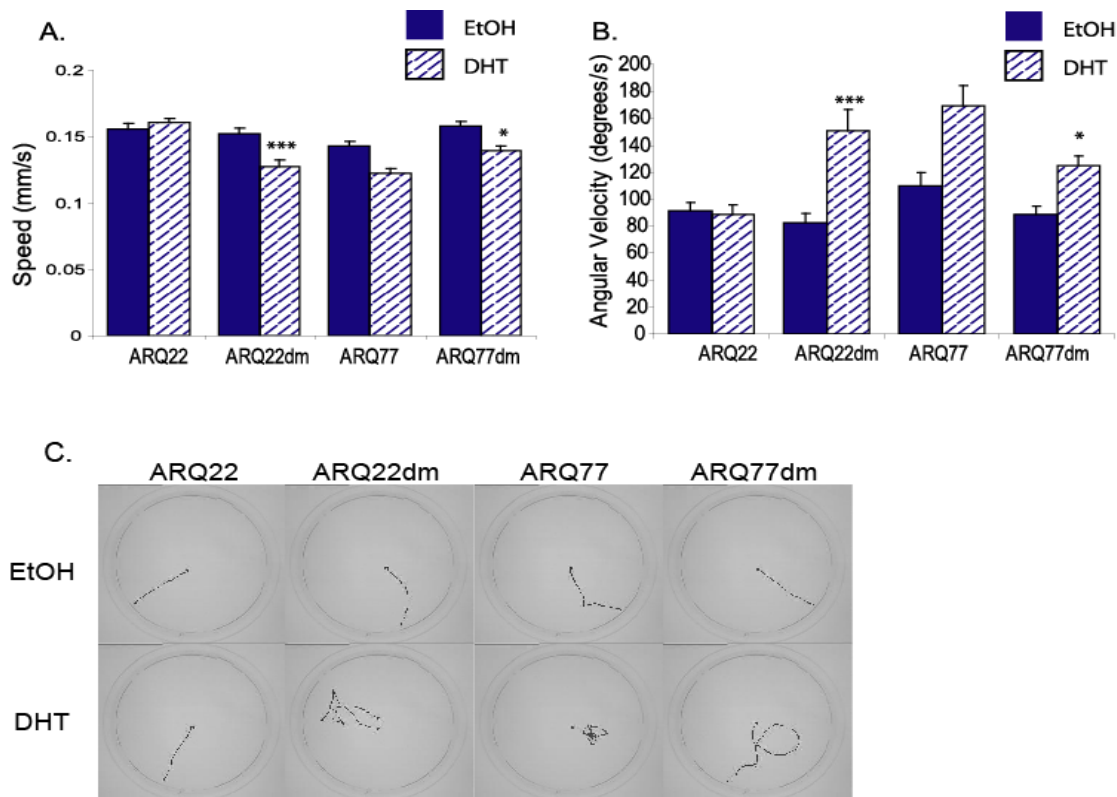


**Figure 3.12 Locomotive and behavioral analysis of transgenic wandering third-instar larvae**

AR fly lines and ELAV-GAL4 flies were crossed on normal stock medium. Progeny were transferred after 72 h to medium containing vehicle (ethanol) or  $10^{-3}$ M DHT for 48 h treatment. A total of 30 larvae were analyzed for each genotype and hormone treatment combination. (A) With hormone treatment ARQ22dm larvae showed a 20% deficit in speed in comparison to their ARQ22 counterparts. ARQ77dm larvae showed a 10% improvement over the ARQ77 larvae. (B) The subtle angular movement of the larvae as measured by angular velocity was greatly increased in the case of the ARQ22dm and ARQ77 larvae. Mutation of the serine residues in the ARQ77 background resulted in a small amelioration of the phenotype. \* $p < 0.05$ , \*\*\* $p < 0.0005$ . (C) Sample overall locomotive paths of the wandering third-instar larvae.

#### ***3.3.4.2 Transgenic lines demonstrate changes in survival dependent upon serine site mutations***

A further way to distinguish between the toxic effects of the polyQ stretch and the serine site mutations was to examine survival rates of the transgenic *Drosophila*. For viability assays the AR was expressed pan-neuronally by crossing transgenic lines with the ELAV promoter line. Directly after hatching, the progeny were transferred to food containing DHT or EtOH alone as vehicle and allowed to feed until pupation for the full effects of hormone treatment. The first developmental stage where a divergence in survival rates could be calculated was the pupal stage, in which the larvae climb out of the food and pupate on the container walls. Therefore, the number of larvae reaching this pupal stage of development (Fig. 3.13A) was determined in addition to determining survival rates for the fully eclosed adult stage (Fig. 3.13B). Both stages of survival rates were calculated based on the total number of original larvae.

The percentage of larvae expressing the ARQ22 that survived to the pupal or adult stages in the absence and presence of hormone was not significantly different, demonstrating no defects in larval development for this wild type group (Figs. 3.13A and B). In contrast, the ARQ22dm demonstrated a marked decrease in survival at both the pupal and adult stages in the presence of hormone. Larvae expressing ARQ77 survived poorly in the presence of hormone. However, in the context of the ARQ77 background, the double mutation showed a small improvement in the survival percentage in the presence of hormone (Figs. 3.13A and B).

The above survival analysis supplemented the data from the locomotion assay, demonstrating again quantitatively that the serine site mutations affected toxicity in a polyQ length-dependent manner. However, although the pathogenicity exhibited by the ARQ22dm was in vast contrast to the normal ARQ22 situation, it was apparent that the toxicity levels were also not quite on par with those of the ARQ77 SBMA model. It was deemed that one method of comparing the types of toxicity was to determine how specific inhibitors of polyQ toxicity would affect the AR variants.

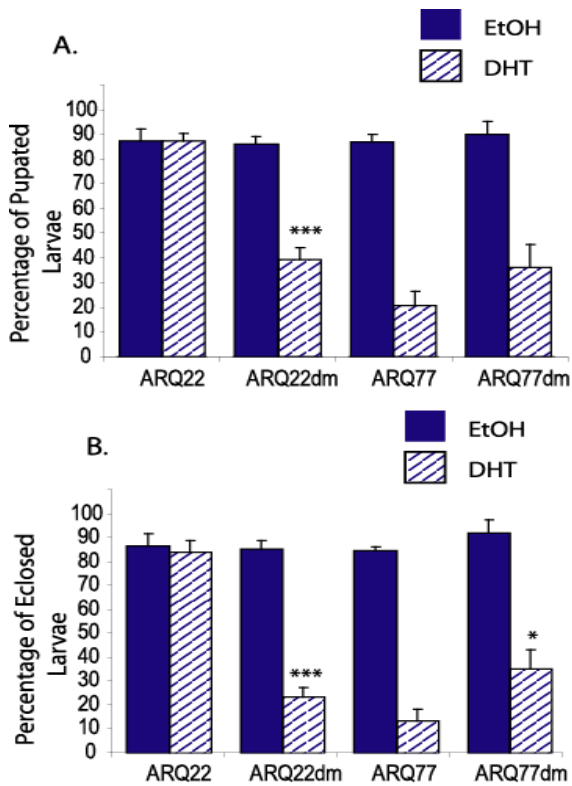


**Figure 3.13 Survival studies of larvae with ubiquitous neuronal expression of AR with amplified polyQ stretch and AR containing mutated serine sites**

AR fly lines and ELAV-GAL4 flies were crossed on normal stock medium. After hatching of progeny, larvae were transferred to medium containing vehicle (ethanol) or  $10^{-3}$ M DHT with a maximum of 50 larvae per vial. The total larvae for each sample was >100. Data are from three separate experiments. The error bars represent standard deviation of the mean. (A) The percentage of larvae surviving to the pupal stage was determined by the number of pupae formed divided by the original number of larvae placed in the vial. (B) The percentage of larvae surviving to posteclosion was determined by the number of eclosed adult flies divided by the original number of larvae placed in the vial. \* $p < 0.05$ , \*\*\* $p < 0.0005$

### **3.4 Inhibitors of polyQ toxicity used to demonstrate differential toxicity due to serine site mutations**

Previous studies have been able to demonstrate in mouse and *Drosophila* models that sodium butyrate, a histone deacetylase (HDAC) inhibitor, is a viable therapeutic agent for polyQ toxicity as well as other forms of neurodegeneration (McCampbell et al., 2001; Steffan et al., 2001; Minamiyama et al., 2004; Fischer et al., 2007). Of the many other drug possibilities that have been examined for the polyQ disorders, Parkinson's, and Alzheimer's disease, melatonin is also a suggested agent due to its widespread effects, which include antioxidant properties (Srinivasan et al., 2006). The effects of treating the four *Drosophila* lines with the known inhibitor sodium butyrate and melatonin were compared in order to determine firstly if melatonin is a capable inhibitor of polyQ toxicity and secondly to compare the effects of tested polyQ inhibitors on the serine mutant lines. The aim was to further distinguish the lesser toxicity seen with the ARQ22dm and ARQ77dm with toxicity caused purely by the expanded polyQ region.

#### **3.4.1 Sodium butyrate and melatonin inhibit neurodegeneration in expanded polyQ fly lines**

The effects of melatonin as an inhibitor of polyQ toxicity were preliminarily tested by examining the neurodegeneration and morphological damage in the eyes of *Drosophila* from crosses between the AR transgenic lines and GMR-GAL4 flies. Flies were treated with DHT or vehicle alone or in combination with the inhibitor compounds for the 5-day period between hatching and pupation. After eclosion, the flies were then examined by light microscopy (Fig. 3.14). The optimum concentration for sodium butyrate treatment was 100mM as determined by published studies (Minamiyama et al., 2004; Agrawal et al., 2005) while a range of concentrations were initially tested for melatonin. Results shown are from treatment with  $10^{-2}$ M melatonin, which was the regimen shown to be the most effective.

The known inhibitor, sodium butyrate, was able to slightly alleviate the neurodegeneration seen in ARQ77 flies treated with DHT alone. However, melatonin demonstrated an even more dramatic effect, eliminating almost all signs of morphological and structural damage (Fig. 3.14A). The results were not nearly as impressive for the flies

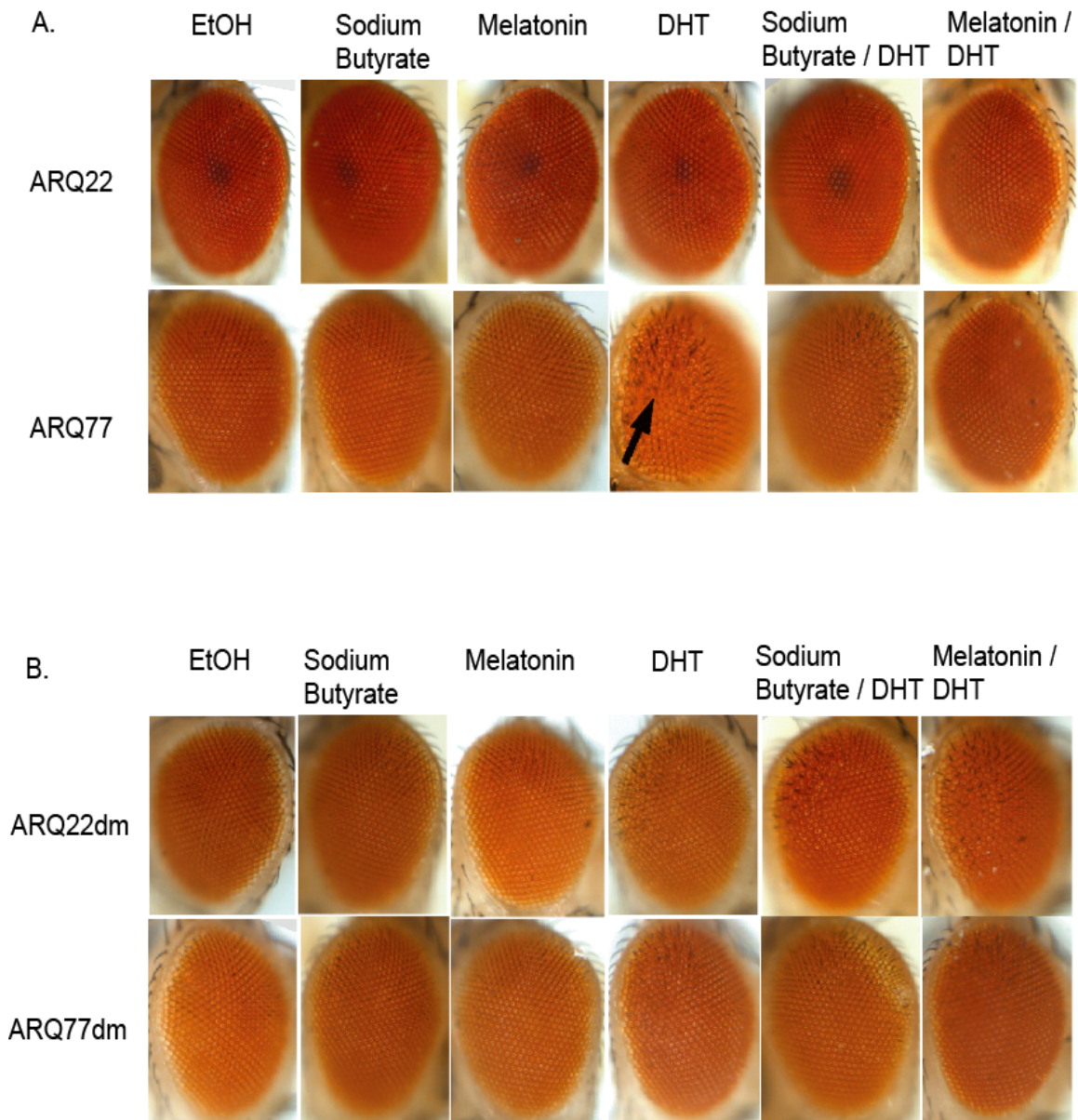


**Figure 3.14 Sodium butyrate and melatonin inhibit polyQ toxicity, but serine mutations alter effectivity.**

AR fly lines and GMR-GAL4 flies were crossed on medium containing vehicle (ethanol),  $10^{-3}$ M DHT, 100mM sodium butyrate,  $10^{-2}$ M melatonin, or a combination. Progeny were allowed to feed for 5 days after hatching and before pupation. Heads were then freshly cut, and pictures were taken using a light microscope. (A) ARQ77 flies treated with DHT demonstrate morphological defects, see black arrow. Defects are significantly reduced with inhibitor treatment. (B) ARQ22dm flies demonstrated little to no recovery with sodium butyrate and melatonin treatment while ARQ77dm flies showed some slight improvement with melatonin.

with AR mutations at serines 424 and 514. Neither sodium butyrate nor melatonin was able to rescue the phenotype of the ARQ22dm flies (Fig 3.14B). ARQ77dm flies appeared to exhibit a slight improvement, but this improvement was not significantly better than the improvement already seen in the ARQ77dm flies in comparison to the toxic ARQ77.

The above results demonstrated that sodium butyrate and melatonin could comparably inhibit neurodegeneration in the SBMA *Drosophila* model. However, as with the previous neurodegeneration assay, these results were qualitative; and the slight improvements of the serine mutant lines were sometimes difficult to discern. For this reason, the locomotion and survival assays were again used for quantitative analysis.

### **3.4.2 Serine mutations affect ability of sodium butyrate and melatonin to rescue polyQ phenotype in quantitative assays**

Use of the sensitive locomotion and survival assays allowed for a more systematic method of testing whether the two mechanistically different compounds sodium butyrate and melatonin would be able to rescue the polyQ toxicity seen in the *Drosophila* models. Both assays were performed in the same manner as previously described in this body of work. The concentrations of sodium butyrate and melatonin that were determined appropriate for the neurodegeneration assay were also used to assess the developmental defects leading to alterations in behavior and survival. Treatments with and without DHT were repeated in conjunction with the new inhibitor compound combinations for accurate comparison. In order to depict the changes in locomotion and survival due to the inhibitor treatment regimens, the percentage recovery was calculated by determining the ratio of the average difference between inhibitor-treated and EtOH-treated larvae to the difference between DHT-treated and EtOH-treated larvae.

#### ***3.4.2.1 Sodium butyrate and melatonin have varying effects on locomotion***

The locomotion assay was first used to confirm that the previously described inhibitor sodium butyrate as well as the newly tested melatonin could positively affect the ARQ77 larvae, the SBMA model. Both sodium butyrate and melatonin were indeed able to significantly increase the speed of ARQ77 larvae that had been treated with DHT (Fig.

3.15A), resulting in a rescue of 46% and 48% respectively (Fig. 3.15C). A vast improvement was also seen for the parameter of angular velocity (Figs. 3.15B and D), 38% for sodium butyrate and 25% for melatonin. Thus it was quantitatively established that both sodium butyrate and melatonin were inhibitors of polyQ toxicity in our model system.

Next it was tested if sodium butyrate and melatonin would be able to rescue the increased toxic effects seen in the ARQ22 background and lessened toxicity in the ARQ77 background that were a result of the serine mutations. In the ARQ22dm and ARQ77dm larvae, the melatonin treated larvae showed a significant recovery in speed of approximately 30% for both cases. However, sodium butyrate was ineffective in improving speed of locomotion (Fig. 3.15C). The opposite scenario was seen for the directional changes of the larvae measured by angular velocity. ARQ22dm and ARQ77dm larvae treated with sodium butyrate showed a 19% and 30% rescue, respectively, while treatment with melatonin provided little to no improvement (Fig 3.15D).

As was hinted at with the previous neurodegeneration assay, the fly lines containing the serine site mutations seemed to display an altered type of toxicity that could not be rescued in the same manner as the ARQ77. Also, the inhibitors themselves showed variations in their ability to act on these mutants. The survival assay was subsequently used as a method of verifying these observations and further quantifying the differences between the AR variant lines.

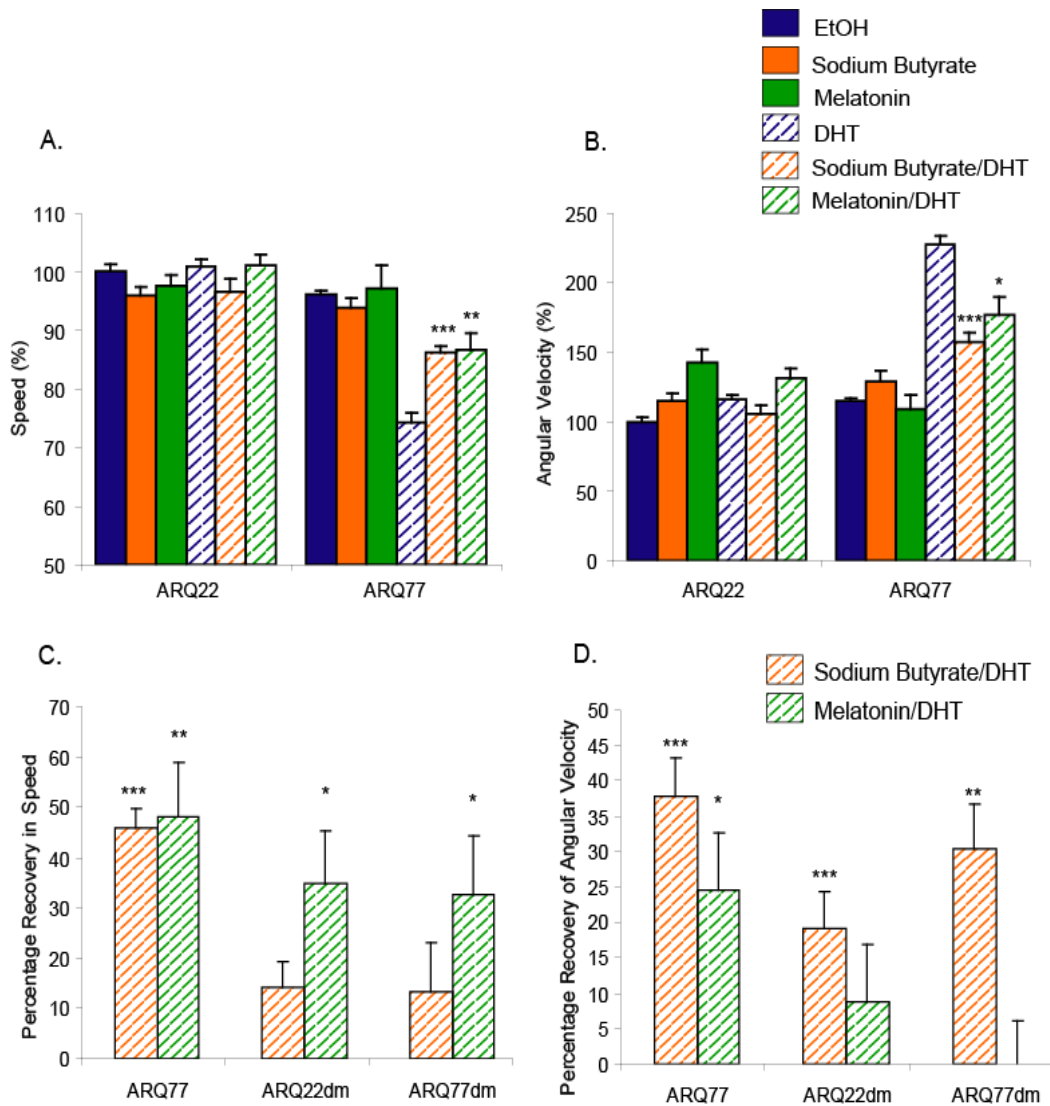


**Figure 3.15 Effects of sodium butyrate and melatonin on larval locomotion**

AR fly lines and ELAV-GAL4 flies were crossed on normal stock medium. Progeny were transferred after 72 h to medium containing vehicle (ethanol),  $10^{-3}$ M DHT, 100mM sodium butyrate,  $10^{-2}$ M melatonin, or a combination. A total of 30 larvae were analyzed for each genotype and hormone treatment combination. Treatment with sodium butyrate and melatonin was able to partially rescue the ARQ77 larvae for both (A) speed and (B) angular velocity. (C) ARQ22dm and ARQ77dm larvae only showed recovery of speed when treated with melatonin while a recovery of angular velocity (D) was preferentially seen with sodium butyrate treatment. \* $p < 0.05$ , \*\* $p < 0.001$ , \*\*\* $p < 0.0005$

### ***3.4.2.2 Sodium butyrate and melatonin differ in ability to rescue AR mutants in survival analyses***

The capabilities of melatonin as well as sodium butyrate as inhibitors of polyQ toxicity were further examined by testing their effects on survival rates. Progeny from crosses between ELAV-GAL4 flies and AR transgenic flies were allowed to feed on DHT or EtOH alone or in combination with the inhibitor compounds until pupation (Figs. 3.17A and D) or eclosion (Figs. 3.16B and C). Sodium butyrate and melatonin's effects were first tested on ARQ77 larvae and compared with the wild type (ARQ22) situation. The known inhibitor sodium butyrate was able to increase survival rates to pupation with a rescue rate of 14% (Figs. 3.16A and C), but the benefits were not extended to eclosion, or full adulthood (Figs. 3.16B and D). Melatonin, on the other hand, partially rescued the ARQ77 larvae in both stages of survival (Figs. 3.16A and B). Melatonin treatment resulted in a 29% rescue in survival to pupation (Fig. 3.16C) and a 20% rescue in survival to eclosion (Fig. 3.16D).

As with locomotion, the story became more complex when it came to rescuing the toxicity/survival in the transgenic *Drosophila* containing the serine site mutations. For these larvae, regardless of the size of the polyQ stretch, sodium butyrate was unable to significantly positively influence survival rates (Figs. 3.16C and D). To the contrary, the survival of the ARQ22dm flies was somewhat hindered with sodium butyrate treatment. However, this hindrance was slight and not statistically significant. Although the ARQ77dm survival appeared to improve after feeding on sodium butyrate food, this difference was also not statistically significant. Melatonin was much more successful in inhibiting the toxicity seen in ARQ77dm and especially ARQ22dm flies (Figs. 3.16C and D). ARQ22dm larvae demonstrated an approximately 40% rescue in survival rates for both survival to pupation (Fig. 3.16C) and survival to eclosion (Fig. 3.16D). ARQ77dm larvae experienced a 44% rescue in survival to eclosion.

The survival data surprisingly showed melatonin to be a potent inhibitor of toxicity, besting the known inhibitor sodium butyrate for each of the AR variants. The differential results between the fly lines also solidified the earlier stated view that the ARQ77, ARQ22dm, and ARQ77dm demonstrate varying forms of toxicity.

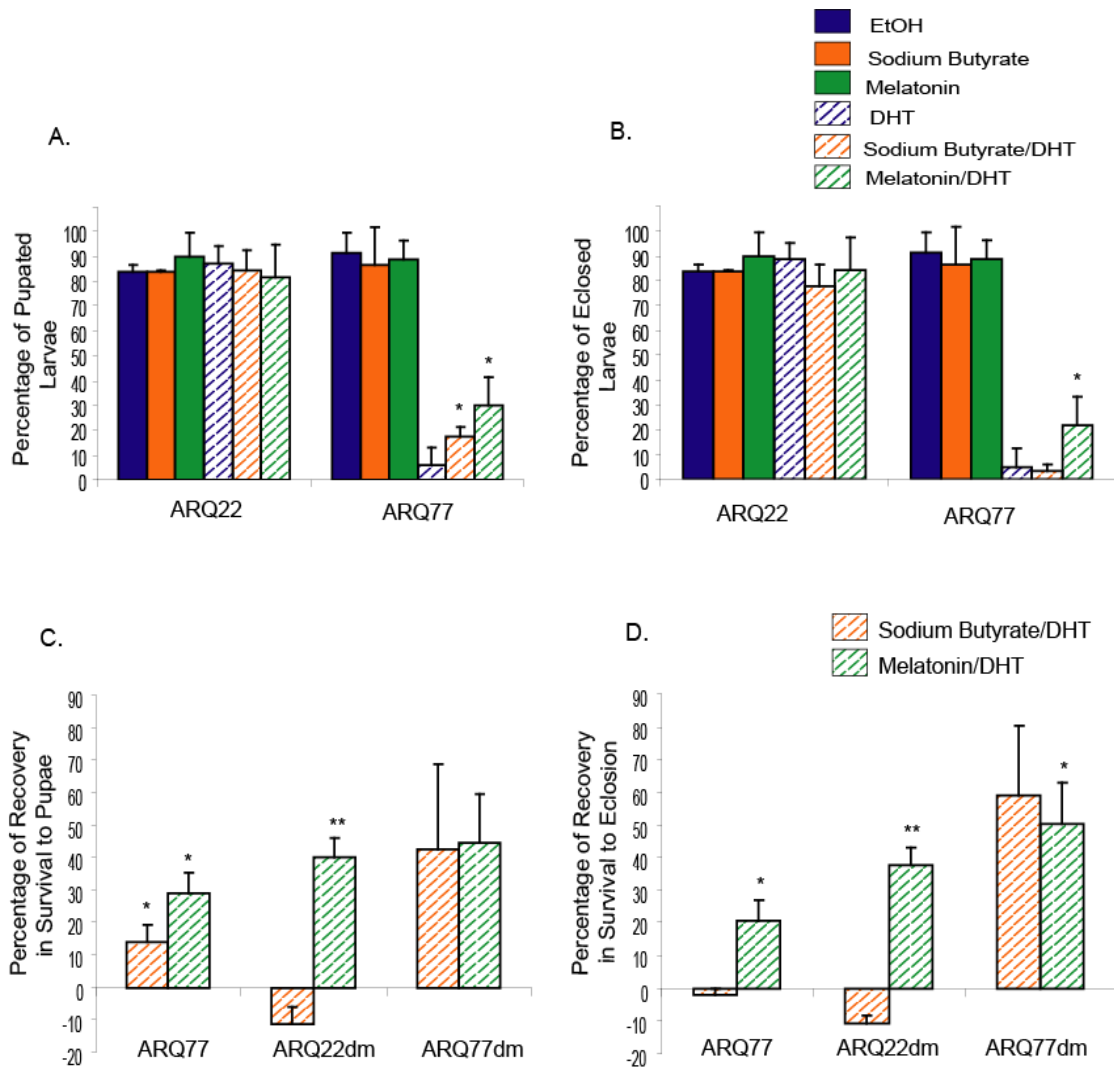


**Figure 3.16 Effects of sodium butyrate and melatonin on survival**

AR fly lines and ELAV-GAL4 flies were crossed on normal stock medium. After hatching of progeny, larvae were transferred to medium containing vehicle (ethanol),  $10^{-3}$ M DHT, 100mM sodium butyrate,  $10^{-2}$ M melatonin, or a combination with a maximum of 50 larvae per vial. The total larvae for each sample was >100. Data are from three separate experiments. The error bars represent standard deviation of the mean. (A) Survival of ARQ77 larvae to pupation was improved with sodium butyrate and melatonin treatment. (B) Survival to eclosion was only affected by melatonin. (C) Only ARQ22dm larvae treated with melatonin showed a significant improvement in survival to pupation while both ARQ22dm and ARQ77dm larvae demonstrated rescue in survival to eclosion with melatonin treatment (D) \* $p < 0.05$ , \*\* $p < 0.001$

## 4.0 DISCUSSION

In this work the effects that alteration of two serine residues at position 424 and 514 in the AR have on the formation of inclusions in cultured cells and on aggregation and toxicity in a *Drosophila* model of SBMA have been analyzed. Individual experiments demonstrated that results in the cell culture model could generally be reproduced in the *Drosophila* model, albeit subtle variations did arise possibly due to the inherent differences in the two systems. Nevertheless, the general reproducibility allowed for comparison of the detailed cell culture inclusion studies with the toxicities and motor impairments exhibited in the more complex *in vivo* system. The collected data thus demonstrate that upon exchange of these two serine residues in the AR to alanine, the wild type receptor becomes toxic while the toxic effects of the normally pathogenic AR with an amplified polyQ stretch are lessened. The results also show that sodium butyrate and melatonin mitigate the toxic effect of the polyQ stretch but show differences toward the serine mutants in their ability to rescue the toxicity. Each of the AR variants therefore exhibits a unique toxic profile.

### 4.1 Alteration of specific residues affects AR conformation and provides model system for evaluating polyQ toxicity

In these studies, the AR serine sites 424 and 514 were chosen for simultaneous analysis because a double mutation was able to block *in vitro* phosphorylation of the AR by ERK whereas single mutations were insufficient. The results presented here show that this double serine to alanine exchange modulates the activity of the expanded polyQ stretch by reducing cellular inclusions and toxicity. However, a study by LaFevre-Brent and Ellerby (2003) showed that the single mutation of serine 514 into alanine was sufficient to block AR-induced cell death and generation of caspase 3-derived products in an AR with a polyQ stretch of 112. At this point, it cannot be determined whether or not a simultaneous mutation of the 424 site would have enhanced the effects seen by Lafevre-Brent and Ellerby, especially if both sites are involved in the ERK signaling that is a central aspect to their results. In the same vein, it is also unclear whether the 514 site alone is sufficient to induce the toxic alterations to the wild type AR that have been

reported here. In any case, these studies do corroborate the work of LaFevre-Brent and Ellerby 2003 in identifying the serine 514 as one of the important sites that when mutated decreases the toxicity of the amplified polyQ tract in the AR.

The previous point leads to the question as to why a single or double amino acid exchange would drastically affect the polyQ toxicity of the AR? One possibility is that the sites mutated destroy interfaces in protein-protein interactions. The other possibility is that they alter the folding (misfolding) of the protein. While there is not yet evidence of altered protein binding by the ARQ22dm and ARQ77dm, the results from the limited protease digestion studies in both *in vitro* and *in vivo* systems show that the conformation of the AR sequences is altered by the amino acid exchanges. The serine double mutation most likely changes the conformation of the ARQ22 and ARQ77 in such a way that the balance of protein folding quality control is disrupted leading to toxic or non-toxic aggregation, among other effects. Perutz and colleagues have reported that a single amino acid replacement can destabilize the native structure of proteins to unfold and form amyloids. Destabilization of no more than 2 kcal/mol can increase the probability of nucleation of disordered aggregates from which amyloids can grow 130,000-fold (Perutz et al., 2002).

If a single amino acid exchange can have such profound effects, one must also question the specificity of these ensuing changes. Would any random amino acid exchange result in altered protein folding for the wild type and polyQ expanded AR? Palazzolo et al., (2007) recently answered this question in their investigation of AR serine sites 215 and 792. This study demonstrated that simultaneous phosphomimetic mutations of serines 215 and 792 reduced ligand binding, ligand-dependent nuclear translocation, transcriptional activation, and toxicity in an AR with a polyQ stretch of 65. However, mutations of these same sites to alanine did not affect the aggregation and toxicity of the wild type or pathogenic AR; thereby showing that only specific residue alterations affect polyQ protein structure and toxicity.

An interesting finding that is perhaps unique to the specific serine mutations in this work is that the serine-to-alanine exchanges had differential effects on aggregation and toxicity depending upon the length of the polyQ stretch. In the context of the wild type receptor, they increase aggregation and make an otherwise non-toxic AR cytotoxic.

Thomas and colleagues had shown previously that mutation of totally different residues (lysine residues at positions 632 and 633 to alanine) in a wild type AR with a polyQ stretch of 24 caused a delay in nuclear transport of the receptor and an accumulation of cytoplasmic inclusions (Thomas et al., 2004). However, although the disruption of acetylation through mutation of these lysine sites resulted in a polyQ phenotype of toxicity in the wild type AR, no significant changes were noted in an AR with a polyQ stretch of 112. The authors hypothesized that reduced acetylation is a key property of AR polyQ pathogenesis; thus they were giving the wild type AR a feature that the mutant polyQ AR already possessed. The aforementioned study of Palazzo et al., where phosphomimetic mutations of serines 215 and 792 positively influenced the toxic polyQ AR, presents a different scenario. In this case, both the wild type and polyQ receptors demonstrated diminished ligand binding and nuclear localization, which contributed to a less toxic polyQ AR but did not alter the benign status of the wild type AR (Palazzolo et al., 2007). Therefore, the central role of these mutations was the disruption of the necessary pathogenic step of translocation to the nucleus. The unique consequences of the alteration of serines 424 and 514 appear to result from a combination of the above scenarios, triggered by the conformational changes that are evident in the limited proteolytic digestion assays. One way to look at the differential effects of these serine mutations is to take the conformational changes as the primary effect. Secondary effects would then be changes in nuclear localization, transcriptional activity, aggregation, and ultimately toxicity. Therefore, the change in conformation of the wild type receptor brought about by the serine mutations resulted in a cascade of secondary effects that gave the wild type AR toxic properties. In the same manner, the change in conformation of the polyQ receptor altered or disrupted some of the secondary effects required for polyQ toxicity. The identification of serines 424 and 514 as specific sites whose manipulation results in different levels of toxicity for the AR is therefore beneficial for studying how the details of AR conformation and secondary effects result in toxic or non-toxic situations.

## **4.2 Altered conformations differentially affect nuclear accumulation and transcriptional activity**

An altered transport pattern of the AR to and from the nucleus, which results in changes in nuclear accumulation as well as possible differences in transcriptional activity, is one of the secondary effects of the altered conformation brought about by the serine mutations. In general, nuclear shuttling activity is one of the few shared characteristics of the polyQ proteins (Truant et al., 2007). Altering this activity by sequestration of the polyQ proteins in the cytoplasmic or nuclear cellular compartments has been shown to have profound effects on polyQ toxicity (Klement et al., 1998; Peters et al., 1999; Bichelmeier et al., 2007). Several groups have shown that blocking the accumulation of the AR in the nucleus eliminates a critical step of the SBMA polyQ disease pathway, thereby blocking aggregation and cell death (Takeyama et al., 2002; Furutani et al., 2005; Palazzolo et al., 2007). However, the subtle difference of delaying rather than blocking nuclear localization can result in an aggravated phenotype (Thomas et al., 2004). The ARQ22dm in this work demonstrated this latter version of delayed accumulation in the nucleus following hormone treatment in cell culture experiments and an overall lack of nuclear accumulation in the *Drosophila* model. A plausible reason for this “delay” is that the altered conformation exhibited by the ARQ22dm yields an AR/chaperone complex that deviates in composition and/or conformation from that of the wild type situation and results in inefficient exposure of the NLS signal. Furthermore, it is plausible that changes in nuclear translocation could ensue if the AR conformation is such that ligand binding is affected. In the case of the AR containing the expanded polyQ stretch, a clinical study found that several SBMA patients exhibited abnormal ligand binding affinity, which correlated with severity of symptoms (MacLean et al., 1995). Ligand association is not only critical for nuclear import but has also been postulated to be required for retaining the AR in the nucleus (Roy et al., 2001). A structural alteration of the NTD due to the serine site mutations and/or the polyQ stretch could modify this association by interfering with an N-/C-terminal interaction of the AR that aids in holding the ligand in the ligand-binding pocket (Ikonen et al., 1997; He et al., 1999). Therefore, an altered binding affinity could explain the observed changes in nuclear accumulation for the AR variants in this work and in other SBMA models (Becker et al., 2000; Thomas et al., 2004).

The conformational state of the AR is also a significant factor for optimal transcriptional activity by the receptor. In the absence of ligand, the LBD of the C-terminus exerts an inhibitory influence on the activity of the AF-1 in the NTD (Jenster et al., 1991). Ligand-binding of the AR allows for a conformational change that not only relieves this inhibitory influence on the AF-1 but also positions the AF-2 for interactions with coregulators. This structural change at the LBD is also thought to create a change in the NTD, enabling the NTD to interact with coactivators as well (Roy et al., 2001). Transcriptional regulation of target genes is reliant upon both the NTD and LBD domains for coordinated AF-1 and AF-2 activity (Jenster et al., 1995). Mutational analyses have demonstrated that almost the entire NTD is necessary for the receptor to reach its maximum transactivation potential (Bevan et al., 1999). Indeed, the transcriptional activity of the N-terminal AR variants containing the amplified polyQ stretch in this work deviated significantly from the wild type ARQ22. The presence of the expanded polyQ region resulted in reduced levels of hormone induction for both the ARQ77 and ARQ77dm, supporting other works that have shown that an amplified polyQ stretch negatively effects AR transcriptional activity (Irvine et al., 2000; Thomas et al., 2006b). The influence of the N-terminal serine residue exchanges, however, was more difficult to discern. While the serine mutations appeared to result in no changes in transcriptional activity for the ARQ77 background, the results for the ARQ22 background were more complex. Although overall levels of transcriptional activity were reduced for the ARQ22dm, hormone induction seemed to be higher than that of its wild type counterpart. In the case of the amplified polyQ stretch, the reduced transcriptional activation of target genes has been proposed to be a contributor to cellular toxicity, possibly through the loss of the AR's trophic capabilities (Thomas et al., 2006b). At present, it is not clear if or how the anomalous result of the ARQ22dm affects the toxicity of this particular AR variant.

In analyzing the effects of the serine site mutations on transcriptional activity, one must keep in mind that the presented COS7 cell culture experiments may only give a limited view of the intricate *in vivo* scenario that involves coactivator and corepressor molecules that may or may not be active in COS7 cells. Along with an altered presence in the nucleus, the ability of coregulators to bind the AR greatly impacts the transactivation

activity of the receptor (Chmelar et al., 2007). Furthermore, the NTD is critical for interaction with the glutamine rich steroid receptor coactivator-1 (SRC-1) as well as other members of the p160 family of coactivators such as the glucocorticoid receptor-interacting protein (GRIP-1)/TIF2 (transcription intermediary factor 2) (Bevan et al., 1999). The length of the polyQ region of the NTD has previously been shown to affect this interaction, demonstrating an inverse correlation with the recruitment of p160 coactivators SRC-1 and GRIP-1 (Irvine et al., 2000; Callewaert et al., 2003). Therefore, it is possible that the proposed alterations in the conformation of the AR NTD due to the exchange of serine residues 424 and 514 could also affect coactivator recruitment and result in changes in transcriptional activity that are not evident in the COS7 model. For this scenario, it is especially important to note that the N-terminal interaction domain of GRIP-1 has previously been mapped to AR amino acids 351-537 (Irvine et al., 2000), which encompasses the serine sites examined in these studies. Another coactivator whose recruitment could potentially be affected by the residue exchanges at serines 424 and 514 is Ran/ARA24. This 24 kDa Ras-like small nuclear GTPase was also found to bind the polyQ region and enhance AR transactivation in a manner that was inversely correlated with the length of the glutamine stretch (Hsiao et al., 1999). A particularly interesting feature of this coactivator is its involvement in the nuclear transport of proteins (Rush et al., 1996). Differential recruitment of ARA24 could therefore also provide another link to the altered nuclear accumulation of the ARQ22dm, ARQ77, and ARQ77dm in addition to any changes in transactivation activity. Thus, overexpression studies investigating the recruitment of coregulators are needed to clarify if and how the serine site mutations alter transcriptional activation by the AR.

When examining the nuclear accumulation and transactivation patterns of the AR variants, changes in nuclear presence did not always directly correspond with changes in transcriptional activity. For example, even though the conformationally different ARQ77dm demonstrated improved nuclear localization kinetics in comparison to the ARQ77, the transcriptional activities of both receptors were similarly impaired. A comparison can also be drawn between the the ARQ22dm and the ARQ77dm; these receptors demonstrated similar nuclear accumulation kinetics but different patterns of transcriptional activation. Therefore, it seems that nuclear localization is a secondary

effect that can be disrupted or improved in a polyQ length-dependent manner due to conformational changes brought about by the serine mutations. However, although the effects of the serine exchanges on transcriptional activity need to be further elucidated in regards to coregulator recruitment, the general picture for the regulation of reporter genes depicted thus far shows alterations for the ARQ22 background but does not show an opposing effect in the ARQ77 background. The implication of these results is that the pathway of toxic secondary effects resulting from the residue exchanges at serines 424 and 514 and the subsequent conformational changes of the wild type receptor likely differs from the pathway of secondary effects that make the ARQ77dm less toxic than its ARQ77 counterpart. Therefore, it is possible to manipulate polyQ toxicity at multiple points and elucidation of these points could reveal multiple therapeutic targets.

### **4.3 Altered AR conformations yield characteristically diverse aggregates**

Aggregate formation as a result of misfolded protein conformations is a critical attribute of polyQ toxicity, and the differing aggregate profiles of the AR variants give further insight into what makes the ARQ22dm “more toxic” and the ARQ77dm “less toxic”. The first most obvious observation from the cell culture model is the differential effects of the serine mutations on the kinetics of inclusion formation with a global increase in inclusions for the ARQ22 background and a decrease for the ARQ77 background. Such global changes in aggregation have been the basis for many reports of alleviation or augmentation of polyQ toxicity (Diamond et al., 2000; Apostol et al., 2003; Scappini et al., 2007). Interestingly, the presented opposing changes in aggregation stemming from the different polyQ lengths and the serine site exchanges actually meant that the ARQ22dm and ARQ77dm demonstrated similar rates for overall formation of inclusions. These similar inclusion/aggregation rates in the cell culture model also corresponded with comparable levels of toxicity as determined by the locomotion and survival assays of the *Drosophila* model. However, focusing only on total inclusion formation numbers can be misleading due to the possibly varying effects of different types of aggregate structures (Bates, 2003; Arrasate et al., 2004). Rather, an association of the specific types of aggregates with alterations in polyQ toxicity has proven more informative (Li et al., 2007; Rusmini et al., 2007). Following this line of reasoning, the ARQ22dm and the ARQ77dm did demonstrate distinct differences when classified in the immunofluorescence and solubility experiments, clarifying that the toxic properties exhibited by these AR variants are not equivalent.

In this work, inclusions were initially classified as to their cellular compartmentalization and globular or fibrous appearance. For all of the AR constructs, most of the differences were only visible in the cytoplasmic compartment. The lack of intranuclear inclusions is most likely due to the specific experimental conditions of the immunofluorescence studies (i.e. cell type or time course of DHT treatment). A previous study reported that nuclear localization of inclusions is indeed more prominent in neuronal cells than COS cell lines (Merry et al., 1998). Nevertheless, examining differences in cytoplasmic inclusions is also relevant due to their presence in SBMA

patients (Adachi et al., 2005) as well as their confirmed toxic influence (Piccioni et al., 2002; Lee et al., 2004). Although the serine mutations resulted in an increase or decrease in both globular and fibrous cytoplasmic inclusions for the ARQ22 and ARQ77 backgrounds respectively, the changes were not entirely symmetric. The percentages of cells containing globular inclusions, which have especially been implicated in pathophysiology (Quist et al., 2005), were relatively equal for both serine mutated receptors. However, the ARQ22dm exhibited a noticeably greater frequency of fibrous cytoplasmic inclusions than the ARQ77dm. Without more intense structural investigation, it is difficult to speculate on the exact role of these extra fibrous inclusions in the pathogenicity of the ARQ22dm.

Differences among the AR variants were investigated by determining aggregate solubility in both COS7 cells and the *Drosophila* model. The aggregates formed by the ARQ22dm in COS7 cells were found to be SDS-insoluble at the earliest time points of androgen treatment. After prolonged hormone treatment, the ARQ22dm aggregates were not retained on the filter that normally traps insoluble aggregates formed by protein with amplified polyQ stretches (Heiser et al., 2002). Thus the ARQ22dm aggregates appeared to be rather transient in nature. Aggregates for both the ARQ77 and ARQ77dm, however, were retained at all time points investigated. As opposed to the cell culture model, all three AR variants expressed in *Drosophila* larvae formed aggregates that were SDS-insoluble over an extended period of hormone treatment. Due to limiting experimental factors with the *Drosophila* model, the transience of these ARQ22dm aggregates could not be determined. However, studies utilizing fluorescence recovery after photobleaching (FRAP) have indicated that polyQ proteins are dynamic and aggregates can actually exchange between soluble and insoluble phases and move between inclusions in their cellular environment (Truant et al., 2007). Therefore, it is possible that the ARQ22dm aggregates of the *Drosophila* system were examined at an insoluble phase. The differences in cellular environmental factors between the two model systems could feasibly play a role in the timing and formation of such soluble and insoluble aggregate phases. In terms of characterizing the AR variants, it could prove beneficial to explore what factors are associated with the various phases of solubility.

The filter retardation assay utilized to determine the solubility states of the four ARs in both the cell and *Drosophila* models was unfortunately not sensitive enough to distinguish quantitatively between the AR variants, especially the ARQ77 and ARQ77dm. The dramatic differences in the appearance of inclusions as visualized by the immunofluorescence studies and the correlation of these results with toxicity levels in *Drosophila* did not translate to comparable differences in the solubility assays. The lack of a correlation between the presence of insoluble aggregates after extended hormone treatment and the exhibited toxicities of the AR variants points toward the argument of soluble intermediates rather than large insoluble inclusions as the toxic species (Ross and Poirier, 2004; Li et al., 2007). The likelihood of the different receptors to form such intermediates would most likely depend on their structural divergences. Attempts to make further conformational distinctions through immunostaining with the 1C2 antibody, however, were also unsuccessful. The aforementioned study by Thomas et al., showed that its AR containing 24 glutamines and acetylation site mutations was recognized by this antibody that normally only recognizes proteins with amplified polyQ stretches, suggesting a conformational change in the protein (Thomas et al., 2004). Although the ARQ22dm presented in this work displayed similar toxic characteristics as the acetylation mutant in the way of delayed nuclear accumulation and increased aggregation, it was not recognized by the 1C2 antibody; indicating that the inclusions formed by this protein are most likely different from those formed by the ARQ24 with the lysine mutations. Therefore, it seems to be generally applicable that polyQ proteins with subtle changes in neighboring sequences produce different types of aggregates with varying toxicities. Furthermore, there is a need to quantitatively and structurally characterize the primary conformational changes and the secondary aggregate formations of the protein variants presented here as well as in other studies (LaFevre-Bernt and Ellerby, 2003; Thomas et al., 2004). This would allow for more direct targeting of specific aggregate types by therapeutic agents.

#### **4.4 Inhibitor compounds act on specific subsets of the varied AR toxicities**

Several compounds have been tested for their ability to ameliorate the toxic effects of the amplified polyQ disorders. Among the successful contenders are inhibitors of histone deacetylases (HDAC). The HDAC inhibitors, sodium butyrate and suberoylanilide hydroxamic acid (SAHA) have been used to mitigate polyQ toxicity in both *Drosophila* and mouse models of SBMA and Huntington's (McCampbell et al., 2001; Steffan et al., 2001; Minamiyama et al., 2004). Sodium butyrate was therefore used along with melatonin, another candidate inhibitor of neurodegenerative disorders (Srinivasan et al., 2006) and a general health supplement (Lewis and Clouatre, 1999) to rescue the toxicity caused by the AR mutants. The inhibitors were initially tested for their capability of rescuing neurodegeneration of the fly eye. The results confirmed published findings that sodium butyrate reduces toxicity caused by the polyQ amplification (Steffan et al., 2001; Marsh and Thompson, 2004). Melatonin was found to function with a similar, perhaps better, efficiency as sodium butyrate in this assay. Interestingly, the toxicities displayed by the serine mutants did not show a significant response to either compound, demonstrating that the pathogenic mechanisms for these mutants diverge from the classical polyQ scenario.

Locomotive and survival studies that were used to distinguish between the toxicities of the AR variants were also used as a more sensitive approach to analyze the effects of the inhibitors. These *Drosophila* assays were employed rather than the frequently used pseudopupil technique that assesses the number of visible rhabdomeres by light microscopy (Steffan et al., 2001; Marsh and Thompson, 2004) due to the relevance of movement impairment and lifespan to the polyQ disorders. As evaluated by both the locomotive and survival assays, sodium butyrate and melatonin again proved capable of ameliorating polyQ toxicity in almost all tested aspects. The efficiencies in increasing lifespan did vary, though, with sodium butyrate only able to improve survival to the pupal stage. However, the two compounds demonstrated an even greater variation in their effect on the two serine mutants. Sodium butyrate was ineffectual in significantly improving locomotive speed and survival for the ARQ22dm and ARQ77dm while melatonin failed to improve the angular velocity of these mutant larvae. The combination

of the above results most likely stems from the demonstrated differing toxicities of the AR variants in addition to the inhibitors' different modes of action. Sodium butyrate, like other HDAC inhibitors, prevents the removal of acetyl groups from core histones and as a result restores histone acetylation and improves neurodegenerative effects in *Drosophila* models (Taylor et al., 2003) and motor impairment in a mouse model of polyQ diseases (Minamiyama et al., 2004). However in a transgenic model of SBMA, it was observed that sodium butyrate ameliorated the neurological phenotype only within a narrow dose range. It did not inhibit aggregation nor the 1C2 staining arising from the amplified polyQ stretch of the AR (Minamiyama et al., 2004). In contrast, melatonin, which also shows neurodegenerative rescue, inhibited progressive formation of  $\beta$ -sheet and amyloid fibrils observed in Alzheimer's disease (Pappolla et al., 1998). This anti-amyloidogenic property possibly results from structural intercalation of melatonin with the A $\beta$  peptide of Alzheimer's disease and possibly other conformationally toxic species. The differential effects of sodium butyrate and melatonin in rescuing specific subsets of the toxic action of polyQ stretches strongly support the idea of combinatorial drug regimens for the future treatment of polyQ disorders. This is underpinned by the fact that the polyQ toxicity involves multiple cellular mechanisms whose contribution to the disease may be additive or even synergistic.

## 4.5 Final conclusions and outlook for AR-specific and general polyglutamine toxicity studies

The presented results have identified a mutant AR with a non-amplified polyQ stretch that demonstrates several characteristics that are similar to those of the pathogenic AR containing a polyQ expansion. These exhibited characteristics include delayed nuclear accumulation, possible alterations in transcriptional activity, and the formation of aggregate species that are toxic in a *Drosophila* model of neurodegeneration. This AR mutant is comparable with the ARQ77dm that also demonstrates a version of lessened polyQ toxicity but through what appears to be a slightly different pathway of alterations. Together with the classical SBMA polyQ receptor, ARQ77, these mutant receptors would provide useful material for future studies on how changes in protein conformation can lead to toxicity. More specifically, these receptors could be utilized to investigate two theoried key features of polyQ pathogenesis, transcriptional dysregulation and aggregate formation. The elucidation of altered transcriptional coregulator interactions with the different receptor versions has the potential to yield mechanistic insight and possible therapeutic targets for SBMA. Structural studies of the aggregates formed by the AR mutants could prove more generally applicable with the possibility of pinpointing specific conformational changes to varying degrees of polyQ toxicity. Furthermore, it would be useful to investigate how these detailed conformational alterations can be rescued by inhibitors that target different cellular processes. Since melatonin was shown to be a capable polyQ inhibitor in the studies presented here and it is known to affect A $\beta$  fibril formation (Pappolla et al., 1998), it would be especially interesting to investigate its specific effects on the proposed different aggregate fomations of the AR mutants. One group has already proven that classification of aggregates can directly lead to therapeutic strategies (Nagai et al., 2003; Armen et al., 2005). In two separate studies, this group identified a toxic conformer peptide (polyQ-binding peptide 1/QBP1) that binds to an alpha-extended chain conformation, thereby inhibiting fibril formation (Armen et al., 2005) and preventing polyQ-induced neurodegeneration in a *Drosophila* model (Nagai et al., 2003). Therefore, with the combination of future structural studies of the AR variants and the running *Drosophila* model presented in this body of work, a similar and perhaps more specific development of therapeutic strategies is feasible.



## REFERENCES

- Abel A, Walcott J, Woods J, Duda J, Merry DE (2001) Expression of expanded repeat androgen receptor produces neurologic disease in transgenic mice. *Hum Mol Genet* 10:107-116.
- Adachi H, Waza M, Tokui K, Katsuno M, Minamiyama M, Tanaka F, Doyu M, Sobue G (2007) CHIP overexpression reduces mutant androgen receptor protein and ameliorates phenotypes of the spinal and bulbar muscular atrophy transgenic mouse model. *J Neurosci* 27:5115-5126.
- Adachi H, Kume A, Li M, Nakagomi Y, Niwa H, Do J, Sang C, Kobayashi Y, Doyu M, Sobue G (2001) Transgenic mice with an expanded CAG repeat controlled by the human AR promoter show polyglutamine nuclear inclusions and neuronal dysfunction without neuronal cell death. *Hum Mol Genet* 10:1039-1048.
- Adachi H, Katsuno M, Minamiyama M, Sang C, Pagoulatos G, Angelidis C, Kusakabe M, Yoshiki A, Kobayashi Y, Doyu M, Sobue G (2003) Heat shock protein 70 chaperone overexpression ameliorates phenotypes of the spinal and bulbar muscular atrophy transgenic mouse model by reducing nuclear-localized mutant androgen receptor protein. *J Neurosci* 23:2203-2211.
- Adachi H, Katsuno M, Minamiyama M, Waza M, Sang C, Nakagomi Y, Kobayashi Y, Tanaka F, Doyu M, Inukai A, Yoshida M, Hashizume Y, Sobue G (2005) Widespread nuclear and cytoplasmic accumulation of mutant androgen receptor in SBMA patients. *Brain* 128:659-670.
- Agrawal N, Pallos J, Slepko N, Apostol BL, Bodai L, Chang LW, Chiang AS, Thompson LM, Marsh JL (2005) Identification of combinatorial drug regimens for treatment of Huntington's disease using *Drosophila*. *Proc Natl Acad Sci U S A* 102:3777-3781.
- Al-Ramahi I, Lam YC, Chen HK, de Gouyon B, Zhang M, Perez AM, Branco J, de Haro M, Patterson C, Zoghbi HY, Botas J (2006) CHIP protects from the neurotoxicity of expanded and wild-type ataxin-1 and promotes their ubiquitination and degradation. *J Biol Chem* 281:26714-26724.
- Allan GF, Leng X, Tsai SY, Weigel NL, Edwards DP, Tsai MJ, O'Malley BW (1992) Hormone and antihormone induce distinct conformational changes which are central to steroid receptor activation. *J Biol Chem* 267:19513-19520.

- Apostol BL, Illes K, Pallos J, Bodai L, Wu J, Strand A, Schweitzer ES, Olson JM, Kazantsev A, Marsh JL, Thompson LM (2006) Mutant huntingtin alters MAPK signaling pathways in PC12 and striatal cells: ERK1/2 protects against mutant huntingtin-associated toxicity. *Hum Mol Genet* 15:273-285.
- Apostol BL, Kazantsev A, Raffioni S, Illes K, Pallos J, Bodai L, Slepko N, Bear JE, Gertler FB, Hersch S, Housman DE, Marsh JL, Thompson LM (2003) A cell-based assay for aggregation inhibitors as therapeutics of polyglutamine-repeat disease and validation in *Drosophila*. *Proc Natl Acad Sci U S A* 100:5950-5955.
- Arbizu T, Santamaria J, Gomez JM, Quilez A, Serra JP (1983) A family with adult spinal and bulbar muscular atrophy, X-linked inheritance and associated testicular failure. *J Neurol Sci* 59:371-382.
- Armen RS, Bernard BM, Day R, Alonso DO, Daggett V (2005) Characterization of a possible amyloidogenic precursor in glutamine-repeat neurodegenerative diseases. *Proc Natl Acad Sci U S A* 102:13433-13438.
- Arrasate M, Mitra S, Schweitzer ES, Segal MR, Finkbeiner S (2004) Inclusion body formation reduces levels of mutant huntingtin and the risk of neuronal death. *Nature* 431:805-810.
- Bailey CK, Andriola IF, Kampinga HH, Merry DE (2002) Molecular chaperones enhance the degradation of expanded polyglutamine repeat androgen receptor in a cellular model of spinal and bulbar muscular atrophy. *Hum Mol Genet* 11:515-523.
- Bain DL, Heneghan AF, Connaghan-Jones KD, Miura MT (2007) Nuclear receptor structure: implications for function. *Annu Rev Physiol* 69:201-220.
- Banfi S, Servadio A, Chung MY, Kwiatkowski TJ, Jr., McCall AE, Duvick LA, Shen Y, Roth EJ, Orr HT, Zoghbi HY (1994) Identification and characterization of the gene causing type 1 spinocerebellar ataxia. *Nat Genet* 7:513-520.
- Bates G (2003) Huntingtin aggregation and toxicity in Huntington's disease. *Lancet* 361:1642-1644.
- Becker M, Martin E, Schneikert J, Krug HF, Cato AC (2000) Cytoplasmic localization and the choice of ligand determine aggregate formation by androgen receptor with amplified polyglutamine stretch. *J Cell Biol* 149:255-262.

- Bevan CL, Hoare S, Claessens F, Heery DM, Parker MG (1999) The AF1 and AF2 domains of the androgen receptor interact with distinct regions of SRC1. *Mol Cell Biol* 19:8383-8392.
- Bhattacharyya A, Thakur AK, Chellgren VM, Thiagarajan G, Williams AD, Chellgren BW, Creamer TP, Wetzel R (2006) Oligoproline effects on polyglutamine conformation and aggregation. *J Mol Biol* 355:524-535.
- Bichelmeier U, Schmidt T, Hubener J, Boy J, Ruttiger L, Habig K, Poths S, Bonin M, Knipper M, Schmidt WJ, Wilbertz J, Wolburg H, Laccone F, Riess O (2007) Nuclear localization of ataxin-3 is required for the manifestation of symptoms in SCA3: in vivo evidence. *J Neurosci* 27:7418-7428.
- Bingham PM, Scott MO, Wang S, McPhaul MJ, Wilson EM, Garbern JY, Merry DE, Fischbeck KH (1995) Stability of an expanded trinucleotide repeat in the androgen receptor gene in transgenic mice. *Nat Genet* 9:191-196.
- Bonini NM (1999) A genetic model for human polyglutamine-repeat disease in *Drosophila melanogaster*. *Philos Trans R Soc Lond B Biol Sci* 354:1057-1060.
- Buee L, Bussiere T, Buee-Scherrer V, Delacourte A, Hof PR (2000) Tau protein isoforms, phosphorylation and role in neurodegenerative disorders. *Brain Res Brain Res Rev* 33:95-130.
- Burright EN, Clark HB, Servadio A, Matilla T, Feddersen RM, Yunis WS, Duvick LA, Zoghbi HY, Orr HT (1995) SCA1 transgenic mice: a model for neurodegeneration caused by an expanded CAG trinucleotide repeat. *Cell* 82:937-948.
- Callewaert L, Christiaens V, Haelens A, Verrijdt G, Verhoeven G, Claessens F (2003) Implications of a polyglutamine tract in the function of the human androgen receptor. *Biochem Biophys Res Commun* 306:46-52.
- Cha JH, Dure LSt (1994) Trinucleotide repeats in neurologic diseases: an hypothesis concerning the pathogenesis of Huntington's disease, Kennedy's disease, and spinocerebellar ataxia type I. *Life Sci* 54:1459-1464.
- Chai Y, Koppenhafer SL, Bonini NM, Paulson HL (1999) Analysis of the role of heat shock protein (Hsp) molecular chaperones in polyglutamine disease. *J Neurosci* 19:10338-10347.

- Chan HY, Warrick JM, Andriola I, Merry D, Bonini NM (2002) Genetic modulation of polyglutamine toxicity by protein conjugation pathways in *Drosophila*. *Hum Mol Genet* 11:2895-2904.
- Chang DT, Rintoul GL, Pandipati S, Reynolds IJ (2006) Mutant huntingtin aggregates impair mitochondrial movement and trafficking in cortical neurons. *Neurobiol Dis* 22:388-400.
- Chen HK, Fernandez-Funez P, Acevedo SF, Lam YC, Kaytor MD, Fernandez MH, Aitken A, Skoulakis EM, Orr HT, Botas J, Zoghbi HY (2003) Interaction of Akt-phosphorylated ataxin-1 with 14-3-3 mediates neurodegeneration in spinocerebellar ataxia type 1. *Cell* 113:457-468.
- Cheng X, van Breemen RB (2005) Mass spectrometry-based screening for inhibitors of beta-amyloid protein aggregation. *Anal Chem* 77:7012-7015.
- Chevalier-Larsen ES, O'Brien CJ, Wang H, Jenkins SC, Holder L, Lieberman AP, Merry DE (2004) Castration restores function and neurofilament alterations of aged symptomatic males in a transgenic mouse model of spinal and bulbar muscular atrophy. *J Neurosci* 24:4778-4786.
- Chmelar R, Buchanan G, Need EF, Tilley W, Greenberg NM (2007) Androgen receptor coregulators and their involvement in the development and progression of prostate cancer. *Int J Cancer* 120:719-733.
- Chou AH, Yeh TH, Kuo YL, Kao YC, Jou MJ, Hsu CY, Tsai SR, Kakizuka A, Wang HL (2006) Polyglutamine-expanded ataxin-3 activates mitochondrial apoptotic pathway by upregulating Bax and downregulating Bcl-xL. *Neurobiol Dis* 21:333-345.
- Cummings CJ, Sun Y, Opal P, Antalffy B, Mestril R, Orr HT, Dillmann WH, Zoghbi HY (2001) Overexpression of inducible HSP70 chaperone suppresses neuropathology and improves motor function in SCA1 mice. *Hum Mol Genet* 10:1511-1518.
- Darrington RS, Leigh PN, Gallo JM (2003) Protective effects of estrogens on polyglutamine-expanded androgen receptor aggregation in mice. *Neurosci Lett* 350:37-40.
- Davies SW, Turmaine M, Cozens BA, Raza AS, Mahal A, Mangiarini L, Bates GP (1999) From neuronal inclusions to neurodegeneration: neuropathological investigation of a transgenic mouse model of Huntington's disease. *Philos Trans R Soc Lond B Biol Sci* 354:981-989.

- Davies SW, Turmaine M, Cozens BA, DiFiglia M, Sharp AH, Ross CA, Scherzinger E, Wanker EE, Mangiarini L, Bates GP (1997) Formation of neuronal intranuclear inclusions underlies the neurological dysfunction in mice transgenic for the HD mutation. *Cell* 90:537-548.
- de Chiara C, Menon RP, Dal Piaz F, Calder L, Pastore A (2005) Polyglutamine is not all: the functional role of the AXH domain in the ataxin-1 protein. *J Mol Biol* 354:883-893.
- Dehay B, Bertolotti A (2006) Critical role of the proline-rich region in Huntingtin for aggregation and cytotoxicity in yeast. *J Biol Chem* 281:35608-35615.
- Dehm SM, Tindall DJ (2007) Androgen Receptor Structural and Functional Elements: Role and Regulation in Prostate Cancer. *Mol Endocrinol*.
- Desai UA, Pallos J, Ma AA, Stockwell BR, Thompson LM, Marsh JL, Diamond MI (2006) Biologically active molecules that reduce polyglutamine aggregation and toxicity. *Hum Mol Genet* 15:2114-2124.
- Diamond MI, Robinson MR, Yamamoto KR (2000) Regulation of expanded polyglutamine protein aggregation and nuclear localization by the glucocorticoid receptor. *Proc Natl Acad Sci U S A* 97:657-661.
- DiFiglia M, Sapp E, Chase KO, Davies SW, Bates GP, Vonsattel JP, Aronin N (1997) Aggregation of huntingtin in neuronal intranuclear inclusions and dystrophic neurites in brain. *Science* 277:1990-1993.
- Dodd JG, Sheppard PC, Matusik RJ (1983) Characterization and cloning of rat dorsal prostate mRNAs. Androgen regulation of two closely related abundant mRNAs. *J Biol Chem* 258:10731-10737.
- Duennwald ML, Jagadish S, Muchowski PJ, Lindquist S (2006) Flanking sequences profoundly alter polyglutamine toxicity in yeast. *Proc Natl Acad Sci U S A* 103:11045-11050.
- Ellerby LM, Andrusiak RL, Wellington CL, Hackam AS, Propp SS, Wood JD, Sharp AH, Margolis RL, Ross CA, Salvesen GS, Hayden MR, Bredesen DE (1999a) Cleavage of atrophin-1 at caspase site aspartic acid 109 modulates cytotoxicity. *J Biol Chem* 274:8730-8736.

- Ellerby LM, Hackam AS, Propp SS, Ellerby HM, Rabizadeh S, Cashman NR, Trifiro MA, Pinsky L, Wellington CL, Salvesen GS, Hayden MR, Bredesen DE (1999b) Kennedy's disease: caspase cleavage of the androgen receptor is a crucial event in cytotoxicity. *J Neurochem* 72:185-195.
- Emamian ES, Kaytor MD, Duvick LA, Zu T, Tousey SK, Zoghbi HY, Clark HB, Orr HT (2003) Serine 776 of ataxin-1 is critical for polyglutamine-induced disease in SCA1 transgenic mice. *Neuron* 38:375-387.
- Faber PW, Alter JR, MacDonald ME, Hart AC (1999) Polyglutamine-mediated dysfunction and apoptotic death of a *Caenorhabditis elegans* sensory neuron. *Proc Natl Acad Sci U S A* 96:179-184.
- Feany MB, Bender WW (2000) A *Drosophila* model of Parkinson's disease. *Nature* 404:394-398.
- Fei E, Jia N, Zhang T, Ma X, Wang H, Liu C, Zhang W, Ding L, Nukina N, Wang G (2007) Phosphorylation of ataxin-3 by glycogen synthase kinase 3beta at serine 256 regulates the aggregation of ataxin-3. *Biochem Biophys Res Commun* 357:487-492.
- Fischer A, Sananbenesi F, Wang X, Dobbin M, Tsai LH (2007) Recovery of learning and memory is associated with chromatin remodelling. *Nature* 447:178-182.
- Fortini ME, Bonini NM (2000) Modeling human neurodegenerative diseases in *Drosophila*: on a wing and a prayer. *Trends Genet* 16:161-167.
- Freeman MR, Cinar B, Lu ML (2005) Membrane rafts as potential sites of nongenomic hormonal signaling in prostate cancer. *Trends Endocrinol Metab* 16:273-279.
- Fu M, Wang C, Reutens AT, Wang J, Angeletti RH, Siconolfi-Baez L, Ogryzko V, Avantaggiati ML, Pestell RG (2000) p300 and p300/cAMP-response element-binding protein-associated factor acetylate the androgen receptor at sites governing hormone-dependent transactivation. *J Biol Chem* 275:20853-20860.
- Fu M, Rao M, Wang C, Sakamaki T, Wang J, Di Vizio D, Zhang X, Albanese C, Balk S, Chang C, Fan S, Rosen E, Palvimo JJ, Janne OA, Muratoglu S, Avantaggiati ML, Pestell RG (2003) Acetylation of androgen receptor enhances coactivator binding and promotes prostate cancer cell growth. *Mol Cell Biol* 23:8563-8575.

- Furutani T, Takeyama K, Tanabe M, Koutoku H, Ito S, Taniguchi N, Suzuki E, Kudoh M, Shibasaki M, Shikama H, Kato S (2005) Human expanded polyglutamine androgen receptor mutants in neurodegeneration as a novel ligand target. *J Pharmacol Exp Ther* 315:545-552.
- Gao T, Marcelli M, McPhaul MJ (1996) Transcriptional activation and transient expression of the human androgen receptor. *J Steroid Biochem Mol Biol* 59:9-20.
- Gatchel JR, Zoghbi HY (2005) Diseases of unstable repeat expansion: mechanisms and common principles. *Nat Rev Genet* 6:743-755.
- Gauthier LR, Charrin BC, Borrell-Pages M, Dompierre JP, Rangone H, Cordelieres FP, De Mey J, MacDonald ME, Lessmann V, Humbert S, Saudou F (2004) Huntingtin controls neurotrophic support and survival of neurons by enhancing BDNF vesicular transport along microtubules. *Cell* 118:127-138.
- Genis D, Matilla T, Volpini V, Rosell J, Davalos A, Ferrer I, Molins A, Estivill X (1995) Clinical, neuropathologic, and genetic studies of a large spinocerebellar ataxia type 1 (SCA1) kindred: (CAG)<sub>n</sub> expansion and early premonitory signs and symptoms. *Neurology* 45:24-30.
- George FW, Wilson JD (1994) Sex determination and Differentiation. In: *The Physiology of Reproduction* (Knobil E, Neill JD, eds). New York: Raven Press Ltd.
- Gidalevitz T, Ben-Zvi A, Ho KH, Brignull HR, Morimoto RI (2006) Progressive disruption of cellular protein folding in models of polyglutamine diseases. *Science* 311:1471-1474.
- Gioeli D, Ficarro SB, Kwiek JJ, Aaronson D, Hancock M, Catling AD, White FM, Christian RE, Settlege RE, Shabanowitz J, Hunt DF, Weber MJ (2002) Androgen receptor phosphorylation. Regulation and identification of the phosphorylation sites. *J Biol Chem* 277:29304-29314.
- Goswami A, Dikshit P, Mishra A, Mulherkar S, Nukina N, Jana NR (2006) Oxidative stress promotes mutant huntingtin aggregation and mutant huntingtin-dependent cell death by mimicking proteasomal malfunction. *Biochem Biophys Res Commun* 342:184-190.
- Grierson AJ, Mootosamy RC, Miller CC (1999) Polyglutamine repeat length influences human androgen receptor/c-Jun mediated transcription. *Neurosci Lett* 277:9-12.

- Ham J, Thomson A, Needham M, Webb P, Parker M (1988) Characterization of response elements for androgens, glucocorticoids and progestins in mouse mammary tumour virus. *Nucleic Acids Res* 16:5263-5276.
- Harding AE, Thomas PK, Baraitser M, Bradbury PG, Morgan-Hughes JA, Ponsford JR (1982) X-linked recessive bulbospinal neuronopathy: a report of ten cases. *J Neurol Neurosurg Psychiatry* 45:1012-1019.
- He B, Kempainen JA, Voegel JJ, Gronemeyer H, Wilson EM (1999) Activation function 2 in the human androgen receptor ligand binding domain mediates interdomain communication with the NH(2)-terminal domain. *J Biol Chem* 274:37219-37225.
- Heiser V, Engemann S, Brocker W, Dunkel I, Boeddrich A, Waelter S, Nordhoff E, Lurz R, Schugardt N, Rautenberg S, Herhaus C, Barnickel G, Bottcher H, Lehrach H, Wanker EE (2002) Identification of benzothiazoles as potential polyglutamine aggregation inhibitors of Huntington's disease by using an automated filter retardation assay. *Proc Natl Acad Sci U S A* 99 Suppl 4:16400-16406.
- Ho LW, Brown R, Maxwell M, Wytenbach A, Rubinsztein DC (2001) Wild type Huntingtin reduces the cellular toxicity of mutant Huntingtin in mammalian cell models of Huntington's disease. *J Med Genet* 38:450-452.
- Hockly E, Richon VM, Woodman B, Smith DL, Zhou X, Rosa E, Sathasivam K, Ghazi-Noori S, Mahal A, Lowden PA, Steffan JS, Marsh JL, Thompson LM, Lewis CM, Marks PA, Bates GP (2003) Suberoylanilide hydroxamic acid, a histone deacetylase inhibitor, ameliorates motor deficits in a mouse model of Huntington's disease. *Proc Natl Acad Sci U S A* 100:2041-2046.
- Hsiao PW, Lin DL, Nakao R, Chang C (1999) The linkage of Kennedy's neuron disease to ARA24, the first identified androgen receptor polyglutamine region-associated coactivator. *J Biol Chem* 274:20229-20234.
- Humbert S, Bryson EA, Cordelieres FP, Connors NC, Datta SR, Finkbeiner S, Greenberg ME, Saudou F (2002) The IGF-1/Akt pathway is neuroprotective in Huntington's disease and involves Huntingtin phosphorylation by Akt. *Dev Cell* 2:831-837.
- Ikonen T, Palvimo JJ, Janne OA (1997) Interaction between the amino- and carboxyl-terminal regions of the rat androgen receptor modulates transcriptional activity and is influenced by nuclear receptor coactivators. *J Biol Chem* 272:29821-29828.

- Irvine RA, Ma H, Yu MC, Ross RK, Stallcup MR, Coetzee GA (2000) Inhibition of p160-mediated coactivation with increasing androgen receptor polyglutamine length. *Hum Mol Genet* 9:267-274.
- Iwata A, Christianson JC, Bucci M, Ellerby LM, Nukina N, Forno LS, Kopito RR (2005) Increased susceptibility of cytoplasmic over nuclear polyglutamine aggregates to autophagic degradation. *Proc Natl Acad Sci U S A* 102:13135-13140.
- Jackson GR, Salecker I, Dong X, Yao X, Arnheim N, Faber PW, MacDonald ME, Zipursky SL (1998) Polyglutamine-expanded human huntingtin transgenes induce degeneration of *Drosophila* photoreceptor neurons. *Neuron* 21:633-642.
- Jana NR, Dikshit P, Goswami A, Kotliarova S, Murata S, Tanaka K, Nukina N (2005) Co-chaperone CHIP associates with expanded polyglutamine protein and promotes their degradation by proteasomes. *J Biol Chem* 280:11635-11640.
- Jenster G (1998) Coactivators and corepressors as mediators of nuclear receptor function: an update. *Mol Cell Endocrinol* 143:1-7.
- Jenster G, van der Korput HA, Trapman J, Brinkmann AO (1995) Identification of two transcription activation units in the N-terminal domain of the human androgen receptor. *J Biol Chem* 270:7341-7346.
- Jenster G, van der Korput HA, van Vroonhoven C, van der Kwast TH, Trapman J, Brinkmann AO (1991) Domains of the human androgen receptor involved in steroid binding, transcriptional activation, and subcellular localization. *Mol Endocrinol* 5:1396-1404.
- Jin K, LaFevre-Bernt M, Sun Y, Chen S, Gafni J, Crippen D, Logvinova A, Ross CA, Greenberg DA, Ellerby LM (2005) FGF-2 promotes neurogenesis and neuroprotection and prolongs survival in a transgenic mouse model of Huntington's disease. *Proc Natl Acad Sci U S A* 102:18189-18194.
- Joseph J, Mudduluru G, Antony S, Vashistha S, Ajitkumar P, Somasundaram K (2004) Expression profiling of sodium butyrate (NaB)-treated cells: identification of regulation of genes related to cytokine signaling and cancer metastasis by NaB. *Oncogene* 23:6304-6315.
- Jung J, Bonini N (2007) CREB-binding protein modulates repeat instability in a *Drosophila* model for polyQ disease. *Science* 315:1857-1859.

- Kariya S, Hirano M, Nagai Y, Furiya Y, Fujikake N, Toda T, Ueno S (2005) Humanin attenuates apoptosis induced by DRPLA proteins with expanded polyglutamine stretches. *J Mol Neurosci* 25:165-169.
- Katsuno M, Adachi H, Tanaka F, Sobue G (2004) Spinal and bulbar muscular atrophy: ligand-dependent pathogenesis and therapeutic perspectives. *J Mol Med* 82:298-307.
- Katsuno M, Adachi H, Doyu M, Minamiyama M, Sang C, Kobayashi Y, Inukai A, Sobue G (2003) Leuprorelin rescues polyglutamine-dependent phenotypes in a transgenic mouse model of spinal and bulbar muscular atrophy. *Nat Med* 9:768-773.
- Katsuno M, Adachi H, Kume A, Li M, Nakagomi Y, Niwa H, Sang C, Kobayashi Y, Doyu M, Sobue G (2002) Testosterone reduction prevents phenotypic expression in a transgenic mouse model of spinal and bulbar muscular atrophy. *Neuron* 35:843-854.
- Kayed R, Head E, Thompson JL, McIntire TM, Milton SC, Cotman CW, Glabe CG (2003) Common structure of soluble amyloid oligomers implies common mechanism of pathogenesis. *Science* 300:486-489.
- Kazantsev A, Preisinger E, Dranovsky A, Goldgaber D, Housman D (1999) Insoluble detergent-resistant aggregates form between pathological and nonpathological lengths of polyglutamine in mammalian cells. *Proc Natl Acad Sci U S A* 96:11404-11409.
- Kazemi-Esfarjani P, Trifiro MA, Pinsky L (1995) Evidence for a repressive function of the long polyglutamine tract in the human androgen receptor: possible pathogenetic relevance for the (CAG)<sub>n</sub>-expanded neuropathies. *Hum Mol Genet* 4:523-527.
- Kennedy WR, Alter M, Sung JH (1968) Progressive proximal spinal and bulbar muscular atrophy of late onset. A sex-linked recessive trait. *Neurology* 18:671-680.
- Klement IA, Skinner PJ, Kaytor MD, Yi H, Hersch SM, Clark HB, Zoghbi HY, Orr HT (1998) Ataxin-1 nuclear localization and aggregation: role in polyglutamine-induced disease in SCA1 transgenic mice. *Cell* 95:41-53.
- kQi ML, Tagawa K, Enokido Y, Yoshimura N, Wada Y, Watase K, Ishiura S, Kanazawa I, Botas J, Saitoe M, Wanker EE, Okazawa H (2007) Proteome analysis of soluble nuclear proteins reveals that HMGB1/2 suppress genotoxic stress in polyglutamine diseases. *Nat Cell Biol* 9:402-414.

- La Spada AR, Taylor JP (2003) Polyglutamines placed into context. *Neuron* 38:681-684.
- La Spada AR, Wilson EM, Lubahn DB, Harding AE, Fischbeck KH (1991) Androgen receptor gene mutations in X-linked spinal and bulbar muscular atrophy. *Nature* 352:77-79.
- La Spada AR, Peterson KR, Meadows SA, McClain ME, Jeng G, Chmelar RS, Haugen HA, Chen K, Singer MJ, Moore D, Trask BJ, Fischbeck KH, Clegg CH, McKnight GS (1998) Androgen receptor YAC transgenic mice carrying CAG 45 alleles show trinucleotide repeat instability. *Hum Mol Genet* 7:959-967.
- LaFevre-Bernt MA, Ellerby LM (2003) Kennedy's disease. Phosphorylation of the polyglutamine-expanded form of androgen receptor regulates its cleavage by caspase-3 and enhances cell death. *J Biol Chem* 278:34918-34924.
- Lambert MP, Barlow AK, Chromy BA, Edwards C, Freed R, Liosatos M, Morgan TE, Rozovsky I, Trommer B, Viola KL, Wals P, Zhang C, Finch CE, Krafft GA, Klein WL (1998) Diffusible, nonfibrillar ligands derived from Abeta1-42 are potent central nervous system neurotoxins. *Proc Natl Acad Sci U S A* 95:6448-6453.
- Latouche M, Lasbleiz C, Martin E, Monnier V, Debeir T, Mouatt-Prigent A, Muriel MP, Morel L, Ruberg M, Brice A, Stevanin G, Tricoire H (2007) A conditional pan-neuronal *Drosophila* model of spinocerebellar ataxia 7 with a reversible adult phenotype suitable for identifying modifier genes. *J Neurosci* 27:2483-2492.
- Lavoie MJ, Cortese GP, Ostaszewski BL, Schlossmacher MG (2007) The effects of oxidative stress on parkin and other E3 ligases. *J Neurochem*.
- Lazennec G, Ediger TR, Petz LN, Nardulli AM, Katzenellenbogen BS (1997) Mechanistic aspects of estrogen receptor activation probed with constitutively active estrogen receptors: correlations with DNA and coregulator interactions and receptor conformational changes. *Mol Endocrinol* 11:1375-1386.
- Leavitt BR, Guttman JA, Hodgson JG, Kimel GH, Singaraja R, Vogl AW, Hayden MR (2001) Wild-type huntingtin reduces the cellular toxicity of mutant huntingtin in vivo. *Am J Hum Genet* 68:313-324.

- Lee WC, Yoshihara M, Littleton JT (2004) Cytoplasmic aggregates trap polyglutamine-containing proteins and block axonal transport in a Drosophila model of Huntington's disease. *Proc Natl Acad Sci U S A* 101:3224-3229.
- Lewis CM, Clouatre D (1999) *Melatonin and the Biological Clock*: McGraw-Hill.
- Li M, Chevalier-Larsen ES, Merry DE, Diamond MI (2007) Soluble androgen receptor oligomers underlie pathology in a mouse model of spinobulbar muscular atrophy. *J Biol Chem* 282:3157-3164.
- Lieberman AP, Harmison G, Strand AD, Olson JM, Fischbeck KH (2002) Altered transcriptional regulation in cells expressing the expanded polyglutamine androgen receptor. *Hum Mol Genet* 11:1967-1976.
- Lin HK, Yeh S, Kang HY, Chang C (2001) Akt suppresses androgen-induced apoptosis by phosphorylating and inhibiting androgen receptor. *Proc Natl Acad Sci U S A* 98:7200-7205.
- Lin HK, Wang L, Hu YC, Altuwaijri S, Chang C (2002) Phosphorylation-dependent ubiquitylation and degradation of androgen receptor by Akt require Mdm2 E3 ligase. *Embo J* 21:4037-4048.
- Link CD (1995) Expression of human beta-amyloid peptide in transgenic *Caenorhabditis elegans*. *Proc Natl Acad Sci U S A* 92:9368-9372.
- Liu YF (1998) Expression of polyglutamine-expanded Huntingtin activates the SEK1-JNK pathway and induces apoptosis in a hippocampal neuronal cell line. *J Biol Chem* 273:28873-28877.
- Luo L, Tully T, White K (1992) Human amyloid precursor protein ameliorates behavioral deficit of flies deleted for *Appl* gene. *Neuron* 9:595-605.
- Luo S, Vacher C, Davies JE, Rubinsztein DC (2005) Cdk5 phosphorylation of huntingtin reduces its cleavage by caspases: implications for mutant huntingtin toxicity. *J Cell Biol* 169:647-656.
- MacLean HE, Chu S, Joske F, Warne GL, Zajac JD (1995) Androgen receptor binding studies on heterozygotes in a family with androgen insensitivity syndrome. *Biochem Mol Med* 55:31-37.
- Mangelsdorf DJ, Thummel C, Beato M, Herrlich P, Schutz G, Umesono K, Blumberg B, Kastner P, Mark M, Chambon P, Evans RM (1995) The nuclear receptor superfamily: the second decade. *Cell* 83:835-839.

- Markesbery WR (1997) Oxidative stress hypothesis in Alzheimer's disease. *Free Radic Biol Med* 23:134-147.
- Marks P, Rifkind RA, Richon VM, Breslow R, Miller T, Kelly WK (2001) Histone deacetylases and cancer: causes and therapies. *Nat Rev Cancer* 1:194-202.
- Marsh JL, Thompson LM (2004) Can flies help humans treat neurodegenerative diseases? *Bioessays* 26:485-496.
- Marsh JL, Walker H, Theisen H, Zhu YZ, Fielder T, Purcell J, Thompson LM (2000) Expanded polyglutamine peptides alone are intrinsically cytotoxic and cause neurodegeneration in *Drosophila*. *Hum Mol Genet* 9:13-25.
- Matias PM, Donner P, Coelho R, Thomaz M, Peixoto C, Macedo S, Otto N, Joschko S, Scholz P, Wegg A, Basler S, Schafer M, Egner U, Carrondo MA (2000) Structural evidence for ligand specificity in the binding domain of the human androgen receptor. Implications for pathogenic gene mutations. *J Biol Chem* 275:26164-26171.
- Matsubara E, Bryant-Thomas T, Pacheco Quinto J, Henry TL, Poeggeler B, Herbert D, Cruz-Sanchez F, Chyan YJ, Smith MA, Perry G, Shoji M, Abe K, Leone A, Grundke-Ikbal I, Wilson GL, Ghiso J, Williams C, Refolo LM, Pappolla MA, Chain DG, Neria E (2003) Melatonin increases survival and inhibits oxidative and amyloid pathology in a transgenic model of Alzheimer's disease. *J Neurochem* 85:1101-1108.
- McBride JL, During MJ, Wu J, Chen EY, Leurgans SE, Kordower JH (2003) Structural and functional neuroprotection in a rat model of Huntington's disease by viral gene transfer of GDNF. *Exp Neurol* 181:213-223.
- McCampbell A, Taye AA, Whitty L, Penney E, Steffan JS, Fischbeck KH (2001) Histone deacetylase inhibitors reduce polyglutamine toxicity. *Proc Natl Acad Sci U S A* 98:15179-15184.
- McCampbell A, Taylor JP, Taye AA, Robitschek J, Li M, Walcott J, Merry D, Chai Y, Paulson H, Sobue G, Fischbeck KH (2000) CREB-binding protein sequestration by expanded polyglutamine. *Hum Mol Genet* 9:2197-2202.

- McManamny P, Chy HS, Finkelstein DI, Craythorn RG, Crack PJ, Kola I, Cheema SS, Horne MK, Wreford NG, O'Bryan MK, De Kretser DM, Morrison JR (2002) A mouse model of spinal and bulbar muscular atrophy. *Hum Mol Genet* 11:2103-2111.
- Merienne K, Friedman J, Akimoto M, Abou-Sleymane G, Weber C, Swaroop A, Trottier Y (2007) Preventing polyglutamine-induced activation of c-Jun delays neuronal dysfunction in a mouse model of SCA7 retinopathy. *Neurobiol Dis* 25:571-581.
- Merry DE (2005) Animal models of Kennedy disease. *NeuroRx* 2:471-479.
- Merry DE, Kobayashi Y, Bailey CK, Taye AA, Fischbeck KH (1998) Cleavage, aggregation and toxicity of the expanded androgen receptor in spinal and bulbar muscular atrophy. *Hum Mol Genet* 7:693-701.
- Minamiyama M, Katsuno M, Adachi H, Waza M, Sang C, Kobayashi Y, Tanaka F, Doyu M, Inukai A, Sobue G (2004) Sodium butyrate ameliorates phenotypic expression in a transgenic mouse model of spinal and bulbar muscular atrophy. *Hum Mol Genet* 13:1183-1192.
- Mukai H, Isagawa T, Goyama E, Tanaka S, Bence NF, Tamura A, Ono Y, Kopito RR (2005) Formation of morphologically similar globular aggregates from diverse aggregation-prone proteins in mammalian cells. *Proc Natl Acad Sci U S A* 102:10887-10892.
- Nagai Y, Fujikake N, Ohno K, Higashiyama H, Popiel HA, Rahadian J, Yamaguchi M, Strittmatter WJ, Burke JR, Toda T (2003) Prevention of polyglutamine oligomerization and neurodegeneration by the peptide inhibitor QBP1 in *Drosophila*. *Hum Mol Genet* 12:1253-1259.
- Neuschmid-Kaspar F, Gast A, Peterziel H, Schneikert J, Muigg A, Ransmayr G, Klocker H, Bartsch G, Cato AC (1996) CAG-repeat expansion in androgen receptor in Kennedy's disease is not a loss of function mutation. *Mol Cell Endocrinol* 117:149-156.
- Nozaki K, Onodera O, Takano H, Tsuji S (2001) Amino acid sequences flanking polyglutamine stretches influence their potential for aggregate formation. *Neuroreport* 12:3357-3364.
- Nucifora FC, Jr., Sasaki M, Peters MF, Huang H, Cooper JK, Yamada M, Takahashi H, Tsuji S, Troncoso J, Dawson VL, Dawson TM, Ross CA (2001) Interference by huntingtin and atrophin-1 with cbp-mediated transcription leading to cellular toxicity. *Science* 291:2423-2428.

- O'Nuallain B, Wetzel R (2002) Conformational Abs recognizing a generic amyloid fibril epitope. *Proc Natl Acad Sci U S A* 99:1485-1490.
- Okamura-Oho Y, Miyashita T, Nagao K, Shima S, Ogata Y, Katada T, Nishina H, Yamada M (2003) Dentatorubral-pallidoluysian atrophy protein is phosphorylated by c-Jun NH2-terminal kinase. *Hum Mol Genet* 12:1535-1542.
- Palazzolo I, Burnett BG, Young JE, Brenne PL, La Spada AR, Fischbeck KH, Howell BW, Pennuto M (2007) Akt blocks ligand binding and protects against expanded polyglutamine androgen receptor toxicity. *Hum Mol Genet* 16:1593-1603.
- Pandey UB, Nie Z, Batlevi Y, McCray BA, Ritson GP, Nedelsky NB, Schwartz SL, DiProspero NA, Knight MA, Schuldiner O, Padmanabhan R, Hild M, Berry DL, Garza D, Hubbert CC, Yao TP, Baehrecke EH, Taylor JP (2007) HDAC6 rescues neurodegeneration and provides an essential link between autophagy and the UPS. *Nature* 447:859-863.
- Pappolla M, Bozner P, Soto C, Shao H, Robakis NK, Zagorski M, Frangione B, Ghiso J (1998) Inhibition of Alzheimer beta-fibrillogenesis by melatonin. *J Biol Chem* 273:7185-7188.
- Parker JA, Metzler M, Georgiou J, Mage M, Roder JC, Rose AM, Hayden MR, Neri C (2007) Huntingtin-interacting protein 1 influences worm and mouse presynaptic function and protects *Caenorhabditis elegans* neurons against mutant polyglutamine toxicity. *J Neurosci* 27:11056-11064.
- Paulson HL, Bonini NM, Roth KA (2000) Polyglutamine disease and neuronal cell death. *Proc Natl Acad Sci U S A* 97:12957-12958.
- Perutz MF, Pope BJ, Owen D, Wanker EE, Scherzinger E (2002) Aggregation of proteins with expanded glutamine and alanine repeats of the glutamine-rich and asparagine-rich domains of Sup35 and of the amyloid beta-peptide of amyloid plaques. *Proc Natl Acad Sci U S A* 99:5596-5600.
- Peters MF, Nucifora FC, Jr., Kushi J, Seaman HC, Cooper JK, Herring WJ, Dawson VL, Dawson TM, Ross CA (1999) Nuclear targeting of mutant Huntingtin increases toxicity. *Mol Cell Neurosci* 14:121-128.
- Phelps CB, Brand AH (1998) Ectopic gene expression in *Drosophila* using GAL4 system. *Methods* 14:367-379.

- Piccioni F, Pinton P, Simeoni S, Pozzi P, Fascio U, Vismara G, Martini L, Rizzuto R, Poletti A (2002) Androgen receptor with elongated polyglutamine tract forms aggregates that alter axonal trafficking and mitochondrial distribution in motor neuronal processes. *FASEB J* 16:1418-1420.
- Pratt WB, Toft DO (1997) Steroid receptor interactions with heat shock protein and immunophilin chaperones. *Endocr Rev* 18:306-360.
- Quist A, Doudevski I, Lin H, Azimova R, Ng D, Frangione B, Kagan B, Ghiso J, Lal R (2005) Amyloid ion channels: a common structural link for protein-misfolding disease. *Proc Natl Acad Sci U S A* 102:10427-10432.
- Reddy PS, Housman DE (1997) The complex pathology of trinucleotide repeats. *Curr Opin Cell Biol* 9:364-372.
- Reid J, Kelly SM, Watt K, Price NC, McEwan IJ (2002) Conformational analysis of the androgen receptor amino-terminal domain involved in transactivation. Influence of structure-stabilizing solutes and protein-protein interactions. *J Biol Chem* 277:20079-20086.
- Rennie PS, Bruchovsky N, Leco KJ, Sheppard PC, McQueen SA, Cheng H, Snoek R, Hamel A, Bock ME, MacDonald BS, et al. (1993) Characterization of two cis-acting DNA elements involved in the androgen regulation of the probasin gene. *Mol Endocrinol* 7:23-36.
- Richon VM, Emiliani S, Verdin E, Webb Y, Breslow R, Rifkind RA, Marks PA (1998) A class of hybrid polar inducers of transformed cell differentiation inhibits histone deacetylases. *Proc Natl Acad Sci U S A* 95:3003-3007.
- Riley BE, Orr HT (2006) Polyglutamine neurodegenerative diseases and regulation of transcription: assembling the puzzle. *Genes Dev* 20:2183-2192.
- Robinson MJ, Cobb MH (1997) Mitogen-activated protein kinase pathways. *Curr Opin Cell Biol* 9:180-186.
- Robitaille Y, Schut L, Kish SJ (1995) Structural and immunocytochemical features of olivopontocerebellar atrophy caused by the spinocerebellar ataxia type 1 (SCA-1) mutation define a unique phenotype. *Acta Neuropathol (Berl)* 90:572-581.

- Ross CA (1997) Intranuclear neuronal inclusions: a common pathogenic mechanism for glutamine-repeat neurodegenerative diseases? *Neuron* 19:1147-1150.
- Ross CA (2002) Polyglutamine pathogenesis: emergence of unifying mechanisms for Huntington's disease and related disorders. *Neuron* 35:819-822.
- Ross CA, Poirier MA (2004) Protein aggregation and neurodegenerative disease. *Nat Med* 10 Suppl:S10-17.
- Roy AK, Tyagi RK, Song CS, Lavrovsky Y, Ahn SC, Oh TS, Chatterjee B (2001) Androgen receptor: structural domains and functional dynamics after ligand-receptor interaction. *Ann N Y Acad Sci* 949:44-57.
- Rush MG, Drivas G, D'Eustachio P (1996) The small nuclear GTPase Ran: how much does it run? *Bioessays* 18:103-112.
- Rusmini P, Sau D, Crippa V, Palazzolo I, Simonini F, Onesto E, Martini L, Poletti A (2007) Aggregation and proteasome: the case of elongated polyglutamine aggregation in spinal and bulbar muscular atrophy. *Neurobiol Aging* 28:1099-1111.
- Russell DW, Wilson JD (1994) Steroid 5 alpha-reductase: two genes/two enzymes. *Annu Rev Biochem* 63:25-61.
- Sanchez I, Xu CJ, Juo P, Kakizaka A, Blenis J, Yuan J (1999) Caspase-8 is required for cell death induced by expanded polyglutamine repeats. *Neuron* 22:623-633.
- Satyal SH, Schmidt E, Kitagawa K, Sondheimer N, Lindquist S, Kramer JM, Morimoto RI (2000) Polyglutamine aggregates alter protein folding homeostasis in *Caenorhabditis elegans*. *Proc Natl Acad Sci U S A* 97:5750-5755.
- Saudou F, Finkbeiner S, Devys D, Greenberg ME (1998) Huntingtin acts in the nucleus to induce apoptosis but death does not correlate with the formation of intranuclear inclusions. *Cell* 95:55-66.
- Scappini E, Koh TW, Martin NP, O'Bryan J P (2007) Intersectin enhances huntingtin aggregation and neurodegeneration through activation of c-Jun-NH2-terminal kinase. *Hum Mol Genet* 16:1862-1871.

- Scherzinger E, Sittler A, Schweiger K, Heiser V, Lurz R, Hasenbank R, Bates GP, Lehrach H, Wanker EE (1999) Self-assembly of polyglutamine-containing huntingtin fragments into amyloid-like fibrils: implications for Huntington's disease pathology. *Proc Natl Acad Sci U S A* 96:4604-4609.
- Schilling B, Gafni J, Torcassi C, Cong X, Row RH, LaFevre-Bernt MA, Cusack MP, Ratovitski T, Hirschhorn R, Ross CA, Gibson BW, Ellerby LM (2006) Huntingtin phosphorylation sites mapped by mass spectrometry. Modulation of cleavage and toxicity. *J Biol Chem* 281:23686-23697.
- Schilling G, Savonenko AV, Klevytska A, Morton JL, Tucker SM, Poirier M, Gale A, Chan N, Gonzales V, Slunt HH, Coonfield ML, Jenkins NA, Copeland NG, Ross CA, Borchelt DR (2004) Nuclear-targeting of mutant huntingtin fragments produces Huntington's disease-like phenotypes in transgenic mice. *Hum Mol Genet* 13:1599-1610.
- Sewerynek E (2002) Melatonin and the cardiovascular system. *Neuro Endocrinol Lett* 23 Suppl 1:79-83.
- Shiu SY (2007) Towards rational and evidence-based use of melatonin in prostate cancer prevention and treatment. *J Pineal Res* 43:1-9.
- Sittler A, Lurz R, Lueder G, Priller J, Lehrach H, Hayer-Hartl MK, Hartl FU, Wanker EE (2001) Geldanamycin activates a heat shock response and inhibits huntingtin aggregation in a cell culture model of Huntington's disease. *Hum Mol Genet* 10:1307-1315.
- Slow EJ, Graham RK, Osmand AP, Devon RS, Lu G, Deng Y, Pearson J, Vaid K, Bissada N, Wetzel R, Leavitt BR, Hayden MR (2005) Absence of behavioral abnormalities and neurodegeneration in vivo despite widespread neuronal huntingtin inclusions. *Proc Natl Acad Sci U S A* 102:11402-11407.
- Sopher BL, Thomas PS, Jr., LaFevre-Bernt MA, Holm IE, Wilke SA, Ware CB, Jin LW, Libby RT, Ellerby LM, La Spada AR (2004) Androgen receptor YAC transgenic mice recapitulate SBMA motor neuronopathy and implicate VEGF164 in the motor neuron degeneration. *Neuron* 41:687-699.
- Srinivasan V (1997) Melatonin, biological rhythm disorders and phototherapy. *Indian J Physiol Pharmacol* 41:309-328.
- Srinivasan V, Pandi-Perumal SR, Cardinali DP, Poeggeler B, Hardeland R (2006) Melatonin in Alzheimer's disease and other neurodegenerative disorders. *Behav Brain Funct* 2:15.

- Stefanis C, Papapetropoulos T, Scarpalezos S, Lygidakis G, Panayiotopoulos CP (1975) X-linked spinal and bulbar muscular atrophy of late onset. A separate type of motor neuron disease? *J Neurol Sci* 24:493-403.
- Steffan JS, Kazantsev A, Spasic-Boskovic O, Greenwald M, Zhu YZ, Gohler H, Wanker EE, Bates GP, Housman DE, Thompson LM (2000) The Huntington's disease protein interacts with p53 and CREB-binding protein and represses transcription. *Proc Natl Acad Sci U S A* 97:6763-6768.
- Steffan JS, Bodai L, Pallos J, Poelman M, McCampbell A, Apostol BL, Kazantsev A, Schmidt E, Zhu YZ, Greenwald M, Kurokawa R, Housman DE, Jackson GR, Marsh JL, Thompson LM (2001) Histone deacetylase inhibitors arrest polyglutamine-dependent neurodegeneration in *Drosophila*. *Nature* 413:739-743.
- Stenoien DL, Mielke M, Mancini MA (2002) Intranuclear ataxin1 inclusions contain both fast- and slow-exchanging components. *Nat Cell Biol* 4:806-810.
- Sunde M, Blake CC (1998) From the globular to the fibrous state: protein structure and structural conversion in amyloid formation. *Q Rev Biophys* 31:1-39.
- Takeyama K, Ito S, Yamamoto A, Tanimoto H, Furutani T, Kanuka H, Miura M, Tabata T, Kato S (2002) Androgen-dependent neurodegeneration by polyglutamine-expanded human androgen receptor in *Drosophila*. *Neuron* 35:855-864.
- Taneja SS, Ha S, Swenson NK, Huang HY, Lee P, Melamed J, Shapiro E, Garabedian MJ, Logan SK (2005) Cell-specific regulation of androgen receptor phosphorylation in vivo. *J Biol Chem* 280:40916-40924.
- Tarlac V, Storey E (2003) Role of proteolysis in polyglutamine disorders. *J Neurosci Res* 74:406-416.
- Taylor JP, Taye AA, Campbell C, Kazemi-Esfarjani P, Fischbeck KH, Min KT (2003) Aberrant histone acetylation, altered transcription, and retinal degeneration in a *Drosophila* model of polyglutamine disease are rescued by CREB-binding protein. *Genes Dev* 17:1463-1468.
- Thomas M, Harrell JM, Morishima Y, Peng HM, Pratt WB, Lieberman AP (2006a) Pharmacologic and genetic inhibition of hsp90-dependent trafficking reduces aggregation and promotes degradation of the expanded glutamine androgen receptor without stress protein induction. *Hum Mol Genet* 15:1876-1883.

- Thomas M, Dadgar N, Aphale A, Harrell JM, Kunkel R, Pratt WB, Lieberman AP (2004) Androgen receptor acetylation site mutations cause trafficking defects, misfolding, and aggregation similar to expanded glutamine tracts. *J Biol Chem* 279:8389-8395.
- Thomas PS, Jr., Fraley GS, Damian V, Woodke LB, Zapata F, Sopher BL, Plymate SR, La Spada AR (2006b) Loss of endogenous androgen receptor protein accelerates motor neuron degeneration and accentuates androgen insensitivity in a mouse model of X-linked spinal and bulbar muscular atrophy. *Hum Mol Genet* 15:2225-2238.
- Trottier Y, Lutz Y, Stevanin G, Imbert G, Devys D, Cancel G, Saudou F, Weber C, David G, Tora L, et al. (1995) Polyglutamine expansion as a pathological epitope in Huntington's disease and four dominant cerebellar ataxias. *Nature* 378:403-406.
- Truant R, Atwal RS, Burtnik A (2007) Nucleocytoplasmic trafficking and transcription effects of huntingtin in Huntington's disease. *Prog Neurobiol*.
- van Laar JH, Bolt-de Vries J, Zegers ND, Trapman J, Brinkmann AO (1990) Androgen receptor heterogeneity and phosphorylation in human LNCaP cells. *Biochem Biophys Res Commun* 166:193-200.
- van Laar JH, Berrevoets CA, Trapman J, Zegers ND, Brinkmann AO (1991) Hormone-dependent androgen receptor phosphorylation is accompanied by receptor transformation in human lymph node carcinoma of the prostate cells. *J Biol Chem* 266:3734-3738.
- Voisine C, Varma H, Walker N, Bates EA, Stockwell BR, Hart AC (2007) Identification of potential therapeutic drugs for huntington's disease using *Caenorhabditis elegans*. *PLoS ONE* 2:e504.
- Wacker JL, Zareie MH, Fong H, Sarikaya M, Muchowski PJ (2004) Hsp70 and Hsp40 attenuate formation of spherical and annular polyglutamine oligomers by partitioning monomer. *Nat Struct Mol Biol* 11:1215-1222.
- Walcott JL, Merry DE (2002) Ligand promotes intranuclear inclusions in a novel cell model of spinal and bulbar muscular atrophy. *J Biol Chem* 277:50855-50859.
- Waldhauser F, Ehrhart B, Forster E (1993) Clinical aspects of the melatonin action: impact of development, aging, and puberty, involvement of melatonin in psychiatric disease and importance of neuroimmunoendocrine interactions. *Experientia* 49:671-681.

- Warrick JM, Paulson HL, Gray-Board GL, Bui QT, Fischbeck KH, Pittman RN, Bonini NM (1998) Expanded polyglutamine protein forms nuclear inclusions and causes neural degeneration in *Drosophila*. *Cell* 93:939-949.
- Watase K, Gatchel JR, Sun Y, Emamian E, Atkinson R, Richman R, Mizusawa H, Orr HT, Shaw C, Zoghbi HY (2007) Lithium therapy improves neurological function and hippocampal dendritic arborization in a spinocerebellar ataxia type 1 mouse model. *PLoS Med* 4:e182.
- Weigmann K, Klapper R, Strasser T, Rickert C, Technau G, Jackle H, Janning W, Klambt C (2003) FlyMove--a new way to look at development of *Drosophila*. *Trends Genet* 19:310-311.
- Wellington CL, Hayden MR (2000) Caspases and neurodegeneration: on the cutting edge of new therapeutic approaches. *Clin Genet* 57:1-10.
- Wellington CL, Singaraja R, Ellerby L, Savill J, Roy S, Leavitt B, Cattaneo E, Hackam A, Sharp A, Thornberry N, Nicholson DW, Bredesen DE, Hayden MR (2000) Inhibiting caspase cleavage of huntingtin reduces toxicity and aggregate formation in neuronal and nonneuronal cells. *J Biol Chem* 275:19831-19838.
- Wellington CL, Ellerby LM, Hackam AS, Margolis RL, Trifiro MA, Singaraja R, McCutcheon K, Salvesen GS, Propp SS, Bromm M, Rowland KJ, Zhang T, Rasper D, Roy S, Thornberry N, Pinsky L, Kakizuka A, Ross CA, Nicholson DW, Bredesen DE, Hayden MR (1998) Caspase cleavage of gene products associated with triplet expansion disorders generates truncated fragments containing the polyglutamine tract. *J Biol Chem* 273:9158-9167.
- Wierman ME (2007) Sex steroid effects at target tissues: mechanisms of action. *Adv Physiol Educ* 31:26-33.
- Wolff T, Martin KA, Rubin GM, Zipursky SL (1997) The development of the *Drosophila* visual system. In: *Molecular and Cellular Approaches to Neuronal Development* (Cowan WM, Jessell TM, Zipursky SL, eds), pp 474–508. New York: Oxford University Press.
- Yamada M, Sato T, Tsuji S, Takahashi H (2007) CAG repeat disorder models and human neuropathology: similarities and differences. *Acta Neuropathol (Berl)*.

- Yang CS, Vitto MJ, Busby SA, Garcia BA, Kesler CT, Gioeli D, Shabanowitz J, Hunt DF, Rundell K, Brautigam DL, Paschal BM (2005) Simian virus 40 small t antigen mediates conformation-dependent transfer of protein phosphatase 2A onto the androgen receptor. *Mol Cell Biol* 25:1298-1308.
- Yang Z, Chang YJ, Yu IC, Yeh S, Wu CC, Miyamoto H, Merry DE, Sobue G, Chen LM, Chang SS, Chang C (2007) ASC-J9 ameliorates spinal and bulbar muscular atrophy phenotype via degradation of androgen receptor. *Nat Med* 13:348-353.
- Yeh S, Lin HK, Kang HY, Thin TH, Lin MF, Chang C (1999) From HER2/Neu signal cascade to androgen receptor and its coactivators: a novel pathway by induction of androgen target genes through MAP kinase in prostate cancer cells. *Proc Natl Acad Sci U S A* 96:5458-5463.
- Ying M, Xu R, Wu X, Zhu H, Zhuang Y, Han M, Xu T (2006) Sodium butyrate ameliorates histone hypoacetylation and neurodegenerative phenotypes in a mouse model for DRPLA. *J Biol Chem* 281:12580-12586.
- Young JE, Gouw L, Propp S, Sopher BL, Taylor J, Lin A, Hermel E, Logvinova A, Chen SF, Chen S, Bredesen DE, Truant R, Ptacek LJ, La Spada AR, Ellerby LM (2007) Proteolytic cleavage of ataxin-7 by caspase-7 modulates cellular toxicity and transcriptional dysregulation. *J Biol Chem*.
- Zhou ZX, Wong CI, Sar M, Wilson EM (1994) The androgen receptor: an overview. *Recent Prog Horm Res* 49:249-274.
- Zoghbi HY, Orr HT (2000) Glutamine repeats and neurodegeneration. *Annu Rev Neurosci* 23:217-247.
- Zoghbi HY, Botas J (2002) Mouse and fly models of neurodegeneration. *Trends Genet* 18:463-471.